AD_____

AWARD NUMBER: W81XWH-04-1-0456

TITLE: Manipulation of NF-KappaB Activity in the Macrophage Lineage as a Novel Therapeutic Approach

PRINCIPAL INVESTIGATOR: Fiona Yull, Ph.D.

CONTRACTING ORGANIZATION: Vanderbilt University Medical Center
Nashville, Tennessee 37232-6917

REPORT DATE: May 2006

TYPE OF REPORT: Annual

PREPARED FOR: U.S. Army Medical Research and Materiel Command
Fort Detrick, Maryland 21702-5012

REPORT DOCUMENTATION PAGE

Form Approved
OMB No. 0704-0188

1. REPORT DATE *(DD-MM-YYYY)*	**2. REPORT TYPE**	**3. DATES COVERED** *(From - To)*
01-05-2006	Annual	19 Apr 2005 – 18 Apr 2006

4. TITLE AND SUBTITLE

Manipulation of NF-KappaB Activity in the Macrophage Lineage as a Novel Therapeutic Approach

5a. CONTRACT NUMBER

5b. GRANT NUMBER
W81XWH-04-1-0456

5c. PROGRAM ELEMENT NUMBER

6. AUTHOR(S)

Fiona Yull, Ph.D.

E-Mail: fiona.yull@vanderbilt.edu

5d. PROJECT NUMBER

5e. TASK NUMBER

5f. WORK UNIT NUMBER

7. PERFORMING ORGANIZATION NAME(S) AND ADDRESS(ES)

Vanderbilt University Medical Center
Nashville, Tennessee 37232-6917

8. PERFORMING ORGANIZATION REPORT NUMBER

9. SPONSORING / MONITORING AGENCY NAME(S) AND ADDRESS(ES)
U.S. Army Medical Research and Materiel Command
Fort Detrick, Maryland 21702-5012

10. SPONSOR/MONITOR'S ACRONYM(S)

11. SPONSOR/MONITOR'S REPORT NUMBER(S)

12. DISTRIBUTION / AVAILABILITY STATEMENT
Approved for Public Release; Distribution Unlimited

13. SUPPLEMENTARY NOTES

14. ABSTRACT
Morphogenesis of the mammary gland is a highly complex process which when misregulated can result in tumorigenesis. It involves the interactions of multiple cell types in a highly regulated manner with complex signal transduction pathways coordinating the physiological processes. Interactions between epithelial and mesenchymal cells are known to be important. However, recent studies are beginning to highlight the importance of other cell types, such as macrophages. One of the signaling molecules that appears to be critical in regulating the dynamic changes during normal and neoplastic development is the nuclear factor-kappa B (NF-κB) family of transcription factors. NF-κ˜ can regulate many genes that are expressed by macrophages that are important for proliferation and apoptosis of cells, as well as remodeling and angiogenesis. This proposal seeks to investigate the contribution of NF-κ˜ signaling within macrophages in defining the macrophage's role in normal and neoplastic mammary development. The proposed studies will provide information regarding the signaling pathways involved in normal mammary development. They will also provide insights into the importance of NF-κB signaling in macrophages for tumor development and progression and will have the potential for identification of novel therapeutic strategies. At this point we have generated a novel transgenic reporter that allows us to investigate patterns of NF-kappaB activity during mammary development.

15. SUBJECT TERMS
NF-kappaB, macrophages, mammary, fetal liver transplantation, doxycycline inducible, transgenic reporter

16. SECURITY CLASSIFICATION OF:			**17. LIMITATION OF ABSTRACT**	**18. NUMBER OF PAGES**	**19a. NAME OF RESPONSIBLE PERSON**
a. REPORT	**b. ABSTRACT**	**c. THIS PAGE**			USAMRMC
U	U	U	UU	79	**19b. TELEPHONE NUMBER** *(include area code)*

Table of Contents

INTRODUCTION

Morphogenesis of the mammary gland is a highly complex process which when misregulated can result in tumorigenesis. It involves the interactions of multiple cell types in a highly regulated manner with complex signal transduction pathways coordinating the physiological processes. Interactions between epithelial and mesenchymal cells are known to be important. However, recent studies are beginning to highlight the importance of other cell types, such as macrophages. One of the signaling molecules that appears to be critical in regulating the dynamic changes during normal and neoplastic development is the nuclear factor-kappa B (NF-κB) family of transcription factors. NF-κB can regulate many genes that are expressed by macrophages that are important for proliferation and apoptosis of cells, as well as remodeling and angiogenesis. This proposal seeks to investigate the contribution of NF-κB signaling within macrophages in defining the macrophage's role in normal and neoplastic mammary development. The proposed experiments use multiple murine lines and novel assay systems. These studies will provide information regarding the signaling pathways involved in normal mammary development. They will also provide insights into the importance of NF-κB signaling in macrophages for tumor development and progression and will have the potential for identification of novel therapeutic strategies.

BODY

Task 1. To investigate the effects of constitutive NF-kappaB activity within macrophages on mammary development (Months 1-24):

a. Perform fetal liver cell transplantation using IkappaB-alpha null and control donors at postnatal day 19 to determine effects on virgin postnatal mammary development of constitutive NF-kappaB activity in reconstituted hematopoietic cells (Months 1-24). [100 mice]
b. Perform fetal liver cell transplantation using IkappaB-alpha null and control donors into recipients at 6 weeks. Allow hematopoetic cell reconstitution for a further 6 weeks. Mate recipient mice and investigate effects on development during pregnancy of constitutive NF-kappaB activity in hematopoietic cells (Months 1-24). [100 mice]

Our lab and others have generated IκBα deficient mice (Chen et al., 2000; Chen et al., 2000b; Beg et al., 1995; Klement et al., 1996). In these animals the major inhibitor of NF-κB is absent resulting in constitutive activity. Neonatal lethality precludes the study of adult mammary gland morphogenesis in these animals. However, fetal liver transplantation and reconstitution of hematopoetic cell lineages enables the effects of constitutive NF-κB activation within these lineages to be investigated in an adult animal (Chen et al., 2000; Everhart et al., 2005).

We have been continuing our program of fetal liver transplantations and have now completed a significant number of experiments. Our accumulated data suggests that constitutive NF-κB in IκBα -/- reconstituted virgin animals may result in a significant decrease in ductal colonization of the mammary fad pat. Mice reconstituted with heterozygote knockout cells display an interesting phenotype in which the extent to which the ductal tree is able to grow into the recipient fad pad appears to be reduced but the ducts themselves appear thicker, representative examples are shown in Figure 1. However, having performed a relatively large number of reconstitution experiments, we became concerned about some of the technical aspects of this approach. Fetal livers are harvested from 14.5dpc embryos resulting from matings between heterozygous knockout animals. The harvested cells are reintroduced into irradiated recipients on the same day. This effectively means that the reconstitutions are performed "blind" because the genotyping of the embryos occurs

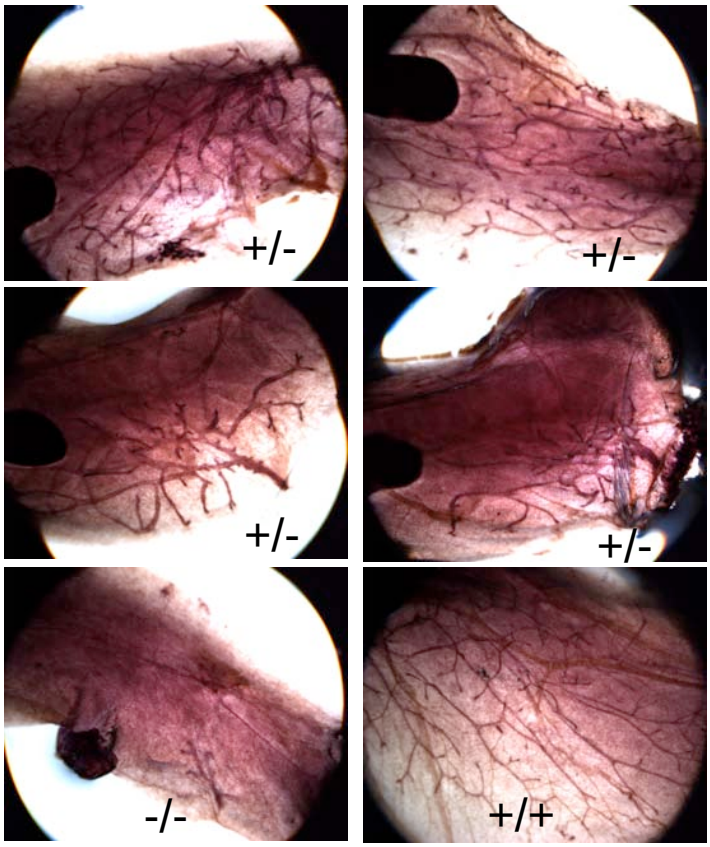

Figure 1 – Wholemount staining of virgin mammary glands after IB- +/-, -/- and +/+ fetal liver transplantation.

after the reconstitutions have been completed. This results in a large number of heterozygote reconstitutions and relatively few homozygous or wildtype reconstitutions. We have also had a couple of complete experiments in which when the mammary tissue was finally harvested we discovered that none of the transplantations had reconstituted. We suspect that this was due to a problem with the irradiator.

We have completed three attempts to perform fetal liver reconstitutions and then obtain pregnant recipient females. Despite attempts to use a decreased level of radiation, the recipient females appear to be sterilized by the irradiation procedure as we have been unsuccessful in our attempts to maintain fertility in reconstituted mice.

We are encouraged by the phenotypes that we have observed as a result of the virgin reconstitution experiments and could probably overcome the technical difficulties that we have been having by persisting with a greater number of reconstitution experiments. In the case of the investigation of mammary development in reconstituted animals during pregnancy it may be feasible to adopt a chemical ablation methodology as opposed to the irradiation prior to reconstitution and maintain fertility. However, the reconstitution experiments have a number of limitations. They are susceptible to a relatively high level of variation due to the variable efficiency of reconstitution. One possibility that we have considered is attempting to control for this using strain specific cell surface markers and FACS analysis of peripheral cells at the point of harvest to determine extent of reconstitution. This method would give us some measure of potential differences due to reconstitution efficiency. Another issue with the reconstitution strategy is that the resulting chimeras have reconstituted populations of multiple cell types of the hematopoetic lineage. In other words, we are not able to specifically assign phenotypic changes to an effect of changed signaling within macrophages as opposed to within B or T cells or a combinatorial effect. Given these considerations, all of which would be addressed by the inducible model proposed as aim 2, we decided to focus our efforts on the inducible model system (see task 2).

In our original proposal we were planning to measure the *in vivo* effects of modulating NF-B activity in macrophages using our HLL reporter transgenics that express luciferase under an NF-B responsive promoter such that luciferase assay of crude protein extracts can be used to quantify NF-B activity. While the HLL reporter mice have provided valuable information regarding NF-B activation *in vivo*, three issues led us to construct a second generation of NF-B reporter transgenic mice. First, although we attempted to identify NF-B activation at a cellular level, we were unable to reproducibly identify luciferase protein or mRNA in individual cells despite repeated efforts with immunohistochemistry and *in situ* hybridization. Second, we would like to be able to sort individual cells that have activated NF-B. Third, the proximal HIV-LTR is an NF-B dependent promoter that by all indications has good fidelity as a read-out for NF-B activation in the

models we have used to date; however, it was still a formal possibility that other transcription factors, including Sp1, could influence transcription of this promoter. Therefore, we decided that it would be valuable to have an additional line of reporter mice with another NF-κB dependent promoter to confirm and validate findings using the HLL mice. These issues led us to collaborate with another group here at Vanderbilt to make a new line of transgenic reporter mice that express a green fluorescent protein (GFP)/luciferase fusion protein under the control of a synthetic NF-κB dependent promoter. Since GFP can be detected in individual cells, these reporter mice allow cell specific determination of NF-κB directed transcription, a crucial factor in understanding NF-κB dependent downstream signaling. The luciferase moiety of the fusion protein also enables luciferase assay from protein extracts and *in vivo* imaging as described above for the HLL reporter transgenics.

The new transgenic NF-κB reporter mice contain tandem copies of a 36 base enhancer from the 5' HIV-LTR that includes both NF-κB binding sites. The proximal 169 base pairs of these promoter constructs, including the TATA box, are from the herpes simplex virus thymidine kinase promoter. We constructed plasmids for expression of enhanced GFP (EGFP)/luciferase fusion protein under the control of 8 replicates of the NF-κB enhancer sequence. The CMV promoter present in pEGFP/Luc (Clontech, Palo Alto, CA) was replaced with our synthetic NF-κB dependent promoter. The 8x construct was microinjected by the Vanderbilt Transgenic/ES Cell Shared Resource to generate transgenic lines (C57Bl6/DBA background) named NGL [for NF-κB-GFP/Luciferase]. Our characterization has shown that the NGL reporter transgenics can be used in the same manner as the HLL, giving comparable results. In fact, the new NGL transgenics are better than the HLL transgenics as they can also enable visualization of specific cell types in which NF-κB is activated by fluorescence microscopy or immunohistochemistry of tissue sections. Activation of NF-κB results in expression of GFP protein that can be detected by fluorescence microscopy or by immunohistochemical analysis of paraffin embedded sections using an anti-GFP antibody. We have tested the efficacy of the new NGL mice by crossing them with transgenics that elevate NF-κB activity in the mammary epithelium. The mice produced from these matings allow us to visualize where the NF-κB is active (Figure 2). The representative examples shown illustrate how it is possible to see both the histological structure of the tissue and to localize and get an indication of NF-κB activity. At 16.5dpc, in an NGL transgenic ie. an animal that is effectively wild-type as far as mammary development is concerned but carries the NF-κB reporter, there is diffuse NF-κB activity throughout the epithelial tissue that is proliferating and filling the mammary fat pad. In double transgenics we are able to visualize both the level and localization of NF-κB activity and determine the effect of the transgene that is modulating NF-κB activity. In the double transgenic animals the level of NF-κB activity is seen to be higher but is confined to a more dense area. Figure 2A shows immunohistochemical staining using a GFP antibody to localize NF-κB activity. It is

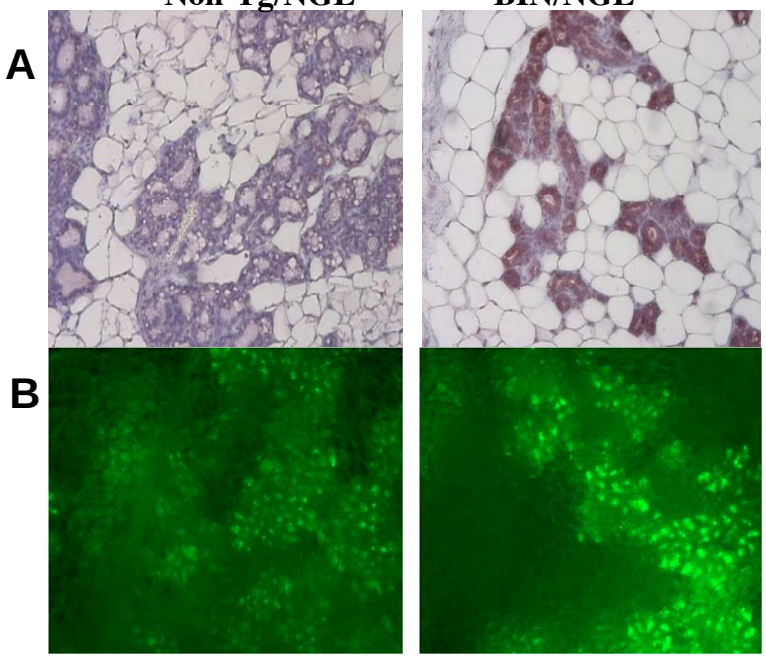

Figure 2 - Immunohistochemistry for GFP expression in single NGL transgenic and double transgenics. Shown are examples of mammary tissue at 16.5dpc. A – immunohistochemistry using a GFP antibody, B – fluorescence in freshly harvested mammary tissue sections.

interesting to note that the fluorescent moiety of the reporter also allows us to place freshly harvested tissue on a slide on a fluorescence microscope and begin to get some idea of the expression pattern in three dimensions (Figure 2B).

One of the anticipated benefits of the new reporter transgenics was the ability to assess NF-□B activity in specific cell types. As macrophages are the focus of these studies we were interested to determine whether the NGL reporter transgenics would allow us to quantify changes in NF-□B activity within macrophages. Therefore, we performed cell culture studies using primary cultures of bone marrow derived macrophages (BMDM) from the NGL reporter transgenics (Figure 3). Luciferase assay of cell extracts demonstrate that NF-□B activity is induced at 4 hours post treatment with LPS (a known activator of NF-□B) and that this stimulation can be blocked by pretreatment with an adenovirus expressing a dominant inhibitor of NF-□B (Sadikot et al, 2006). This data provides evidence that the activity of NF-□B within primary NGL macrophages can be easily measured.

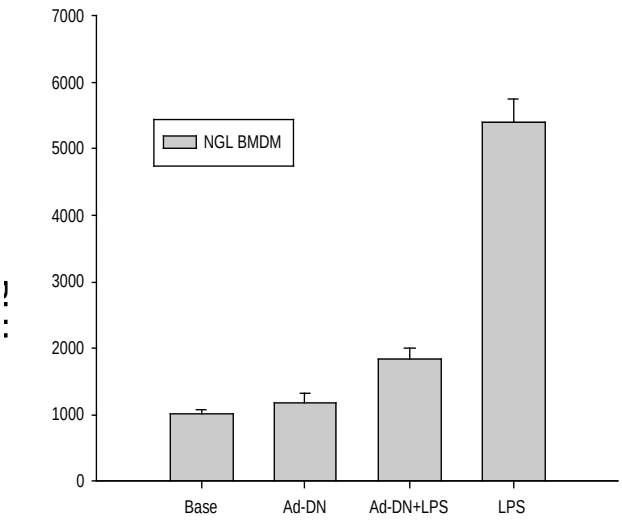

Figure 3– Luciferase assay of NGL BMDM extracts after 4 hrs treatment with LPS in the presence or absence of an NF-kB dominant-inhibitor virus.

In order to carry out more extensive cell culture studies, we have also generated an immortalized NGL bone marrow derived macrophage cell line. The cell surface markers on this line were investigated to confirm that the cells were derived from macrophages and maintained the appropriate characteristics.

Cell surface marker of J2-BM cells (day 14)

Surface marker	% Positive J2-BM cells	Distribution
MAC-1	96.8	Macrophage, granulocytes
Fc receptor	85.7	Macrophage, B Cells
Ly 1.1	2.8	Pan-T cells, some B cells
Lyt 2.1	0.4	T-cell subsets, thymocyte
L3T4	3.2	T-cell subsets, thymocyte
Surface immunoglobulin	0.7	B cells

Having confirmed that the characteristics of the immortalized line were consistent with macrophage cells we tested to determine whether they have the appropriate NF-□B response to LPS stimulation and whether we can measure this using a luciferase assay. The data showed that the response to LPS stimulation of the

immortalized cell lines was not significantly different to that of primary BMDC (Figure 4). In combination, the studies suggest that we have generated an immortalized macrophage cell line from the NGL mice that can be used in future *in vitro* studies as required.

In addition to investigating our ability to assess NF- □B activity in specific cell types using our NGL reporter we have cultured BMDM from wildtype (I□B□ +/+) and I□B□ +/- mice. In order to confirm that NF-□B signaling was altered in macrophages derived from heterozygous knockout animals we performed western analyses using cytoplasmic and nuclear extracts from wildtype and heterozygous BMDM and assessed the response to LPS stimulation (Figure 5). I□B-□+/- BMDM contained decreased I□B-□ and increased RelA protein at baseline compared to WT BMDM. Four hours after LPS stimulation, increased RelA was detected in both WT and I□B□ +/- BMDM; however, I□B-□ protein was virtually undetectable in I□B□ +/- BMDM. While I□B-□ protein had returned to basal levels by 24 hours after LPS stimulation, nuclear RelA protein was significantly higher in I□B□ +/- BMDM compared to WT BMDM. These results demonstrate our ability to obtain BMDM from both wildtype and heterozygous knockout mice and that NF-□B signaling is altered in heterozygous knockout mice.

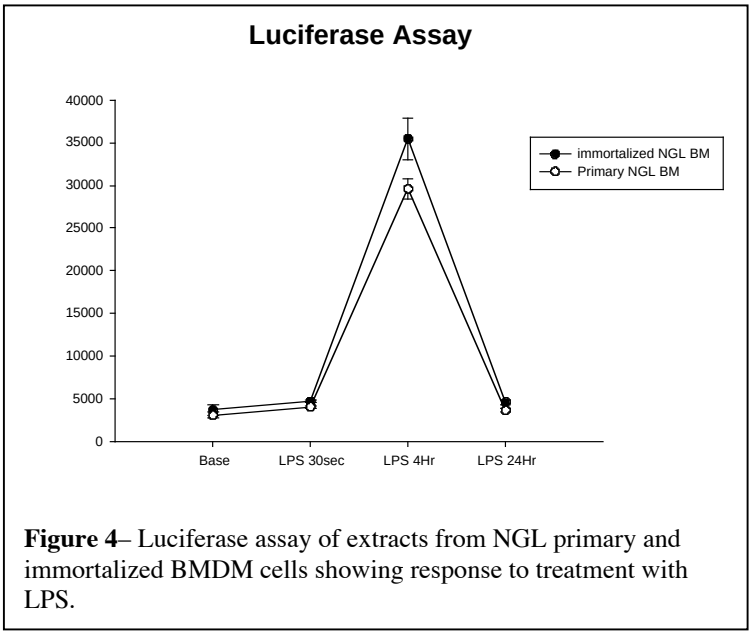

Figure 4– Luciferase assay of extracts from NGL primary and immortalized BMDM cells showing response to treatment with LPS.

Should we encounter a significant delay in our ability to use the macrophage directed inducible model (see task 2), we propose to commence *in vitro* co-culture studies in which role of NF-□B in macrophage/epithelium communication will be investigated using BMDM derived from lines with altered NF-□B signaling. In these experiments BMDM will be placed in the top chamber of our co-culture apparatus with epithelial cells in the bottom. Differential cytokine/chemokine production and effects on epithelial proliferation and apoptosis will be measured. The inclusion of our NGL reporter will also enable us to assess effects on NF-□B activity.

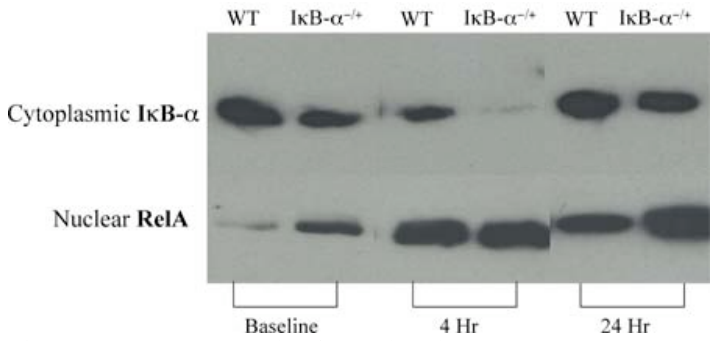

Figure 5– western analysis of cytoplasmic and nuclear extracts from wildtype and I□B□ +/- BMDM cells showing differential response to treatment with LPS.

These studies would begin to dissect the potential mechanism by which altered NF-□B signaling within the macrophages impacts epithelial cell behavior during mammary development.

In summary, we have completed additional fetal liver reconstitution studies and the data that we have obtained are strongly suggestive that increased NF-□B signaling in cells of the hematopoetic lineage (and our biased prediction would be that the macrophages are likely to be the responsible cell type) can have significant effects on mammary ductal development. In collaborative efforts with the group of Dr Timothy Blackwell we have developed new reporter transgenics that are providing the kind of data that was hitherto not possible to collect. These mice have already led to a collaborative publication (Everhart et al, 2006) and will be extremely useful in ongoing studies.

Task 2. Assess effects on mammary development of induced and inhibited NF-kappaB activity using novel inducible transgenics (Months 1-36).

a. Investigate postnatal development in doxycycline-induced macrophage-restricted constitutive activator double transgenic mice (IKMRP) and controls (Months 1-36). [300 mice]
b. Investigate postnatal development doxycycline-induced macrophage-restricted dominant inhibitor double transgenic mice in (DNMRP) and controls (Months 1-36). [300 mice]

In collaboration with the group of Dr Timothy Blackwell, we have been developing conditional transgenic modular mouse models, based on the tetracycline inducible system, to over-express IκB-DN (dominant inhibitor) or cIKK2 (constitutive activator) in response to treatment with doxycycline in drinking water. The components of this system include transgenics expressing the reverse tetracycline transactivator (rtTA) in the appropriate cell type, and transgenics in which the tetracycline operator $(tet\text{-}O)_7$ and a minimal CMV promoter drive expression of either the dominant inhibitor (IκB-DN), or a constitutively active IKK2 mutant. Key DNA components for the system were obtained from Dr Jay Tichelaar (Perl et al., 2002). In the presence of doxycycline, the rtTA binds to tet-O and induces downstream gene expression within 24 hours. In these transgenics, the IκB-DN construct that we have has mutations of the critical phosphorylation targets (serine residues) that are normally phosphorylated in response to signaling resulting in degradation of the inhibitor (Chen et al., 1999). This mutated form of inhibitor is not degraded in response to phosphorylation signals and therefore functions to block NF-κB signaling. To facilitate detection of induced transgene products we have attached a FLAG tag to the cIKK2 and a Myc-His tag to the dominant inhibitor. The transgenics expressing the inhibitor are named DN. The transgenics expressing the activator are named IKK. In order to modulate expression in macrophages, we have been collaborating with the group of Dr. John Christman (formerly at Vanderbilt and now in Chicago). We designed a transgenic construct to achieve macrophage restricted expression of the reverse tetracycline transactivator (rtTA)(Perl et al., 2002). Expression was targeted to macrophages using a promoter based on the mannose receptor promoter (MRP)(Eichbaum et al., 1997) and including 3 repeats of a PU.1 responsive element (DeKoter et al., 2000). The transactivator transgenics are named MRP. With the assistance of the Vanderbilt Transgenic/ES Cell Shared Resource we generated 4 independent lines each of the DN, IKK and MRP transgenics.

We have now completed extensive collaborative studies using the DN and IKK transgenics crossed with an existing, well-characterized lung-specific CC-10rtTA transgenic (Perl et al., 2002). In last years report we included evidence demonstrating that expression of either the IKK or DN transgenes could be induced in the lung in response to treatment with doxycycline in drinking water (1mg/ml) for 3 days prior to collection of tissue samples. We have now tested all 4 lines of IKK transgenics and all 4 lines of DN transgenics in crosses with the lung specific rtTA. The levels of induced protein expression in response to the same concentration of doxycycline in the drinking water differ between lines. We have identified the strongest expressing line of each type and have confirmed that in these lines there is no uninduced expression in the absence of doxycycline in the drinking water and no detectable non tissue-specific expression, therefore the system is not leaky. The response to doxycycline administration in the drinking water is dose dependent allowing manipulation of levels of transgene expression. As shown in preliminary data in last years report the induced DN transgene is able to inhibit NF-κB activation in the lung in response to LPS treatment that would normally be expected to increase NF-κB activity and hence binding in a gel mobility shift assay and the induced IKK transgene is able to enhance NF-κB activation in the lung. Thus, we have generated transgenic lines in which expression of the NF-κB dominant inhibitor or constitutive activator transgenes is inducible in the presence of the transactivator protein and administration of doxycycline in the drinking water. The DN and IKK transgene products are functional and able to modulate NF-κB activity *in vivo*. We have used this form of the modular inducible

transgenic system in collaborative studies that have recently been submitted to Nature Medicine (see appended manuscript).

We also generated 4 independent lines of MRP transgenics. Last year we reported preliminary data showing that we could detect the rtTA mRNA using RT-PCR in alveolar macrophages harvested from bronchiolar lavage fluid and in bone marrow-derived macrophage cultures. We had begun to generate double transgenic animals carrying a combination of the DN and MRP transgenes (DNMP) or the IKK and MRP transgenes (IKMP). A small number of double transgenics and controls had been treated with doxycycline to induce transgene expression but our initial attempts to detect expression of the transgenes by western analysis of macrophages harvested from bronchiolar lavage fluid had been unsuccessful.

We continued analysis of the 4 MRP lines. Only a small subset of the data obtained will be shown here as the majority of the data has proved to be negative. All 4 of the separately generated MRP lines were crossed with a strong IKK transgenic line. In our extensive studies using the lung specific rtTA; this transgene has been easily detected by western analysis using the FLAG tag. In initial harvest s of lung, spleen, bone marrow and peritoneal macrophages from induced animals we were unable to detect transgene expression. Therefore, we decided to obtain a more concentrated cell population by culturing bone marrow derived macrophages. As we were a little concerned at our inability to detect transgene expression, we designed a second set of primers and repeated our RT PCR analysis looking for mRNA expression of the rtTA in double transgenic and control BMDM (Figure 6). In each case, we were able to detect expression of the rtTA transgene in BMDM.. Shown are examples harvested after 10 days of non-adherent culture or after culture and 24 hours for cells to adhere. An antibody that recognizes this form of the rtTA is not available and therefore, we cannot perform western analysis to detect rtTA expression at the protein level.

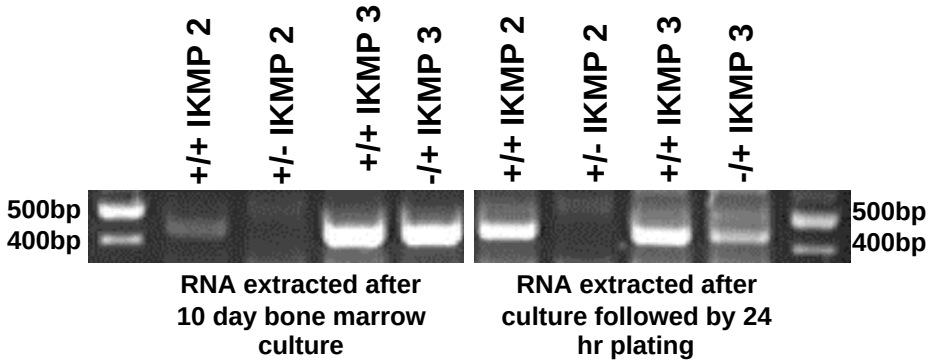

Figure 6– IKMP – bone marrow derived macrophages, RT PCR for rtTA mRNA expression.

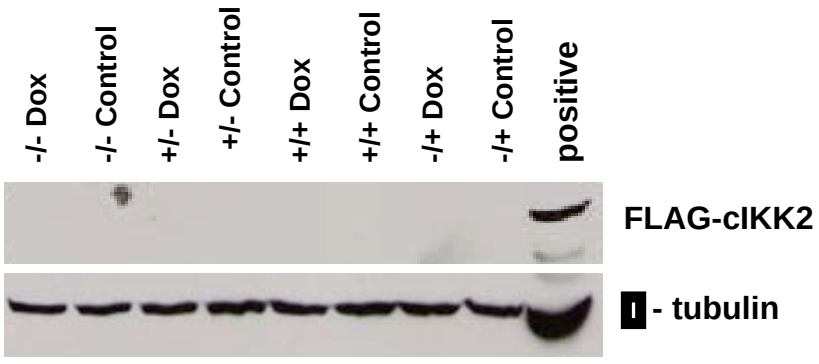

Figure 7– IKMP – bone marrow derived macrophages, treated with Dox 1μg/ml for 24 hrs

Despite our continued ability to detect rtTA at the mRNA level our attempts to detect FLAG-tagged IKK protein in doxycyline induced BMDM have failed. Shown is a representative example (Figure 7). We have tested all four MRP lines in crosses with the IKK transgenics and tested different lengths of induction (24 hours to 1 week) and different concentrations of doxycycline (1-5 g/ml). In combination with

the lung rtTA transgenic, 0.5 g/ml and 24 hours of doxycycline induction is sufficient for clear induction of expression. Although no deleterious effects were apparent in terms of the survival of the BMDM we were concerned that the induction of the constitutive IKK was in some way altering the behavior of the macrophages such that the rtTA was then silenced. However, in crosses with the DN transgenics (also extremely effective in combination with the lung rtTA) we have also been unable to detect transgene induction by western analysis (data not shown).

We were still not ready to conclude that the MRP transgenics were not useful and wondered whether perhaps despite our inability to detect the induced IKK or DN transgenes at the level of a western, there may be low level induction of the transgenes that was still sufficient to have an effect on macrophage function. Therefore we decided to determine whether the function of the macrophages in induced double transgenics was altered.

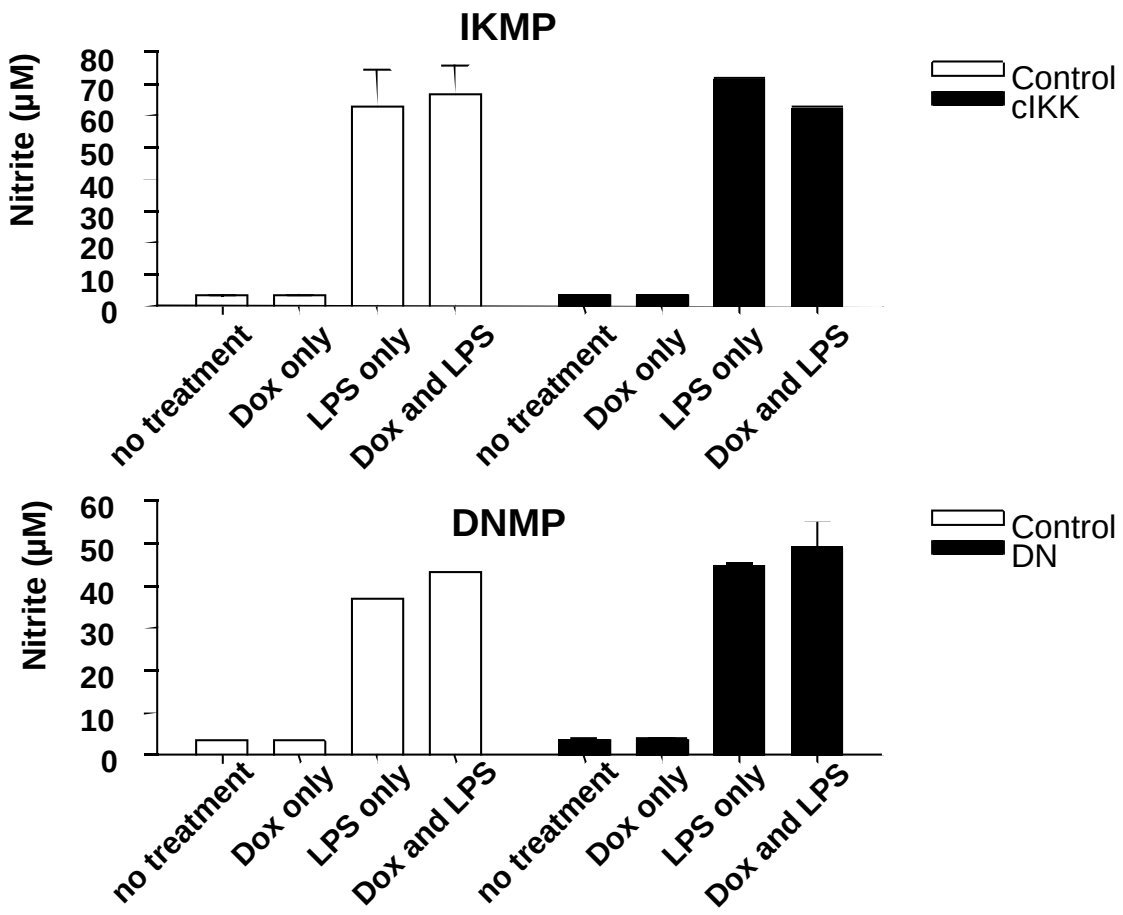

Figure 8 - Production of nitrite in response to LPS stimulation by induced and uninduced double transgenic and control macrophages.

We would have predicted that induction of the constitutive IKK transgene would result in increased nitrite production and that induction of the DN inhibitor transgene would result in decreased nitrite production. In neither case were we able to detect any significant effect of attempted induction of the transgenes. Taking

into consideration all of the above data we have been forced to conclude that the four lines of MRP transgenics do not result in sufficient expression of the rtTA to be of use for the inducible system.

As our proposed research would benefit greatly from having the inducible system within macrophages we sought an alternative strategy. The c-fms gene encodes the receptor for macrophage colony-stimulating factor (CSF-1). The c-fms promoter has been successfully used to generate macrophage specific transgenics (Sasmono et al., 2003; Burnett et al., 2004). In trying to find a source for this promoter we made contact with Professor Michael Ostrowski at Ohio State University, Columbus, Ohio. We discovered that his research group are also attempting to make a macrophage-targeted rtTA transgenic. They have founder animals from two different transgene constructs each of which uses a different form of the c-fms promoter. Both types of transgenics express high levels of the transgene as determined by RT-PCR. Dr. Ostrowski has kindly agreed to collaborate with us and representative males from the two different types of founder lines are currently being serology tested for transfer to our facility. As soon as we obtain these founder animals they will be mated with our IKK and DN transgenics to determine whether they have sufficient levels of rtTA expression to be effective in our inducible system.

While our modular inducible transgenic system is not yet functional in macrophages, we have confirmed efficacy of the DN and IKK component transgenics in the lung epithelium and therefore, expect the system will be effective once we have the macrophage rtTA component transgenics.

Task 3. To determine whether manipulation of NF-kappaB activity within macrophage populations effects tumorigenesis (Months 25-36).

a. Investigate effects on tumorigenesis in PyMT/IKMRP doxycycline-induced transgenics and controls. ie. does constitutive NF-□B activity within macrophages exacerbate tumorigenesis? (Months 25-36). [100 mice]
b. Investigate effects on tumorigenesis in PyMT/DNMRP doxycycline-induced transgenics and controls. ie. does reduced NF-kappaB activity within macrophages inhibit tumorigenesis? (Months 25-36). [100 mice]

As originally proposed this task was dependent on establishing the model described in task 2 and was not scheduled to commence until month 25. However, due to the difficulties we were experiencing in establishing the critical macrophage targeted rtTA transgenic component of the inducible modular system we are adopting an intermediate strategy to obtain worthwhile data in the event that we are unsuccessful in developing the modular system in time to make significant progress with this aim.

We have obtained the PyMT transgenic mice and have established a small colony within our laboratory. While this model of mammary cancer has been used in a number of studies, little is known concerning the pattern of NF-□B activation during the development of the tumors. Our new NGL reporter transgenics provide us with a unique opportunity to investigate the stages during tumor progression in which NF-□B is active and the specific cell types involved. We have commenced breeding the PyMT transgenics with the NGL reporter transgenics to enable us to investigate the pattern of NF-□B activation at the various stages of tumor development; pre-tumor, primary mammary tumor and lung metastasis.

Should the new macrophage rtTA transgenics that we are obtaining as part of a collaboration with Dr Ostrowski also prove to be ineffective as inducers, we propose to complete a small pilot cohort of animals in which the I□B□ knockout is crossed with the PyMT transgenics and we complete a comparative study of primary tumor development and lung metastasis in PyMT: I□B□ +/+ versus PyMT: I□B□ +/- animals. Clearly we would prefer to use or originally proposed inducible model, but this represents a “Plan B”.

In order to be in a position to rapidly commence some of the original proposed studies should the new macrophage transgenics prove effective, we have commenced breeding strategies to generate homozygous forms of the IKK and DN transgenics.

While this task was not scheduled to start until month 25, we have made some pre-emptive efforts in case we encounter further difficulties with task 2.

KEY RESEARCH ACCOMPLISHMENTS

1) Results obtained using our fetal liver reconstitution strategy using I□B□ deficient cells and controls suggest that cells of the hematopoetic lineage (including macrophages) play a significant role in development of the mammary ductal epithelium.
2) In collaboration with the group of Dr. Timothy Blackwell, we have generated a novel GFP/luciferase transgenic reporter of *in vivo* NF-kappaB activity that we can use to obtain information concerning NF-kappaB activity at the resolution of single cells on tissue sections. These transgenics have now been fully characterized and have led to a recent publication (see reportable outcomes).
3) In collaboration with the group of Dr. Timothy Blackwell, we have generated transgenics in which the dominant inhibitor of NF-kappaB is under the control of an inducible promoter and confirmed that they are functional. These transgenics have now been fully characterized, have been used in collaborative studies and have been included in a recently submitted manuscript (see reportable outcomes).
4) In collaboration with the group of Dr. Timothy Blackwell, we have generated transgenics in which a constitutive activator of NF-kappaB is under the control of an inducible promoter and confirmed that they are functional. These transgenics have now been fully characterized, have been used in collaborative studies and have been included in a recently submitted manuscript (see reportable outcomes).
5) In collaboration with the group of Dr. John Christman, we generated several lines of transgenics designed to target expression of the reverse transactivator protein (rtTA) to macrophages. As of last years report we were commencing their characterization. Despite promising initial data and after considerable effort, we have been forced to conclude that while these transgenics express RNA that is detectable by RTPCR the levels of rtTA protein expression are insufficient to make any one of the transgenic lines that we have tested useful as a component of our doxycycline inducible model.
6) We have commenced a new collaboration and are in the process of obtaining potential macrophage targeted rtTA transgenic mice from the laboratory of Professor M. Ostrowski, Ohio State University. We will test these for their utility in our inducible model and are optimistic that they will enable us to complete more elegant studies to determine the effects of NF-kappaB signaling within macrophages on mammary development.

REPORTABLE OUTCOMES

In a collaborative effort with the laboratory of Dr. Timothy Blackwell we have developed three novel transgenics; an *in vivo* reporter of NF-kappaB activity, an inducible dominant inhibitor of NF-kappaB activity and an inducible constitutive activator of NF-kappaB activity. These efforts have currently led to one accepted manuscript and one submitted manuscript.

In vivo reporter of NF-kappaB activity transgenics. Everhart MB, Han W, Sherrill TP, Arutiunov M, Polosukhin VV, Burke JR, Sadikot RT, Christman JW, Yull FE, Blackwell TS. (2006) Duration and intensity of NF-kappaB activity determine the severity of endotoxin-induced acute lung injury. J Immunol. 176:4995-5005.

Airway epithelium controls development of acute lung injury through the NF-□B pathway. Cheng, D-S.C., Han, W., Chen, S., Sherrill, T.P., Chont, M., Park, G-Y., Sheller, J.R., Polosukhin, V.V., Christman, J.W., Yull, F.E.,

and Blackwell, T.S. Submitted to Nature Medicine (note that last two authors contributed equally to the publication).

CONCLUSIONS

In summary, we have succeeded in generating and characterizing 3 of the 4 originally proposed transgenics. All of these transgenics have considerable potential for further studies for not only our groups but for many others within the scientific community. Collaborative studies with the reporter NGL, constitutive activator IKK and dominant inhibitor DN transgenics have led to one accepted and one submitted publication. While we have encountered some difficulties in the generation of the 4th transgenic we have established a new collaboration with Dr M Ostrowski and will commence characterization of these new transgenics as soon as they are released from quarantine. We have included discussion of our amended strategies to take into account the unpredicted hurdles that we have encountered and acquire further valuable information within the body of the report. Our data from task 1 and increasing numbers of reported studies in the literature result in our continued optimism that our approaches will reveal an important role for NF-□B signaling within macrophages on both normal development and tumorigenesis and also lead to further publications within the time frame of this funding.

REFERENCES

Beg, A.A., Sha, W.C., Bronson, R.T., Baltimore, D. (1995) Constitutive NF-kappa B activation, enhanced granulopoiesis, and neonatal lethality in I kappa B alpha-deficient mice. *Genes Dev*. 9:2736-46.

Burnett, S.H., Kershen, E.J., Zhang, J., Zeng, L., Straley, S.C., Kaplan, A.M., Cohen, D.A. (2004) Conditional macrophage ablation in transgenic mice expressing a Fas-based suicide gene. *J Leukoc Biol.* 75:612-23.

Chen, C-L., Yull, F.E., Kerr, L.D. (1999) Differential serine phosphorylation regulates I□B-□ inactivation. *Biochem. Biophys. Res. Comm.* 257, 798-806.

Chen, C-L., Singh, N., Yull, F.E., Strayhorn, D., Van Kaer, L., Kerr, L.D. (2000). Lymphocytes lacking I□B-□ develop normally, but have selective defects in proliferation and function. *Journal of Immunology* 165: 5418-5427.

Chen, C-L., Yull, F.E., Cardwell, N., Nanney, L., Kerr, L.D. (2000b) RAG2-/-, I□B-□-/- chimeras display a psoriasis-like skin disease. *Journal of Investigative Dermatology*, 115: 1124-1133.

DeKoter, R.P., Singh, H. (2000). Regulation of B lymphocyte and macrophage development by graded expression of PU.1. *Science*. 288: 1439-41.

Eichbaum, Q., Heney, D., Raveh, D., Chung, M., Davidson, M., Epstin, J., Ezekowitz, A.B. (1997) Murine macrophage mannose receptor promoter is regulated by the transcription factors PU.1 and SP1. Blood 90: 4135-143.

Everhart, M.B., Han, W., Parman, K.S., Polosukhin, VV., Zeng, H., Sadikot, R.T., Li, B., Yull, F.E., Christman, J.W., Blackwell, T.S. 2005. Intratracheal administration of liposomal clodronate accelerates alveolar macrophage reconstitution following fetal liver transplantation. *J Leukoc Biol.* 77:173-80.

Everhart, M.B., Han, W., Sherrill, T.P., Arutiunov, M., Polosukhin, V.V., Burke, J.R., Sadikot, R.T., Christman, J.W., Yull, F.E., Blackwell, T.S. Duration and Intensity of NF-{kappa}B Activity Determine the Severity of Endotoxin-Induced Acute Lung Injury. J Immunol. 2006 176:4995-5005.

Klement, J.F., Rice, N.R., Car, B.D., Abbondanzo, S.J., Powers, G.D., Bhatt, P.H., Chen, C.H., Rosen, C.A., Stewart, C.L. (1996) IkappaBalpha deficiency results in a sustained NF-kappaB response and severe widespread dermatitis in mice. *Mol Cell Biol.* 16:2341-9.

Sasmono, R.T., Oceandy, D., Pollard, J.W., Tong, W., Pavli, P., Wainwright, B.J., Ostrowski, M.C., Himes, S.R., Hume, D.A. (2003) A macrophage colony-stimulating factor receptor-green fluorescent protein transgene is expressed throughout the mononuclear phagocyte system of the mouse. *Blood* 101:1155-63.
Perl, A.K., Tichelaar, J.W., Whitsett, J.A. (2002) Conditional gene expression in the respiratory epithelium of the mouse. *Transgenic Research*. 11:21-9.
Sadikot, R.T., Zeng, H., Joo, M., Everhart, M.B., Sherrill, T.P., Li, B., Cheng, D.S., Yull, F.E., Christman, J.W., Blackwell, T.S. (2006) Targeted Immunomodulation of the NF-{kappa}B Pathway in Airway Epithelium Impacts Host Defense against Pseudomonas aeruginosa. *J Immunol*. 176:4923-30.

APPENDICES

In vivo reporter of NF-kappaB activity transgenics. Everhart MB, Han W, Sherrill TP, Arutiunov M, Polosukhin VV, Burke JR, Sadikot RT, Christman JW, Yull FE, Blackwell TS. (2006) Duration and intensity of NF-kappaB activity determine the severity of endotoxin-induced acute lung injury. J Immunol. 176:4995-5005.

Airway epithelium controls development of acute lung injury through the NF-□B pathway. Cheng, D-S.C., Han, W., Chen, S., Sherrill, T.P., Chont, M., Park, G-Y., Sheller, J.R., Polosukhin, V.V., Christman, J.W., Yull, F.E., and Blackwell, T.S. Submitted to Nature Medicine (note that last two authors contributed equally to the publication).

Duration and Intensity of NF-κB Activity Determine the Severity of Endotoxin-Induced Acute Lung Injury[1]

M. Brett Everhart,[2]* Wei Han,[2†] Taylor P. Sherrill,[†] Melissa Arutiunov,[‡] Vasiliy V. Polosukhin,[†] James R. Burke,[‖] Ruxana T. Sadikot,[†§] John W. Christman,[¶] Fiona E. Yull,[‡] and Timothy S. Blackwell[3]*[†‡§]

Activation of innate immunity in the lungs can lead to a self-limited inflammatory response or progress to severe lung injury. We investigated whether specific parameters of NF-κB pathway activation determine the outcome of acute lung inflammation using a novel line of transgenic reporter mice. Following a single i.p. injection of *Escherichia coli* LPS, transient NF-κB activation was identified in a variety of lung cell types, and neutrophilic inflammation resolved without substantial tissue injury. However, administration of LPS over 24 h by osmotic pump (LPS pump) implanted into the peritoneum resulted in sustained, widespread NF-κB activation and neutrophilic inflammation that culminated in lung injury at 48 h. To determine whether intervention in the NF-κB pathway could prevent progression to lung injury in the LPS pump model, we administered a specific IκB kinase inhibitor (BMS-345541) to down-regulate NF-κB activation following the onset of inflammation. Treatment with BMS-345541 beginning at 20 h after osmotic pump implantation reduced lung NF-κB activation, concentration of KC and MIP-2 in lung lavage, neutrophil influx, and lung edema measured at 48 h. Therefore, sustained NF-κB activation correlates with severity of lung injury, and interdiction in the NF-κB pathway is beneficial even after the onset of lung inflammation. *The Journal of Immunology,* **2006, 176: 4995–5005.**

Although inflammation generated through activation of innate immune pathways is critical for effective host responses to infection, dysregulated inflammation can contribute to tissue injury, thereby preventing recovery of the organism. The factors that govern whether an inflammatory response is adaptive or maladaptive (leading to injury) are not well understood and may vary depending on the initiating stimulus. The NF-κB pathway, which regulates transcription of a variety of proinflammatory mediators, is involved in generation of neutrophilic lung inflammation; however, it is unknown whether specific parameters of NF-κB activation determine whether lung inflammation resolves or progresses to lung injury. Elucidating the relationships between NF-κB activation, lung inflammation, and lung injury could provide important insights into the pathobiology of a variety of human lung diseases, including the acute respiratory distress syndrome (ARDS).[4]

In the lungs, many noxious/inflammatory stimuli have been shown to activate NF-κB, implicating the NF-κB pathway as a focal point for induction of lung inflammation. In vivo activators of NF-κB in the lungs include intact bacteria, Gram-negative bacterial LPS, ozone, and silica delivered directly to the airways, as well as systemic inflammatory insults such as sepsis, hemorrhage, and direct liver injury (1–10). In rodent models of lung inflammation induced by LPS, pretreatment with relatively nonspecific inhibitors of NF-κB activation has been found to diminish lung inflammation (11–13). Additionally, mice deficient in RelA (the transactivating subunit of NF-κB) and TNFR type 1 have impaired neutrophil recruitment to the lungs in response to LPS compared with wild-type controls and TNFR1-deficient mice (14). Together, these studies indicate that NF-κB plays an important role in initiation of inflammatory signaling in the lungs in response to LPS, a prototypical inflammatory stimulus. After establishment of an inflammatory response, however, it has been suggested that NF-κB has a role in resolution of inflammation through antiapoptotic effects and expression of proteins that function to limit inflammation (15). The importance of NF-κB in regulating ongoing lung inflammation or progression to lung injury is unknown.

We hypothesized that specific parameters of NF-κB activation in the lungs, including cellular distribution, intensity, and/or duration of NF-κB activity, determine whether lung inflammation is self-limited or progresses to injury. Further, we proposed that focused intervention to inhibit NF-κB activity could limit lung injury and convert an injurious stimulus to a phenotype of transient inflammation that resolves without significant tissue injury. To investigate this hypothesis, we generated novel transgenic NF-κB reporter mice to allow cell-specific detection of NF-κB activity.

*Department of Cell and Developmental Biology, †Department of Medicine, Division of Allergy, Pulmonary, and Critical Care Medicine, ‡Department of Cancer Biology, Vanderbilt University School of Medicine, and §Department of Veterans Affairs, Nashville, TN 37232; ¶Section of Pulmonary, Critical Care, and Sleep Medicine, University of Illinois, Chicago, IL 60612; and ‖Department of Immunology, Inflammation, and Pulmonary Drug Discovery, Bristol-Myers Squibb Pharmaceutical Research Institute, Princeton, NJ 08543

Received for publication September 19, 2005. Accepted for publication February 2, 2006.

The costs of publication of this article were defrayed in part by the payment of page charges. This article must therefore be hereby marked *advertisement* in accordance with 18 U.S.C. Section 1734 solely to indicate this fact.

[1] This work is supported by Grants HL61419 and HL66196 from the National Institutes of Health, by the U.S. Department of Veterans Affairs, Vanderbilt Ingram Cancer Center, by Grant BCTR02-1728 from the Susan G. Komen Foundation, and by Grant WX1XWH-04-1-0456 from the U.S. Department of Defense Breast Cancer Program.

[2] M.B.E. and W.H. contributed equally to this work.

[3] Address correspondence and reprint requests to Dr. Timothy S. Blackwell, Division of Allergy, Pulmonary, and Critical Care Medicine, T-1218 Medical Center North, Vanderbilt University Medical Center, Nashville, TN 37232-2650. E-mail address: timothy.blackwell@vanderbilt.edu

[4] Abbreviations used in this paper: ARDS, acute respiratory distress syndrome; IKK, IκB kinase; BAL, bronchoalveolar lavage; RLU, relative light unit.

0022-1767/06/$02.00

We determined parameters of NF-κB activation in a mouse model of transient lung inflammation following i.p. injection of *Escherichia coli* LPS and a model of lung inflammation and injury following prolonged delivery of LPS via an osmotic pump implanted into the peritoneum. We then intervened using a selective inhibitor of IκB kinase (IKK) to down-regulate NF-κB activation during a period in which we identified differential NF-κB activation between the two models. Information from these studies provides evidence that inhibition of the NF-κB pathway in vivo can ablate lung injury and identifies NF-κB as a critical target for limiting ongoing, maladaptive inflammation in the lungs.

Materials and Methods

Animal models

Transgenic NF-κB reporter mice were generated that contain four tandem copies of a 36-base enhancer from the 5′ HIV-long terminal repeat (containing two NF-κB binding sites, GGGACTTTCC) placed upstream of the HSV minimal thymidine kinase promoter. This enhancer-promoter construct was cloned into pEGFPluc (BD Clontech) for expression of an enhanced GFP-luciferase fusion protein. The 8xNF-κB-GFP-luciferase construct was excised and purified using a GELase Agarose Gel-Digesting preparation kit following the manufacturer's instruction (Epicentre Technologies). This construct was then injected at the Vanderbilt Transgenic/ES Cell Shared Resource to generate NGL (NF-κB-GFP-luciferase construct) transgenic mouse lines on C57B6/DBA background. Founder animals were genotyped by Southern blot and then further generations were genotyped by PCR analysis for increased efficiency.

Male and female NGL transgenic mice weighing between 20 and 25 g were used for these studies. *E. coli* LPS (serotype O55:B5) was obtained from Sigma-Aldrich. LPS was delivered by a single i.p. injection of 3 μg/g body weight (1 μg/μl solution in sterile PBS). For prolonged delivery of LPS, an osmotic pump (2001D Alzet pump; ALZA) was filled with LPS solution (1 μg/μl in PBS) and surgically implanted in the peritoneal cavity using sterile technique. The pump delivered 8 μg LPS (8 μl) per hour for 24 h. A priming dose of 3 μg of LPS/g body weight was injected i.p. following pump implantation.

A selective inhibitor of IKK, BMS-345541, was obtained from Bristol-Myers Squibb. The compound was formulated as a 7.5 mg/ml solution in 3% Tween 80 and sterile water. Body weight (75 μg/g) of this solution or an equivalent volume of vehicle (without BMS-345541) was administered by peroral gavage after anesthesia with inhaled isoflurane.

Neutrophil depletion was performed as previously reported (16). Undiluted rabbit antineutrophil Abs (200 μl; Accurate Chemical and Scientific) or control rabbit IgG (1 μg/μl; Sigma-Aldrich) were administered by i.p. injection daily for 2 days. On days 3 and 4, 300 μl of a 1/15 dilution of Ab preparations (in 1× PBS) were injected i.p. On day 5, peripheral white blood cell counts and differentials were measured to verify neutrophil depletion.

The experimental protocol was reviewed and approved by the Institutional Animal Care and Use Committee at Vanderbilt University (Nashville, TN).

Bioluminescence imaging and photon count quantification

Mice were anesthetized and shaved over the chest before imaging. Luciferin (1 mg/mouse in 100 μl isotonic saline) was administered by i.v. injection and mice were imaged with an intensified charge-coupled device (ICCD) camera (IVIS 200; Xenogen). For the duration of photon counting, mice were placed inside a light tight box that housed the camera. Light emission from the mouse was detected as photon counts by the ICCD camera and customized with image processing hardware and software (Living Image software; Xenogen). The imaging duration (30 s) was selected to avoid saturation of the camera during image acquisition. Quantitative analysis was performed by defining a standard area over the mid-lung zone and determining the total integrated photon intensity over the area of interest. For presentation, a digital false-color photon emission image was generated for each captured image.

Bone marrow-derived macrophage experiments

Bone marrow-derived macrophages were generated from NGL mice as previously described (17). Adenoviral vectors expressing a dominant inhibitor of NF-κB (IκBdn), which represents a S36-40A mutant of the avian IκB-α that cannot be phosphorylated or degraded, and β-galactosidase have been previously reported (10, 18). Cells were treated with adenoviral vectors (multiplicity of infection = 300) 48 h before LPS treatment. LPS was added to cultures (200 ng/ml) and cells were harvested 4 h later. In separate experiments, cells were treated with BMS-345541 (20 μM) 30 min before LPS.

Histology and immunohistochemistry

After euthanasia, lungs were inflated with 1 ml of 10% neutral buffered formalin. Lungs were then removed en bloc after tracheal ligation and preserved in 10% neutral buffered formalin for 24 h at 4°C, and subsequently embedded in paraffin. Lung tissue sections (5 μm) were prepared in the Mouse Pathology Core Facility (Vanderbilt University). H&E stains were performed using standard protocol. For GFP immunohistochemistry, 5-μm sections were cut and placed on charged slides. Following paraffin removal, sections were rehydrated and placed in heated Target Retrieval Solution (high pH; (DakoCytomation) for 20 min. Tissues were incubated with rabbit anti-GFP 1/200 (BD Clontech) for 30 min. Sections without primary Ab served as negative controls. The Vectastain ABC Elite System (Vector Laboratories) and diaminobenzidine (DAB^+; DakoCytomation) were used to produce localized, visible staining. Slides then were lightly counterstained with Mayer's hematoxylin, dehydrated, and coverslipped.

Measurement of neutrophil influx

For tissue neutrophil quantification, H&E-stained lung tissue sections were used to count the number of neutrophils per high power field. For each slide, neutrophils were counted in a blinded fashion on 10 sequential, non-overlapping high power fields (magnification, ×400) of lung parenchyma beginning at the periphery of the section. Three separate H&E-stained sections were evaluated per mouse, and the mean number of neutrophils per high power field was reported.

Lung lavage neutrophil counts

For bronchoalveolar lavage (BAL) neutrophil quantification, BAL cells were collected after lavage with 3 aliquots of 1 ml of sterile PBS. BAL was combined and centrifuged at 400 × *g* for 10 min to separate cells from supernatant. Supernatant was saved separately and frozen at −70°C. The cell pellet was suspended in PBS with 1% BSA, and total cell counts were determined on a grid hemocytometer. Differential cell counts were determined by staining cytocentrifuge slides with a modified Wright stain (Diff-Quick; Baxter Scientific Products) and counting 200–300 cells in complete cross-section.

Tissue luciferase assay

Lungs were removed en bloc and homogenized in 1 ml of lysis buffer (Promega) using a dounce homogenizer. After pulse centrifugation, luciferase activity was measured in a Monolight 3010 Luminometer (Analytical Luminescence Laboratory) after adding 100 μl of freshly reconstituted luciferase assay buffer to 20 μl of lung tissue homogenate. Results were expressed as relative light units (RLU) normalized for protein content, which was measured by Bradford assay (Bio-Rad).

Western blots

One hundred micrograms of protein from lung tissue homogenates were separated on a 10% acrylamide gel, transblotted, and immunodetected using phosphospecific Abs to an epitope of IKK1 containing phosphorylated serine 176 and serine 180 (BioSource International). The blots were also probed with Abs to MAPK p44 and p42 (Cell Signaling Technology), then stripped and reprobed for total IKK1 (Santa Cruz Biotechnology).

Lung wet to dry ratio

Lungs were removed and the wet weight recorded. Lungs were then placed in an incubator at 65°C for 48 h and the dry weight was determined.

MIP-2 and KC quantification

MIP-2 and KC levels in BAL fluid were measured using a specific ELISA according to manufacturer's instructions (R&D Systems).

Statistical analysis

To assess differences among groups, analyses were performed with GraphPad Instat software using an unpaired *t* test or one-way ANOVA. Results are presented as the mean ± SEM. Two-tailed values of $p < 0.05$ were considered significant.

Results

Construction of reporter mice to identify cell-specific NF-κB activation

After testing a variety of NF-κB-driven promoter constructs, we determined that basal expression and inducibility characteristics were optimal with a construct that contained four tandem copies of a 36-base enhancer from the 5′ HIV-long terminal repeat (containing two NF-κB binding sites, GGGACTTTCC). This NF-κB-dependent promoter was placed upstream of GFP-luciferase expression cassette, and the construct was tested in vitro using multiple cell lines (A549, RAW 267.4, NIH-3T3, HeLa) to ensure reliable expression in a wide range of cell types (data not shown). Subsequently, the NF-κB reporter construct was excised, purified, and microinjected at the Vanderbilt Transgenic/ES Cell Shared Resource to produce transgenic mice (NGL mice).

To investigate regulation of the reporter expression in primary cells, we obtained bone marrow macrophages and treated them in vitro with *E. coli* LPS (200 ng/ml) for 4 h to stimulate NF-κB activation. Adenoviral vectors expressing a transdominant inhibitor of the NF-κB pathway (Ad-IκBdn) (10, 18) were used to specifically block NF-κB activation in these cells. Cells were infected with adenoviral vectors 48 h before experimentation. Expression of the GFP-luciferase reporter was determined by luciferase assays and fluorescence microscopy (Fig. 1, *A* and *B*). By luciferase assay, no difference in reporter activity was detected between untreated and Ad-IκBdn-treated macrophages (1015.2 ± 67.2 vs 1257.3 ± 174.17 RLU, respectively). Compared with untreated and Ad-IκBdn-treated macrophages, LPS stimulation resulted in a significant increase in luciferase activity (5450.0 ± 265.59 RLU, $p < 0.05$); however, infection of cells with Ad-IκBdn before LPS blocked induction of luciferase expression (1841.3 ± 171.1 RLU). Infection of macrophages with control adenoviral vectors did not affect LPS-induced luciferase activity (data not shown). Using fluorescence microscopy to detect GFP expression before cell harvest, we corroborated the results obtained by luciferase assays (Fig. 1*B*). In addition to Ad-IκBdn, we treated macrophages from NGL mice with a specific inhibitor of the NF-κB pathway, BMS-345541 (19) (Fig. 1*C*). In these studies, cells were treated with BMS-345541 (20 μM) or vehicle 30 min before addition of LPS (200 ng/ml) and cells were harvested 4 h later. Similar to IκBdn, BMS-345541 treatment blocked LPS-induced luciferase activity in macrophages. Together, these findings confirm that LPS-induced expression of GFP-luciferase reflects NF-κB activation in NGL cells.

We performed additional studies to determine the half-life of the GFP-luciferase fusion protein in bone marrow-derived NGL macrophages. At 3 h after LPS treatment, cycloheximide (20 μg/ml) was added to cell cultures to block protein synthesis, and luciferase measurements were obtained every 30 min until return to baseline. In these studies, the half-life of the GFP-luciferase fusion protein was determined to be 2.5 h, making it suitable as a reporter of NF-κB transcriptional activity.

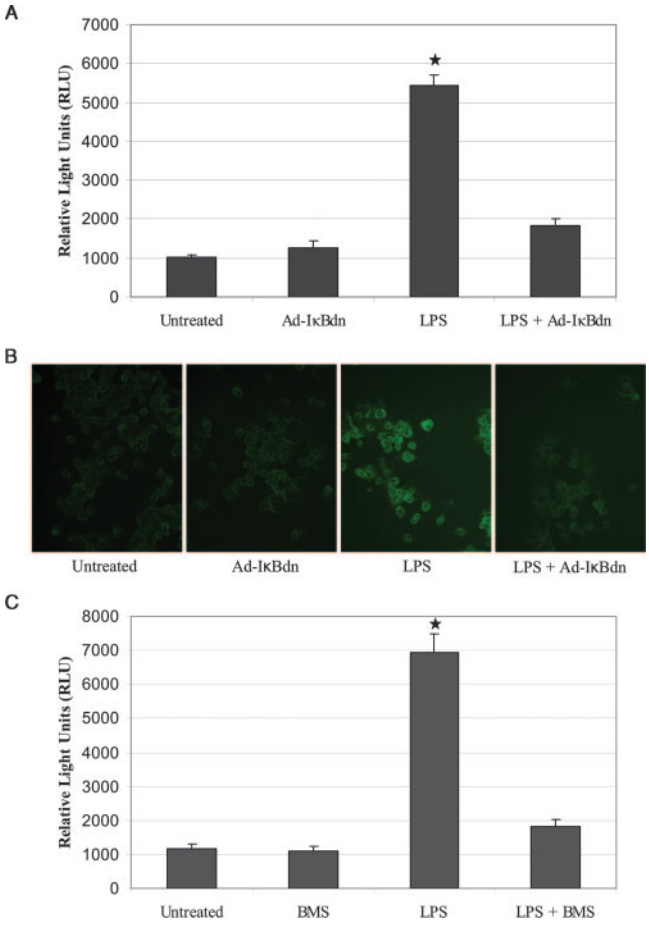

FIGURE 1. NF-κB regulation of the NGL reporter construct in bone marrow-derived macrophages from NGL mice. *A*, Luciferase activity (measured as RLU) from cell homogenates following treatment with LPS (200 ng/ml) for 4 h. Specificity of the reporter for NF-κB was shown by infection with adenoviral vectors expressing a dominant inhibitor of the NF-κB pathway (IκBdn). Cells were infected with adenoviral (multiplicity of infection = 300) 48 h before LPS treatment. Each bar represents the mean RLU ± SEM (for $n = 3$ wells per treatment group) and the experiment was repeated two times (∗, $p < 0.05$ compared with other groups). *B*, Representative fluorescence microscopy images of each treatment group showing GFP fluorescence at the time of harvest. *C*, Luciferase activity from cells treated with NF-κB inhibitor BMS-345541 (20 μM) or vehicle 30 min before LPS and harvested at 4 h. Each bar represents the mean RLU ± SEM (for $n = 3$ wells per treatment group). ∗, $p < 0.05$ vs other groups.

Cellular distribution, intensity, and duration of NF-κB activation in LPS-induced lung inflammation and injury

To model transient neutrophilic lung inflammation, a single dose of *E. coli* LPS (3 μg/g) was administered to NGL mice by i.p. injection (IP LPS treatment). Because established models of LPS-induced lung inflammation in mice do not produce consistent lung injury (20), we developed a model of LPS delivery into the peritoneal cavity over 24 h that produces severe lung inflammation and injury (Fig. 2*A*). In this model, an osmotic pump delivering *E. coli* LPS at 8 μg/h for 24 h was surgically implanted into the peritoneal space followed by a priming dose of 3 μg/g LPS by direct i.p. injection (LPS pump treatment). Although single-dose i.p. LPS produced only mild interstitial thickening and cellular infiltrate at 48 h, LPS delivered by osmotic pump caused lung inflammation and injury (edema, interstitial thickening, hemorrhage, and inflammatory cell influx). Persistent lung inflammation in the LPS pump model was confirmed by counting neutrophils on H&E-stained lung tissue sections. Although single-dose IP LPS treatment resulted in a transient influx of neutrophils at 4 h, LPS pump treatment resulted in persistent neutrophil influx through 48 h (Fig. 2*B*). The LPS pump model also resulted in a significant increase in lung edema as assessed by the wet to dry ratio at 48 h (3.81 ± 0.03 in untreated mice vs 4.65 ± 0.04 in the LPS pump group, $p < 0.05$), whereas the lung wet to dry ratio in the IP LPS group was similar to baseline. Delivery of LPS over 24 h into the peritoneum was required to induce this phenotype as treatment with an equal LPS

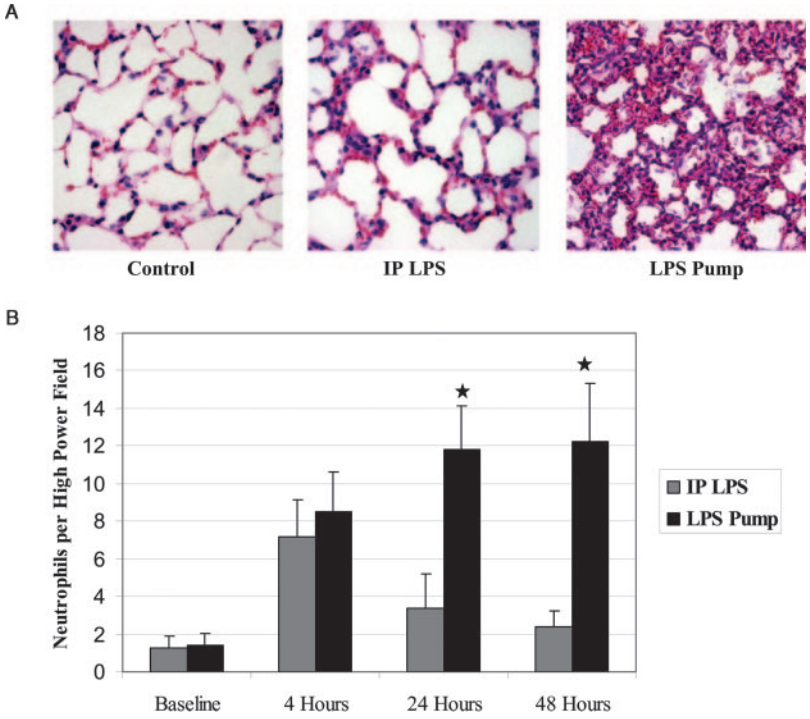

FIGURE 2. A single i.p. injection of LPS (IP LPS treatment) results in transient neutrophilic inflammation, but delivery of LPS by osmotic pump (LPS pump treatment) implanted in the peritoneum leads to persistent neutrophilic lung inflammation and injury. *A*, H&E-stained lung sections from a control NGL mouse and NGL mice harvested 48 h after a single i.p. injection of LPS (IP LPS) or LPS delivered by osmotic pump (LPS Pump). Increased edema, inflammatory cell influx and edema are identified in the LPS pump treatment group. *B*, Quantification of neutrophils per high power field on H&E-stained lung tissue sections. The number of neutrophils per high power field was counted for 10 consecutive, nonoverlapping fields per slide. Each bar represents the mean for each mouse ± SEM (for $n = 6$ mice per group at each time point). ∗, $p < 0.05$ vs IP LPS).

dose by single i.p. injection or implantation of pumps alone did not induce sustained lung inflammation and injury (data not shown).

After establishing these models of transient inflammation without substantial injury and persistent lung inflammation and injury, we investigated whether NF-κB was differentially activated in these models. Expression of the NF-κB-driven reporter in NGL mice was identified by bioluminescence imaging (following i.v. injection of 1 mg of luciferin) to detect luciferase activity in the lungs of intact mice and by immunohistochemistry for detection of GFP in lung sections. Consistent with our previous reports (10, 21), single-dose IP LPS treatment resulted in a transient increase in NF-κB-driven luciferase activity by 4 h. However, by 24 h, photon emission from the lungs returned near baseline, indicating transient NF-κB activation (Fig. 3*A*). In contrast, NGL mice treated with LPS delivered by osmotic pump showed sustained lung luciferase activity at 4, 24, and 48 h. Peak photon emission from the lungs at 4 h did not differ between the two models.

We correlated bioluminescence imaging of luciferase activity in the lungs of NGL mice with cellular localization of NF-κB activity by immunohistochemistry for GFP on lung sections (Fig. 3*B*). At baseline, minimal GFP staining was identified in the lungs. LPS treatment (either IP LPS or LPS pump) resulted in widespread GFP staining in multiple lung cell types at 4 h, including airway epithelium, endothelium, and leukocytes (macrophages and neutrophils). GFP staining was also noted in alveolar epithelium, particularly type II cells. At 24 h after IP LPS treatment, GFP immunoreactivity in the lungs was limited to a few, scattered positive cells, and by 48 h, GFP staining returned to baseline. In the LPS pump model, widespread GFP staining persisted in the lungs through 48 h, consistent with bioluminescence detection of NF-κB driven transgene expression. Together, these studies indicate that endotoxemia induces NF-κB activation in a variety of lung cells. Although the cell-specific pattern of NF-κB activity and peak intensity of lung NF-κB intensity did not differ depending on the method of LPS delivery, prolonged duration of high-level NF-κB activation in the lungs correlated with LPS-induced lung injury.

Early NF-κB inhibition limits neutrophilic lung inflammation whereas late NF-κB inhibition prevents lung injury

To evaluate the role of NF-κB in determining the course of lung inflammation and injury, we used BMS-345541, which is a selective inhibitor of IKK1 and IKK2 (19). In prior studies, BMS-345541 at doses as high as 100 μg/g daily for 6 wk in mice showed no toxicologic changes, either by gross or by histopathologic evaluation, of major organs including the liver (22).

In the IP LPS treatment model, BMS-345541 (75 μg/g) or vehicle was administered to NGL mice by peroral gavage 2 h before injection of LPS and again 4 h after LPS treatment. By bioluminescence imaging, photon emission from the lungs was reduced at 8 h after IP LPS in the group that received BMS-345541 compared with controls treated with vehicle, although no significant difference between the groups was identified at 4 h (Fig. 4, *A* and *B*). At the time of harvest (8 h), luciferase activity in lung homogenates was also significantly reduced in mice treated with BMS-345541 before LPS (1347 ± 51 RLU/μg protein in the BMS-345541 group vs 2089 ± 134 RLU/μg protein in the control vehicle-treated group, $p < 0.05$) (Fig. 4*C*). Neutrophil influx was quantified on lung sections as a measure of lung inflammation. As shown in Fig. 4*D*, a marked reduction in lung neutrophils was identified in lungs treated with BMS-345541 before LPS compared with controls treated with vehicle before LPS. These experiments indicate that treatment with BMS-345541 inhibits lung NF-κB activation and neutrophilic lung inflammation in response to IP LPS treatment.

Based on the differential NF-κB activation that we observed between the IP LPS and LPS pump treatment models, we investigated whether sustained lung NF-κB activation in the LPS pump model mediates lung injury. Therefore, we targeted the late phase of NF-κB activation by beginning BMS-345541 after the establishment of lung inflammation in NGL mice treated with LPS via osmotic pump. Mice were treated with BMS-345541 or vehicle by

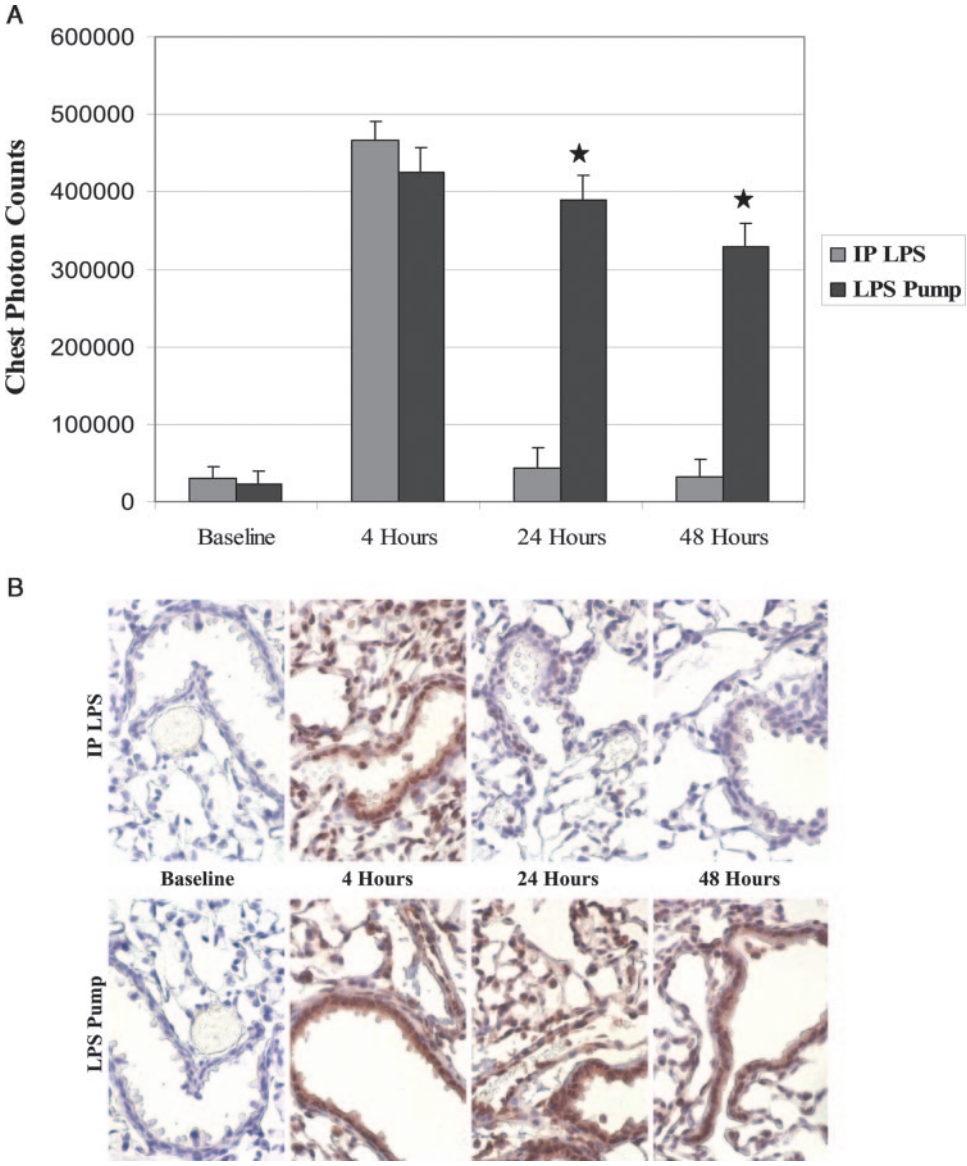

FIGURE 3. Differential NF-κB activation in lungs following a single i.p. dose of LPS (IP LPS) or LPS delivered by osmotic pump (LPS Pump) is identified by reporter gene expression in NGL mice. *A*, Bioluminescence imaging of NGL mice to determine luciferase activity in lungs at baseline, 4, 24, and 48 h after LPS delivered by single i.p. injection or LPS pump. Images were obtained after i.v. injection of 1 mg luciferin and photon detection was quantified over a standard region of the anterior chest corresponding to the mid-lung zones. Each bar represents the mean ± SEM (for $n = 6$ mice per group). ∗, $p < 0.05$ vs IP LPS. *B*, Representative immunohistochemistry for GFP^+ cells in lung sections from NGL mice.

peroral gavage beginning at 20 h after osmotic pump implantation. BMS-345541 dosing was repeated every 4 h for a total of five doses. Multiple doses were used because of the relatively short half-life of the compound in vivo (19). Bioluminescent imaging was performed at baseline, 20, 24, and 48 h after initiation of LPS to evaluate NF-κB-dependent reporter gene expression (Fig. 5, *A* and *B*). In both, vehicle or BMS-345541 treatment groups, similar induction of photon emission from the lungs was observed at 20 h, before intervention. By 24 h, there was a trend toward lower chest bioluminescence in the group treated with BMS-345541, and at 48 h, a marked reduction in photon emission from the lungs was observed in the group treated with BMS-345541 compared with vehicle-treated controls. Treatment with BMS-345541 resulted in ~50% reduction in chest bioluminescence compared with the measurement before treatment (20 h). These findings were confirmed by postmortem measurement of lung tissue luciferase activity. Luciferase activity in BMS-345541 treated mice was 1061 ± 233 RLU/μg protein compared with 2521 ± 462 RLU/μg protein in the vehicle-treated group ($p < 0.05$) (Fig. 5*C*). To show that treatment with BMS-345541 reduces IKK activation in the lungs, we performed Western blot analysis for IKK1 using Abs that specifically identify the phosphorylated (activated) kinase. Fig. 5*D* indicates that IKK1 phosphorylation was reduced in lungs treated with BMS-345541 at 48 h after LPS pump implantation. Therefore, oral delivery of the IKK inhibitor was sufficient to reduce IKK activity and thereby block NF-κB activation in the lungs.

To examine the impact of BMS-345541 therapy on the distribution of cells with active NF-κB, we performed immunostaining for GFP on lung tissue sections from NGL mice (Fig. 6). Interestingly, we found that BMS-345541 treatment broadly diminished GFP staining compared with vehicle-treated controls. Less GFP staining was observed in epithelium, endothelium, and leukocytes at 48 h after LPS pump implantation in BMS-345541-treated mice compared with vehicle-treated mice. By evaluation of H&E-stained lung sections, we observed a dramatic reduction in lung inflammation and injury in mice treated with the IKK inhibitor (Fig. 6). Mice treated with BMS-345541 showed preserved alveolar architecture with minimal edema, septal thickening, and hemorrhage.

To quantify lung inflammation and injury, we measured lung neutrophils, chemokine concentration in BAL fluid, and lung edema at 48 h after implantation of LPS pumps. Lung neutrophil influx was evaluated by counting of neutrophils on H&E lung tissue sections and by quantifying the number of neutrophils in BAL.

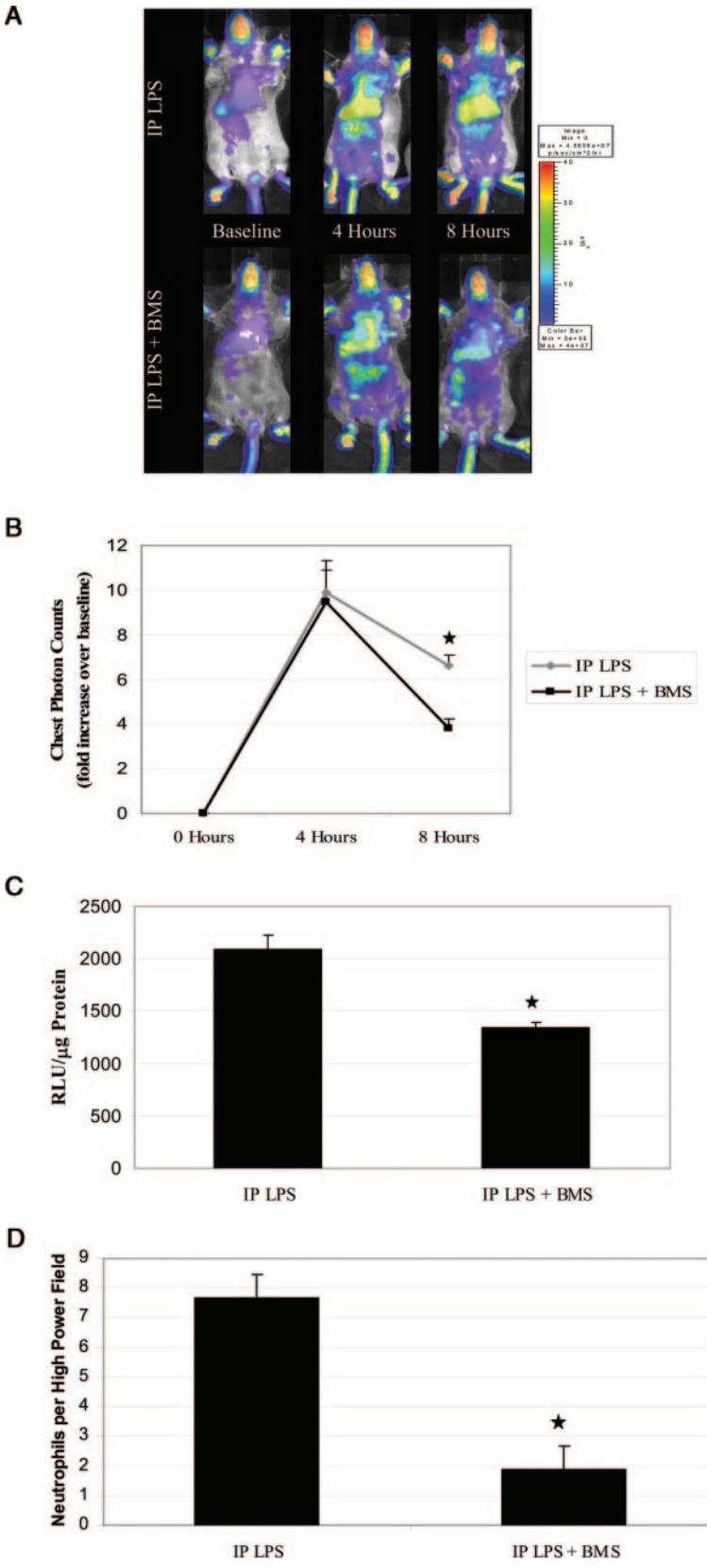

FIGURE 4. Treatment with the specific NF-κB inhibitor BMS-345541 results in decreased NF-κB activity and lung inflammation following a single i.p. dose of LPS. BMS-345541 or vehicle was delivered by gavage (75 μg/g) 2 h before and 4 h after i.p. injection of LPS (3 μg/g). *A*, Representative bioluminescence images of NGL mice obtained before LPS (0 h) and 4 and 8 h after i.p. dose of LPS (IP LPS). *B*, Quantification of chest photon emission from bioluminescence images (fold increase over baseline) (n = 6 mice). ∗, $p < 0.05$ vs IP LPS+BMS group. *C*, Luciferase activity measured in lung tissue homogenates at the time of harvest (RLU/μg protein) for $n = 6$ mice per group. ∗, $p < 0.05$). *D*, Measurement of neutrophils per high power field on H&E lung tissue sections. Each bar represents the mean ± SEM for $n = 6$ mice per group. ∗, $p < 0.05$.

A significant decrease in the number of neutrophils per high power field was detected on lung sections from BMS-345541-treated mice compared with vehicle treated mice (Fig. 7*A*). Similarly, a significant reduction of neutrophils was identified in BAL from mice treated with BMS-345541 (Fig. 7*B*). Because LPS-induced neutrophilic alveolitis in mice is largely determined by expression of the CXC chemokines MIP-2 and KC (23), we measured levels of these mediators in lung lavage fluid from mice treated with BMS-345541 or vehicle in addition to LPS pump treatment. BMS-345541 treatment resulted in deceased production of both MIP-2

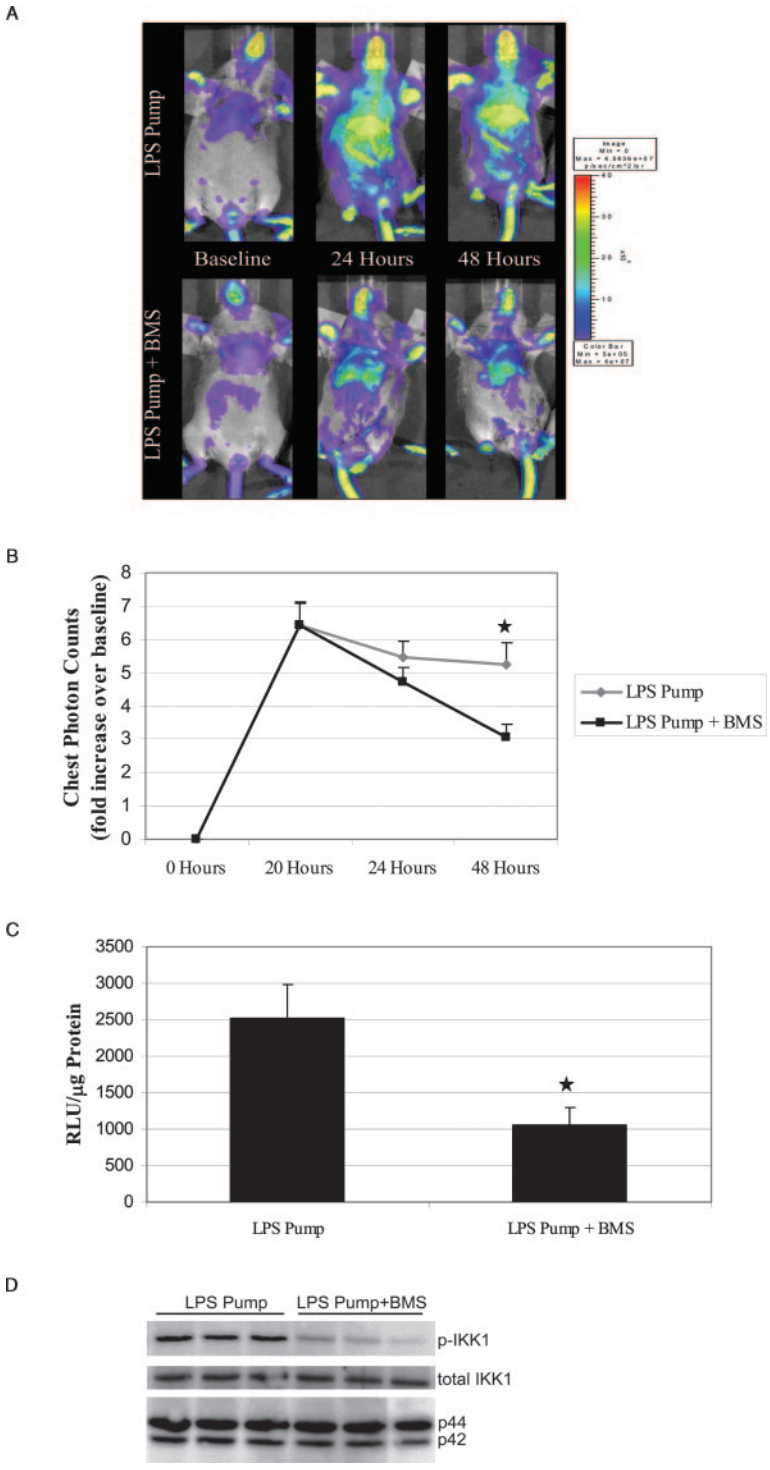

FIGURE 5. Treatment with BMS-345541 after the onset of inflammation in the LPS pump model reduces lung NF-κB activation. BMS-345541 or vehicle was delivered by gavage (75 μg/g) beginning at 20 h after LPS pump implantation and repeated every 4 h for total of five doses. *A*, Representative bioluminescence images of NGL mice obtained before LPS (0 h) and 24 and 48 h after implantation of osmotic pump (LPS Pump). *B*, Quantification of chest photon emission from bioluminescence images (fold increase over baseline) for $n = 12$ mice per group. *, $p < 0.05$ vs group treated with vehicle. *C*, Luciferase activity is measured in lung tissue homogenates at the time of harvest (RLU/μg protein). Each bar represents the mean ± SEM ($n = 12$ per group). *, $p < 0.05$. *D*, Western blot for phosphorylated IKK1 (p-IKK1) in lung tissue homogenates at 48 h after LPS pump implantation, normalized for total IKK1 and p44 and p42 MAPK. Each lane represents protein from a different mouse.

(127.4 ± 48.9 pg/ml in vehicle-treated mice vs 13.9 ± 3.7 pg/ml in BMS-345541-treated mice, $p < 0.05$) and KC (531.2 ± 34.0 pg/ml in vehicle-treated mice vs 21.6 ± 17.9 pg/ml in BMS-345541-treated mice, $p < 0.05$). Lung edema was evaluated by determining lung wet to dry ratio (Fig. 7*C*). The increased wet to dry ratio observed in vehicle-treated mice was completely ablated by BMS-345541 treatment, consistent with the histological improvement observed in the lungs of these mice. Together, these studies show that specific inhibition of NF-κB activation after establishment of lung inflammation reduces lung inflammation and prevents injury.

Neutrophil depletion reduces lung inflammation and injury

To evaluate whether reduction of neutrophil recruitment to the lungs accounts for prevention of lung injury resulting from NF-κB inhibition, we depleted neutrophils and determined the impact on LPS-induced lung inflammation and injury. Neutrophil depletion was achieved by repeated i.p. injection of antineutrophil Abs using a previously published protocol (16). After 4 daily injections of antineutrophil Abs, we detected an 80% reduction in peripheral neutrophil counts compared with mice treated with control IgG (Fig. 8*A*). After documenting PMN depletion, LPS pumps were

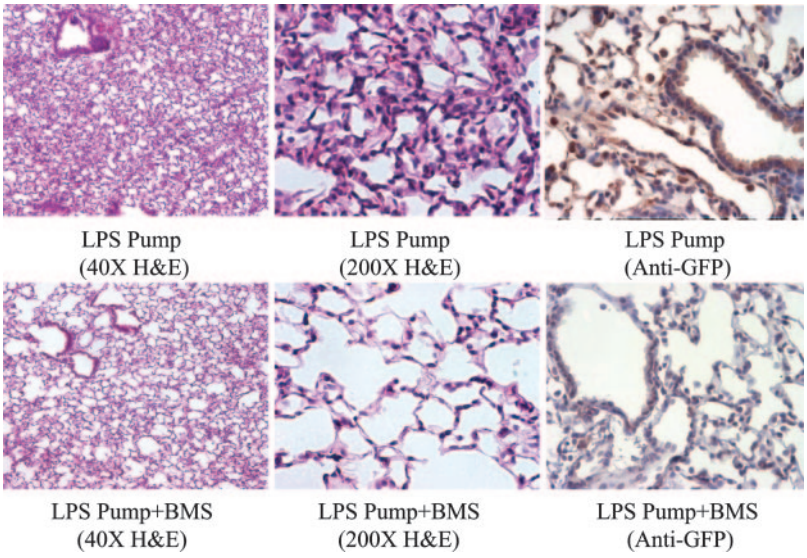

FIGURE 6. Treatment with NF-κB inhibitor after the onset of inflammation in the LPS pump model reduces lung inflammation and injury at 48 h. Representative H&E-stained lung sections were obtained from mice treated with BMS-345541 (LPS Pump+BMS) or vehicle (LPS Pump) in addition to LPS by osmotic pump. Immunohistochemistry for GFP demonstrates widespread reduction in NF-κB-driven reporter expression following treatment with BMS-345541.

implanted and bioluminescent detection of NF-κB-dependent luciferase expression was performed at 24 and 48 h (Fig. 8*B*). As shown, reduction of circulating neutrophils did not affect luciferase expression in NGL mice, implying that neutrophils do not make major contributions to the total lung NF-κB activation in this model. At 48 h, neutrophils were found to be reduced in BAL (Fig. 8*C*) and the lung wet-to-dry ratio was significantly decreased in neutrophil-depleted mice compared with IgG-treated controls (Fig. 8*D*). However, the wet-to-dry ratio in the lungs of neutrophil-depleted mice treated with LPS pump was significantly greater than the ratio in untreated controls, indicating that the achieved degree of neutrophil depletion was only partially effective in preventing lung edema formation. By histological examination of lung sections, mice treated with antineutrophil Abs were found to have a reduction in lung neutrophil influx with a mild diminution in edema and evidence of lung injury compared with IgG-treated controls (data not shown). Accounting for the reduction in neutrophils, immunohistochemistry for GFP did not show any differences in intensity or distribution of GFP staining in the lungs of mice treated with antineutrophil Abs or control IgG before LPS pumps.

Discussion

To comprehensively determine the extent of NF-κB activation in vivo, we developed a reporter system that allows identification of NF-κB-positive cells using GFP detection, as well as quantification of NF-κB activity in cells and tissue using luciferase detection methodologies. The NGL reporter construct was validated as an indicator of NF-κB activation in cell lines, primary cells from transgenic mice, and intact animals. Following a single i.p. injection of LPS, the time course for increased bioluminescence over the chest was similar to our previous report with NF-κB reporter mice that express luciferase under the control of the proximal promoter for the 5′ HIV-long terminal repeat (21).

LPS activates NF-κB in cells directly by interaction with cell surface molecules CD14 and TLR4. Although initial studies identified TLR4 on leukocytes, more recent studies have identified TLR4 expression in other cell types, including endothelium and bronchial epithelial cells, indicating that LPS may directly stimulate inflammatory signaling in a variety of cell types (24, 25). In addition to direct cellular effects, inflammatory signaling by LPS is amplified by rapid production and secretion of "proximal" cytokines, including TNF-α and IL-β, by macrophages. Through specific receptors, these molecules have the ability to activate NF-κB signaling and amplify the host inflammatory response. In NGL mice, we showed that NF-κB was efficiently activated throughout the lungs in response to systemic LPS. Within 4 h, most cells in the lungs were GFP^+; however, in the absence of continued activation, inflammation resolved without substantial tissue injury.

We evaluated NF-κB activation in the lungs in a model of transient lung inflammation (single-dose IP LPS treatment) and a model of LPS-induced lung inflammation that progresses to lung injury (LPS pump treatment). One limitation of previously reported models of LPS-induced lung inflammation in mice is that they produce relatively minor lung injury, even at near lethal doses; therefore, we chose to deliver LPS over 24 h by osmotic pump in a model that resembles subacute LPS release from i.p. infection. Using these two models, we observed clear differences in NF-κB activation. Like other parameters of the inflammatory response, NF-κB activation was transient in the IP LPS model but persisted in the LPS pump model up to 24 h after LPS delivery ceased. In the LPS pump model, obvious lung injury was present by 48 h after implantation of the osmotic pump. In our studies, mice were harvested at 48 h in the LPS pump model because substantial mortality was observed when mice were followed beyond this time point. The cellular distribution of NF-κB activation as measured by GFP^+ cells, and peak intensity of NF-κB activation as determined by bioluminescence imaging of luciferase activity did not differ between the IP LPS and LPS pump treatment models, indicating that these parameters are not the critical determinants of progression to lung injury. However, widespread sustained cellular activation of NF-κB correlated with lung injury.

To evaluate whether a causal relationship exists between sustained lung NF-κB activation and lung injury, we used a specific inhibitor of the NF-κB pathway. BMS-345541 is a selective inhibitor of the catalytic subunit of IKK2 (IC_{50} = 0.3 mM) and IKK1 (IC_{50} = 4 μM) through binding to an allosteric site (19). Peroral administration of BMS-345541 inhibits serum TNF-α production following LPS injection in a dose-dependent manner (19). Additional studies support the use of BMS-345541 as a selective NF-κB inhibitor and anti-inflammatory agent, including findings of reduced joint inflammation and destruction in a collagen-induced arthritis model, reduced severity

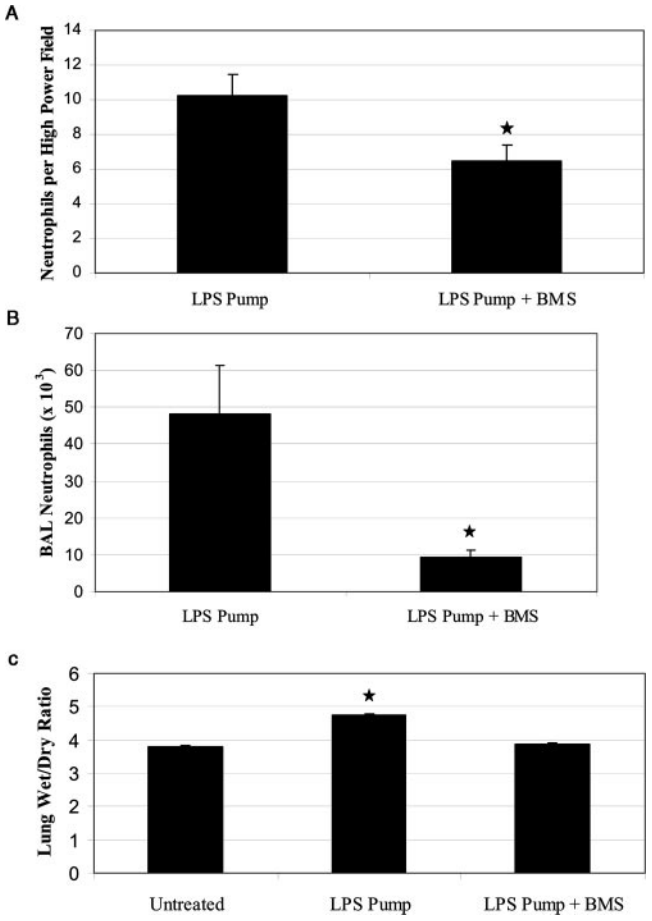

FIGURE 7. Treatment with NF-κB inhibitor decreases neutrophil influx into the lungs and eliminates lung edema in the LPS pump model. Lungs were harvested at 48 h after initiation of LPS treatment in mice treated with BMS-345541 (LPS Pump+BMS) or vehicle (LPS Pump). *A*, Quantification of lung neutrophils on H&E-stained lung sections for $n = 6$ mice per group. *, $p < 0.05$. *B*, Total neutrophils in BAL fluid for $n = 6$ mice per group. *, $p < 0.05$. *C*, Lung wet-to-dry ratio is represented. Each bar represents the mean ± SEM for $n = 6$ mice per group. *, $p < 0.05$ vs the other two groups.

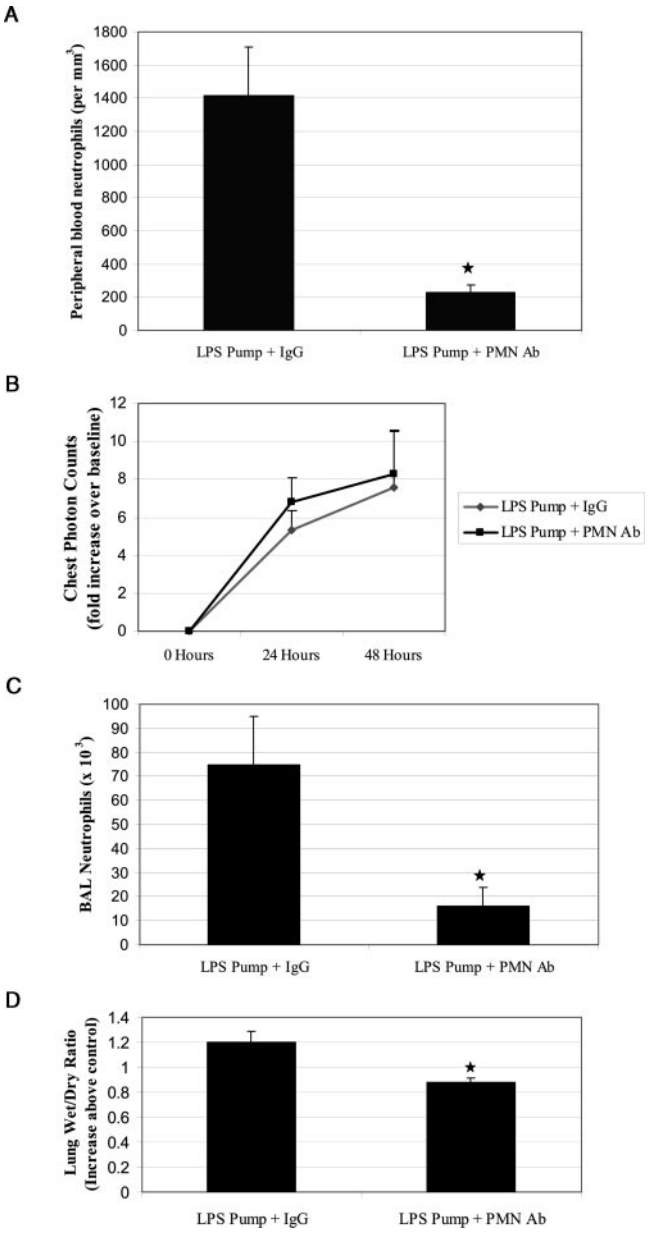

FIGURE 8. Neutrophil depletion reduces lung edema but not NF-κB activation in the LPS pump model. NGL mice were treated with antineutrophil Abs (PMN Ab) or control IgG before implantation of LPS pumps. Mice were harvested at 48 h. *A*, Peripheral blood neutrophils (PMN) were quantified after Ab treatment and before implantation of LPS pumps. *B*, Quantification of chest photon emission from bioluminescence images of mice at baseline, 24, and 48 h after LPS pumps. *C*, Total neutrophils in BAL fluid. *D*, Lung wet-to-dry ratio is reported as the increase above the mean value for an untreated control group. Each bar represents the mean ± SEM for $n = 5$ mice per group for each end point. *, $p < 0.05$ vs IgG control.

of colitis in a dextran sulfate sodium-induced colitis model, and improved graft survival in a murine model of cardiac graft rejection (22, 26, 27). In our experiments, we found that when administered before LPS, BMS-345541 treatment decreased NF-κB activation and neutrophilic lung inflammation measured at 8 h. Subsequently, we treated mice with BMS-345541 during the period when NF-κB activity was differentially up-regulated in the LPS pump model to investigate whether attenuation of NF-κB activation would convert this model of lung injury to one of transient inflammation. We initiated treatment with BMS-345541 at 20 h after LPS pump implantation. At the time of harvest, NF-κB activation, CXC chemokine production, and neutrophilic inflammation were markedly reduced in mice by BMS-345541 treatment. In addition, the histological appearance of lungs from BMS-345541-treated mice was improved and lung edema formation, as measured by wet-to-dry ratio, was eliminated. It appears that part of the benefit of NF-κB depletion results from reducing the neutrophil influx into the lungs consequent to LPS pump implantation. Activated neutrophils produce a variety of oxidants and proteases that have the potential to disrupt the alveolar-capillary barrier and contribute to lung injury (28). By treatment with antineutrophil Abs, we were able to reduce lung neutrophil influx (measured in BAL) to a similar degree as that achieved by treatment with the NF-κB inhibitor; however, the NF-κB inhibitor had a much more profound benefit in protecting from lung injury. These findings imply that NF-κB inhibition reduces lung injury in this model by reduction of neutrophil recruitment to the lungs and through other mechanisms (currently not well defined) that prevent disruption of the alveolar capillary barrier.

In contrast with our findings, a study by Lawrence et al. (15) found that NF-κB played opposing roles in the onset and resolution of inflammation in rat carrageenin pleurisy and mouse carrageenin air pouch models. Using nonspecific inhibitors, decreased NF-κB activation after establishment of inflammation was associated with protracted inflammation and prevention of leukocyte clearance, suggesting NF-κB may not be a suitable target for therapeutic intervention to limit and/or resolve established inflammation. Our findings, however, indicate that NF-κB could be an important target for limiting injury in the setting of ongoing inflammation in the lung parenchyma. The differences in our findings and those previously reported may be related to differences in the models of inflammation and/or the specificity of the agents used to inhibit the NF-κB pathway.

In humans, lung injury resulting from pneumonia, systemic infection, or trauma can cause ARDS (29, 30). The inflammatory phenotype associated with ARDS supports a role for NF-κB in the pathogenesis of this syndrome, including increased concentrations of a variety of NF-κB-linked cytokines and chemokines in BAL fluid from patients with ARDS (31–33). Increased concentration of the NF-κB-dependent CXC chemokine IL-8 correlates with neutrophilia in BAL, and prolonged neutrophilic alveolitis is associated with increased mortality in patients with ARDS (34–37). In addition, NF-κB activation has been identified in alveolar macrophages from humans with ARDS (38). Together, these data from human studies implicate the NF-κB pathway as a potentially important determinant of lung injury in humans with ARDS. Based on our findings in relevant rodent models of lung inflammation and injury, NF-κB may prove to be a beneficial target for therapeutic intervention to treat ongoing lung inflammation and prevent or limit lung injury. Although NF-κB inhibition has the potential to reduce lung injury, innate immune functions that depend on NF-κB may be required for adequate lung host defense against infection (39); therefore, application of these findings to human disease should proceed with caution. Hopefully, a better understanding of the intricacies of proinflammatory pathways that contribute to lung injury and host defense will lead to targeted therapies that limit injury while preserving lung defenses.

Disclosures

J. R. Burke is employed by Bristol-Myers Squibb Pharmaceutical Research Institute, the company that manufactured BMS-345541, which was used in these studies.

References

1. Blackwell, T. S., E. P. Holden, T. R. Blackwell, J. E. DeLarco, and J. W. Christman. 1994. Cytokine-induced neutrophil chemoattractant mediates neutrophilic alveolitis in rats: association with nuclear factor κB activation. *Am. J. Respir. Cell Mol. Biol.* 11: 464–472.
2. Haddad, E. B., M. Salmon, H. Koto, P. J. Barnes, I. Adcock, and K. F. Chung. 1996. Ozone induction of cytokine-induced neutrophil chemoattractant (CINC) and nuclear factor-κb in rat lung: inhibition by corticosteroids. *FEBS Lett.* 379: 265–268.
3. Shenkar, R., M. D. Schwartz, L. S. Terada, J. E. Repine, J. McCord, and E. Abraham. 1996. Hemorrhage activates NF-κB in murine lung mononuclear cells in vivo. *Am. J. Physiol.* 270: L729–L735.
4. Sacks, M., J. Gordon, J. Bylander, D. Porter, X. L. Shi, V. Castranova, W. Kaczmarczyk, K. Van Dyke, and M. J. Reasor. 1998. Silica-induced pulmonary inflammation in rats: activation of NF-κB and its suppression by dexamethasone. *Biochem. Biophys. Res. Commun.* 253: 181–184.
5. Browder, W., T. Ha, L. Chuanfu, J. H. Kalbfleisch, D. A. Ferguson, Jr., and D. L. Williams. 1999. Early activation of pulmonary nuclear factor κB and nuclear factor interleukin-6 in polymicrobial sepsis. *J. Trauma* 46: 590–596.
6. Mizgerd, J. P., J. J. Peschon, and C. M. Doerschuk. 2000. Roles of tumor necrosis factor receptor signaling during murine *Escherichia coli* pneumonia. *Am. J. Respir. Cell Mol. Biol.* 22: 85–91.
7. Mizgerd, J. P., M. R. Spieker, and C. M. Doerschuk. 2001. Early response cytokines and innate immunity: essential roles for TNF receptor 1 and type I IL-1 receptor during *Escherichia coli* pneumonia in mice. *J. Immunol.* 166: 4042–4048.
8. Sadikot, R. T., E. D. Jansen, T. R. Blackwell, O. Zoia, F. Yull, J. W. Christman, and T. S. Blackwell. 2001. High-dose dexamethasone accentuates nuclear factor-κB activation in endotoxin-treated mice. *Am. J. Respir. Crit. Care Med.* 164: 873–878.
9. Blackwell, T. S., J. P. Debelak, A. Venkatakrishnan, D. J. Schot, D. H. Harley, C. W. Pinson, P. Williams, K. Washington, J. W. Christman, and W. C. Chapman. 1999. Acute lung injury after hepatic cryoablation: correlation with NF-κB activation and cytokine production. *Surgery* 126: 518–526.
10. Blackwell, T. S., F. E. Yull, C. L. Chen, A. Venkatakrishnan, T. R. Blackwell, D. J. Hicks, L. H. Lancaster, J. W. Christman, and L. D. Kerr. 2000. Multiorgan nuclear factor κB activation in a transgenic mouse model of systemic inflammation. *Am. J. Respir. Crit. Care Med.* 162: 1095–1101.
11. Lauzurica, P., S. Martínez-Martínez, M. Marazuela, P. Gómez del Arco, C. Martínez-A, F. Sánchez-Madrid, and J. M. Redondo. 1999. Pyrrolidine dithiocarbamate protects mice from lethal shock induced by LPS or TNF-α. *Eur. J. Immunol.* 29: 1890–1900.
12. Liu, S. F., X. Ye, and A. B. Malik. 1999. Pyrrolidine dithiocarbamate prevents I-κB degradation and reduces microvascular injury induced by lipopolysaccharide in multiple organs. *Mol. Pharmacol.* 55: 658–667.
13. Blackwell, T. S., T. R. Blackwell, E. P. Holden, B. W. Christman, and J. W. Christman. 1996. In vivo antioxidant treatment suppresses nuclear factor-κB activation and neutrophilic lung inflammation. *J. Immunol.* 157: 1630–1637.
14. Alcamo, E., J. P. Mizgerd, B. H. Horwitz, R. Bronson, A. A. Beg, M. Scott, C. M. Doerschuk, R. O. Hynes, and D. Baltimore. 2001. Targeted mutation of TNF receptor I rescues the RelA-deficient mouse and reveals a critical role for NF-κB in leukocyte recruitment. *J. Immunol.* 167: 1592–1600.
15. Lawrence, T., D. W. Gilroy, P. R. Colville-Nash, and D. A. Willoughby. 2001. Possible new role for NF-κB in the resolution of inflammation. *Nat. Med.* 7: 1291–1297.
16. Abraham, E., A. Carmody, R. Shenkar, and J. Arcaroli. 2000. Neutrophils as early immunologic effectors in hemorrhage- or endotoxemia-induced acute lung injury. *Am. J. Physiol.* 279: L1137–L1145.
17. Sadikot, R. T., H. Zeng, F. E. Yull, B. Li, D. S. Cheng, D. S. Kernodle, E. D. Jansen, C. H. Contag, B. H. Segal, S. M. Holland, et al. 2004. p47^{phox} deficiency impairs NF-κB activation and host defense in *Pseudomonas* pneumonia. *J. Immunol.* 172: 1801–1808.
18. Sadikot, R. T., W. Han, M. B. Everhart, O. Zoia, R. S. Peebles, E. D. Jansen, F. E. Yull, J. W. Christman, and T. S. Blackwell. 2003. Selective IκB kinase expression in airway epithelium generates neutrophilic lung inflammation. *J. Immunol.* 170: 1091–1098.
19. Burke, J. R., M. A. Pattoli, K. R. Gregor, P. J. Brassil, J. F. MacMaster, K. W. McIntyre, X. Yang, V. S. Iotzova, W. Clarke, J. Strnad, et al. 2003. BMS-345541 is a highly selective inhibitor of IκB kinase that binds at an allosteric site of the enzyme and blocks NF-κB-dependent transcription in mice. *J. Biol. Chem.* 278: 1450–1456.
20. Rojas, M., C. R. Woods, A. L. Mora, J. Xu, and K. L. Brigham. 2005. Endotoxin-induced lung injury in mice: structural, functional, and biochemical responses. *Am. J. Physiol.* 288: L333–L341.
21. Yull, F. E., W. Han, E. D. Jansen, M. B. Everhart, R. T. Sadikot, J. W. Christman, and T. S. Blackwell. 2003. Bioluminescent detection of endotoxin effects on HIV-1 LTR-driven transcription in vivo. *J. Histochem. Cytochem.* 51: 741–749.
22. McIntyre, K. W., D. J. Shuster, K. M. Gillooly, D. M. Dambach, M. A. Pattoli, P. Lu, X.-D. Zhou, Y. Qiu, F. C. Zusi, and J. R. Burke. 2003. A highly selective inhibitor of IκB kinase, BMS-345541, blocks both joint inflammation and destruction in collagen-induced arthritis in mice. *Arthritis Rheum.* 48: 2652–2659.
23. Gonçalves, A. S., and R. Appelberg. 2002. The involvement of the chemokine receptor CXCR2 in neutrophil recruitment in LPS-induced inflammation and in *Mycobacterium avium* infection. *Scand. J. Immunol.* 55: 585–591.
24. Muir, A., G. Soong, S. Sokol, B. Reddy, M. I. Gomez, A. Van Heeckeren, and A. Prince. 2004. Toll-like receptors in normal and cystic fibrosis airway epithelial cells. *Am. J. Respir. Cell Mol. Biol.* 30: 777–783.
25. Fan, J., R. S. Frey, and A. B. Malik. 2003. TLR4 signaling induces TLR2 expression in endothelial cells via neutrophil NADPH oxidase. *J. Clin. Invest.* 112: 1234–1243.
26. MacMaster, J. F., D. M. Dambach, D. B. Lee, K. K. Berry, Y. Qiu, F. C. Zusi, and J. R. Burke. 2003. An inhibitor of IκB kinase, BMS-345541, blocks endothelial cell adhesion molecule expression and reduces the severity of dextran sulfate sodium-induced colitis in mice. *Inflamm. Res.* 52: 508–511.
27. Townsend, R. M., J. Postelnek, V. Susulic, K. W. McIntyre, D. J. Shuster, Y. Qiu, F. C. Zusi, and J. R. Burke. 2004. A highly selective inhibitor of IκB kinase, BMS-345541, augments graft survival mediated by suboptimal immunosuppression in a murine model of cardiac graft rejection. *Transplantation* 77: 1090–1094.
28. Matthay, M. A., and G. A. Zimmerman. 2005. Acute lung injury and the acute respiratory distress syndrome: four decades of inquiry into pathogenesis and rational management. *Am. J. Respir. Cell Mol. Biol.* 33: 319–327.
29. Kollef, M. H., and D. P. Schuster. 1995. The acute respiratory distress syndrome. *N. Engl. J. Med.* 332: 27–37.
30. Ware, L. B., and M. A. Matthay. 2000. The acute respiratory distress syndrome. *N. Engl. J. Med.* 342: 1334–1349.

31. Bhatia, M., and S. Moochhala. 2004. Role of inflammatory mediators in the pathophysiology of acute respiratory distress syndrome. *J. Pathol.* 202: 145–156.
32. Goodman, R. B., R. M. Strieter, D. P. Martin, K. P. Steinberg, J. A. Milberg, R. J. Maunder, S. L. Kunkel, A. Walz, L. D. Hudson, and T. R. Martin. 1996. Inflammatory cytokines in patients with persistence of the acute respiratory distress syndrome. *Am. J. Respir. Crit. Care Med.* 154: 602–611.
33. Schütte, H., J. Lohmeyer, S. Rosseau, S. Ziegler, C. Siebert, H. Kielisch, H. Pralle, F. Grimminger, H. Morr, and W. Seeger. 1996. Bronchoalveolar and systemic cytokine profiles in patients with ARDS, severe pneumonia and cardiogenic pulmonary oedema. *Eur. Respir. J.* 9: 1858–1867.
34. Miller, E. J., A. B. Cohen, S. Nagao, D. Griffith, R. J. Maunder, T. R. Martin, J. P. Weiner-Kronish, M. Sticherling, E. Christophers, and M. A. Matthay. 1992. Elevated levels of NAP-1/interleukin-8 are present in the airspaces of patients with the adult respiratory distress syndrome and are associated with increased mortality. *Am. Rev. Respir. Dis.* 146: 427–432.
35. Donnelly, S. C., R. M. Strieter, S. L. Kunkel, A. Walz, C. R. Robertson, D. C. Carter, I. S. Grant, A. J. Pollok, and C. Haslett. 1993. Interleukin-8 and development of adult respiratory distress syndrome in at-risk patient groups. *Lancet* 341: 643–647.
36. Baughman, R. P., K. L. Gunther, M. C. Rashkin, D. A. Keeton, and E. N. Pattishall. 1996. Changes in the inflammatory response of the lung during acute respiratory distress syndrome: prognostic indicators. *Am. J. Respir. Crit. Care Med.* 154: 76–81.
37. Steinberg, K. P., J. A. Milberg, T. R. Martin, R. J. Maunder, B. A. Cockrill, and L. D. Hudson. 1994. Evolution of bronchoalveolar cell populations in the adult respiratory distress syndrome. *Am. J. Respir. Crit. Care Med.* 150: 113–122.
38. Schwartz, M. D., E. E. Moore, F. A. Moore, R. Shenkar, P. Moine, J. B. Haenel, and E. Abraham. 1996. Nuclear factor-κB is activated in alveolar macrophages from patients with acute respiratory distress syndrome. *Crit. Care Med.* 24: 1285–1292.
39. Sadikot, R. T., H. Zeng, M. Joo, M. B. Everhart, T. P. Sherrill, B. Li, D.-S. Cheng, F. E. Yull, J. W. Christman, and T. S. Blackwell. 2006. Targeted immunomodulation of the NF-κβ pathway in airway epithelium impacts host defense against *Pseudomonas aeruginosa. J. Immunol.* In press.

Airway Epithelium Controls Development of Acute Lung Injury Through the NF-κB Pathway

Dong-sheng Cheng[1], Wei Han[1], Sabrina M. Chen[1], Taylor P. Sherrill[1], Melissa Chont[3], Gye-Young Park[5], James R. Sheller[1], Vasiliy V. Polosukhin[1], John W. Christman[4,5], Fiona E. Yull[3*], and Timothy S. Blackwell[1-4*]

[1]Department of Medicine, Division of Allergy, Pulmonary and Critical Care Medicine,
[2]Department of Cell and Developmental Biology
[3]Department of Cancer Biology
Vanderbilt University School of Medicine, Nashville, TN
[4]Department of Veterans Affairs
[5]Section of Pulmonary, Critical Care, and Sleep Medicine, University of Illinois, Chicago, IL.

Address correspondence to:
Timothy S. Blackwell, M.D.
Associate Professor of Medicine
Associate Director of Research, Division of Allergy, Pulmonary
and Critical Care Medicine
Associate Professor of Cell and Developmental Biology
Vanderbilt University School of Medicine
T-1218 MCN
Nashville, TN 37232-2650

phone: 615-322-3412
fax: 615-322-2582
email: timothy.blackwell@vanderbilt.edu

Supported by: NIH HL61419, HL66196, HL 07123, the U.S. Department of Veterans Affairs, Vanderbilt Ingram Cancer Center, Susan G Komen Foundation grant BCTR02-1728 and Department of Defense Breast Cancer Program grant WX1XWH-04-1-0456

* These authors contributed equally to this manuscript.

Key words: transgenic, cytokine, neutrophil, acute respiratory distress syndrome

Abstract

To investigate the role of airway epithelium in regulating lung inflammation and injury, we used a tetracycline-inducible system to achieve selective NF-κB activation or inhibition in airway epithelial cells *in vivo*. In transgenic mice that express a constitutively active form of IκB kinase 2 under control of the CC10 promoter, treatment with doxycycline (dox) induces NF-κB activation with consequent up-regulation of pro-inflammatory cytokines, pulmonary edema, and neutrophilic alveolitis. Continued treatment with dox causes progressive lung injury, hypoxemia, and high mortality. In contrast, dox-inducible expression of a dominant inhibitor of NF-κB in airway epithelium prevents lung injury and death in a model of systemic endotoxemia in which *E. coli* endotoxin is delivered via osmotic pump implanted in the peritoneal cavity. Therefore, airway epithelium critically regulates lung injury through the NF-κB pathway and may represent an important target for therapies designed to improve outcomes from the acute respiratory distress syndrome.

Innate immunity is critical for host defense against bacterial pathogens, but dysregulated or exaggerated immune responses can result in tissue injury. In the lungs, this form of host-derived tissue injury characterizes the acute respiratory distress syndrome (ARDS). ARDS is a common cause of morbidity and mortality in critically ill patients, resulting from local or systemic infection, trauma or other inflammatory/injurious stimuli[1,2]. The inflammatory phenotype underlying the pathogenesis of ARDS includes neutrophilic alveolitis and increased levels of a number of cytokines and chemokines in the airways[1,3]. Improved understanding of critical cell types and biological pathways that regulate innate immunity in the lungs could be useful in designing therapies to limit or prevent lung injury in patients at risk for ARDS.

The ubiquitous NF-κB pathway regulates transcription of important pro-inflammatory cytokines, chemokines, adhesion molecules, and enzymes[4,5]. Following cell stimulation, inhibitors of NF-κB (IκBs) are phosphorylated on serine residues in the amino-terminus by IκB kinase 2 (IKK2), targeting them for destruction by the ubiquitin/proteasome (26S) degradation pathway[6]. IκB degradation allows NF-κB nuclear translocation and transcriptional activation of target genes. In the lungs, many noxious/inflammatory stimuli have been shown to activate NF-κB, including bacterial products, ozone and silica, as well as systemic inflammatory insults such as sepsis, trauma, and hemorrhage.

Airway epithelium provides a physical border between host and environment that protects from injurious and infectious stimuli that gain access to the respiratory tract through inspiration or aspiration. Well recognized functions of airway epithelium include mechanical clearance of offending agents and production of antimicrobial agents; however, a crucial role for airway epithelium in coordinating the innate immune response in the lungs has not been elucidated. Airway epithelial cells express a number of toll-like receptors and we have recently

shown that local and systemic inflammation results in prominent activation of the NF-κB pathway in these cells[7-9]. Therefore, we hypothesized that epithelial cells in the lung are important for transducing NF-κB dependent inflammatory signals and that prolonged NF-κB activation in airway epithelial cells leads to a dysfunctional (injurious) inflammatory response culminating in lung injury. To evaluate whether airway epithelial cells critically regulate lung inflammation and injury, we generated inducible transgenic mice that express an activator or dominant inhibitor of the NF-κB pathway in CC10 expressing epithelial cells. We then determined the effects of cell type-specific NF-κB activation or inhibition on parameters of lung inflammation and injury. Our data indicate that activation of NF-κB in airway epithelial cells is sufficient for generating full-blown acute lung injury and is necessary for mediating the pulmonary effects of endotoxemia.

Results

Construction of transgenic mice with inducible activation of NF-κB in airway epithelium.

To achieve inducible NF-κB activation using the tet-on system, we placed a FLAG-tagged constitutively active mutant form of human IκB kinase 2 (cIKK2)[6] under the control of the (tet-O)$_7$-CMV promoter (**Fig. 1a**). To prevent basal leakiness of transgene expression, a construct expressing tetracycline-controlled transcriptional silencer (tTS) under the control of the Clara cell specific CC10 promoter (obtained from Dr. Jack Elias, Yale University, with permission of Andrew Farmer, BD Clontech, Palo Alto, CA) was co-injected with (tet-O)$_7$-FLAG-cIKK2 to generate double transgenic mice. Unbound tTS interacts with tet-O sites and functions as a transcriptional repressor; however, binding of dox to tTS results in dissociation from DNA, allowing rtTA binding and promoter activation[10-12]. Double transgenic mice were bred with transgenic mice expressing rtTA under the control of the rat CC10 promoter (obtained from Dr. Jeffrey Whitsett, Univ. of Cincinnati) to generate triple transgenic mice, designated IKTA (for cIKK2 TransActivated).

In initial experiments, IKTA transgenic mice were treated with dox in drinking water (2 g/l) for 3 days. Western blots for the FLAG-tagged transgene product identified cIKK2 expression exclusively in the lungs of dox-treated IKTA mice (**Fig. 1b**). No leakiness of FLAG-cIKK2 expression was detectable in other tissues following dox treatment or in the lungs in the absence of dox. By immunohistochemistry, FLAG-cIKK2 expression was localized to the airway epithelium (**Fig. 1c**). We investigated whether FLAG-cIKK2 expression in airway epithelium was sufficient to activate NF-κB by performing electrophoretic mobility shift assays using lung tissue nuclear protein extracts. Compared to controls, NF-κB activation was increased in lungs of dox-treated IKTA mice (**figure 1d**). Together, these data show that

treatment of IKTA mice with dox induces expression of FLAG-cIKK2 exclusively in airway epithelial cells at levels sufficient to activate NF-κB.

Sustained NF-κB activation in airway epithelium results in neutrophilic lung inflammation and severe lung injury.

Although untreated IKTA mice exhibited normal lung histology, IKTA mice showed progressive lung inflammation and injury after 3 and 7 days of dox treatment (**Fig. 2a**). After 3 days of dox treatment, lungs from IKTA mice showed evidence of edema and a cellular infiltrate consisting of neutrophils and macrophages. By 7 days of dox treatment, however, a massive infiltration of inflammatory cells into the lung parenchyma was present, along with septal thickening, edema, and alveolar hemorrhage. Other organs, including liver, spleen and kidney, showed no evidence of inflammation or architectural abnormalities (not shown).

By lung lavage, increased numbers of neutrophils and macrophages were identified in the airways of IKTA mice at 3 days after introduction of dox (**Fig. 2b**). After 7 days of dox treatment, increased numbers of neutrophils, macrophages, and lymphocytes were present in lung lavage from IKTA mice compared to dox-treated wild-type (WT) mice, and neutrophils were further elevated compared to IKTA mice treated with dox for 3 days. We measured protein concentration in lung lavage from IKTA mice and WT controls at baseline and after dox treatment as an indicator of vascular permeability (**Fig. 2c**). Compared to baseline, protein concentration in IKTA mice increased 3-fold by 3 days of dox treatment, and by day 7 of dox treatment protein concentration had increased >10-fold above baseline. Lung lavage protein concentration was similar in untreated WT and IKTA mice and did not change in WT mice

following dox treatment. Consistent with these results, wet/dry ratios were increased in dox-treated IKTA mice treated with dox for 3 days compared to controls (**Fig. 2d**).

Activation of NF-κB in airway epithelium resulted in production of a variety of inflammatory mediators. **Table 1** shows the profile of cytokines and chemokines up-regulated in lung lavage from IKTA mice treated with dox for 7 days compared to dox-treated WT mice and IKTA mice without dox treatment. Significantly increased levels of IL-1α, IL-1β, IL-5, IL-6, IL-12, IL-17, RANTES, MIP-2, KC, MCP-1 and G-CSF were observed in dox-treated IKTA mice. No differences in mediator production were identified between WT mice and IKTA mice in the absence of dox treatment. We used multiprobe ribonuclease protection assays to confirm that mRNA expression of selected chemokines was increased in the lungs of dox-treated IKTA mice (**Supplemental Fig. 1**). Protein and mRNA measurements of mediators correlated well with the exception of MCP-1, which was increased in lung lavage fluid by Luminex assay but increased mRNA expression was not identified in the lungs at this time point. Together, these studies show that sustained activation of NF-κB in IKTA mice (in the absence of a specific inflammatory stimulus) results in a pattern of progressive lung inflammation and injury associated with production of a number of NF-κB dependent cytokines and chemokines.

To determine which inflammatory mediators are produced directly by airway epithelial cells following NF-κB activation, we harvested mouse tracheal epithelial cells (MTEC) and grew them in air-liquid interface conditions to obtain highly differentiated airway epithelium (**Supplemental Fig. 2a**)[13]. Cultures of MTEC cells from IKTA mice were treated with dox (0.5 μg/ml) for 48 hours and transgene induction was identified by immunofluorescent staining of FLAG-cIKK2 (**Supplemental Fig. 2b**). Increased concentrations of IL-6, G-CSF, GM-CSF, MIP-2, KC, and RANTES were identified in cell culture supernatants of dox-treated IKTA cells

compared to IKTA cells in the absence of dox (**Supplemental table 1**). These findings suggest that direct NF-κB activation in airway epithelial cells is sufficient to produce a number of mediators, including IL-6, G-CSF, MIP-2, KC and RANTES, that are increased in the lungs of dox-treated IKTA mice. Other mediators that are increased in lung lavage fluid from dox-treated IKTA mice, such as IL-1α, IL-1β, and IL-12p40, may be up-regulated indirectly through recruitment or activation of inflammatory cells in the lungs.

We sought to determine the physiological effects of lung inflammation/injury resulting from epithelial NF-κB activation in IKTA mice by measuring arterial PO_2. Serial arterial blood gas analysis was done with indwelling carotid artery catheters in unanesthetized IKTA mice treated with dox (**Fig. 3a**). Baseline PO_2 (123.9 ± 4.67 mmHg) and PCO_2 (20.1 ± 0.93 mmHg) in IKTA mice were similar to WT controls (data not shown). With continued dox treatment, arterial PO_2 in IKTA mice decreased to 50.3 ± 2.81 mmHg by day 7 and PCO_2 increased to 30.5 ± 4.33 mmHg. Arterial oxygen saturation decreased from 99 ± 0.1% at baseline to 81±2.7% after 7 days of dox treatment in IKTA mice ($p<0.001$). WT controls with indwelling carotid artery catheters treated with dox for 1 week did not show any changes from baseline in arterial PO_2, PCO_2, or arterial oxygen saturation (not shown).

Continued dox treatment resulted in substantial mortality in IKTA mice between 1 and 2 weeks (**Fig. 3b**). In 2 separate lines of IKTA mice, mortality rates of 60 and 70% were found by 2 weeks of dox treatment, whereas no mortality was observed in WT control mice treated with dox for 2 weeks. Taken together, these studies demonstrate that persistent induction of NF-κB in airway epithelial cells is sufficient to cause lung inflammation and injury. Lung injury in this model results in progressive hypoxemia with a high mortality rate.

Construction and characterization of transgenic mice that express a dominant inhibitor of NF-κB in airway epithelium.

We placed a Myc-His tagged dominant inhibitor of the NF-κB pathway (IκB-αDN) under control of the $(tet\text{-}O)_7$-CMV promoter (**Fig. 4a**). IκB-αDN is an avian IκB-α with adenine substitutions at serines 36 and 40 that inhibit phosphorylation and degradation of the protein, therefore blocking NF-κB nuclear translocation[8,14,15]. Double transgenic mice containing $(tet\text{-}O)_7$-IκB-αDN-Myc-His and CC-10-tTS constructs were produced and cross-mated with CC10-rtTA mice to create triple transgenic mice with inducible expression of IκB-αDN-Myc-His in airway epithelium, designated DNTA (for IκB-αDN TransActivated). As with IKTA mice, dox treatment resulted in transgene expression exclusively in the lungs (**Fig. 4b**). No leakiness of transgene expression was identified in the absence of dox. Immunohistochemistry for the Myc tag on IκB-αDN localized transgene expression to the airway epithelium in dox-treated mice (not shown). Lungs of dox-treated DNTA mice were histologically normal.

To show that IκB-αDN expression was sufficient to block NF-κB activation in DNTA mice, we crossed IKTA and DNTA mice to obtain mice that inducibly expressed both transgenes (cIKK2 and IκB-αDN-Myc-His). **Figure 4c** shows that dox treatment of these mice (IKDNTA) results in suppression of lung inflammation induced by cIKK2. These experiments indicate that expression of IκB-αDN in epithelium inhibits NF-κB activation and confirm that cIKK2-induced lung inflammation is transduced through activation of the NF-κB pathway.

Prevention of acute lung injury by blocking NF-κB activation in airway epithelium.

We investigated whether blocking NF-κB activation in airway epithelium could reduce lung injury resulting from delivery of *E. coli* endotoxin (lipopolysaccharide, LPS) (8 μg/hour)

into the peritoneum over 24 hours via a surgically implanted osmotic pump[9]. We have recently reported that this model results in persistent lung NF-κB activation that prominently involves airway epithelium[9]. For these studies, we treated WT or DNTA mice with dox for 1 week, followed by implantation of the LPS pump. At 4 hours after osmotic pump implantation, NF-κB activation was reduced in DNTA mice as indicated by western blots for RelA in lung nuclear protein extracts (**Fig. 5a**). At 48 hours after implantation, WT mice exhibited histological evidence of lung injury with edema and inflammatory cell influx, which was markedly reduced in DNTA mice (**Fig 5b**). Consistent with these findings, lung lavage neutrophils were reduced in DNTA mice (**Fig. 5c**). In addition, total lung lavage cells were lower in dox-treated DNTA mice than controls at 48 hours after placement of LPS pumps ($16.5 \pm 1.6 \times 10^4$ cells in DNTA mice compared with $35.0 \pm 4.6 \times 10^4$ cells in WT mice, $n = 10$ per group, $p<0.01$). Evidence of lung injury was reduced in dox-treated DNTA mice as indicated by a reduction in lung wet/dry ratio and lung lavage protein concentration compared to dox-treated WT mice (**Figs. 5d and 5e**). WT and DNTA mice treated with LPS pumps in the absence of dox treatment showed lung inflammation and wet/dry ratios that were similar to dox-treated WT mice (data not shown). No differences in peripheral white blood cell counts were identified between WT or DNTA mice (with or without dox) at baseline, 4 hours, or 48 hours after placement of LPS pumps (data not shown).

We performed multiplex cytokine analysis to evaluate the effects of epithelial NF-κB inhibition on the mediator profile in lung lavage fluid obtained at the time of harvest (**Supplemental table 2**). Levels of MIP-2 and KC were lower in dox-treated DNTA mice than in dox-treated WT mice, consistent with the reduced neutrophilic lung inflammation observed in

these mice. Other mediators reduced in DNTA mice included RANTES, MIP-1β, MCP-1, G-CSF and GM-CSF.

To determine whether reduced lung injury in DNTA mice could lead to improved survival, we performed peritoneal implantation of osmotic pumps that deliver LPS (8 μg/hour) for 72 hours into dox-treated WT and DNTA mice. As shown in **figure 5f**, delivery of LPS over 72 hours resulted in 50% mortality in WT mice at day 7; however, DNTA mice were completely protected. Together, these experiments show that expression of a dominant inhibitor of the NF-κB pathway in airway epithelium blocks acute lung injury and improves survival from systemic endotoxemia. Therefore, persistent activation of the NF-κB pathway in airway epithelial cells is not only sufficient to produce lung injury but is also a focal point for controlling acute lung injury in the clinically relevant setting of endotoxemia.

Discussion

These studies define a pivotal role for the NF-κB pathway in lung inflammation and injury. Persistent expression of cIKK2 in epithelial cells, in the absence of an additional stimulus, induces cytokine expression, inflammatory cell recruitment, lung injury, hypoxemia, and death. Lung histopathology in this model largely recapitulates the findings in patients with ARDS. Studies in transgenic mice cross-bred to express both cIKK2 and IκB-αDN, which functions downstream of cIKK2, support the conclusion that the phenotype observed in dox-treated IKTA mice is directly related to activation of the NF-κB pathway in epithelial cells. Dox treatment of cultured tracheal epithelial cells from IKTA mice up-regulates expression of a group of cytokines and chemokines that are found in the lungs of dox-treated IKTA mice, indicating airway epithelium as a source for these mediators. In addition to direct effects of cIKK2 expression in airway epithelium, recruitment and activation of inflammatory cells (particularly neutrophils and macrophages) likely contribute to the mediator profile identified in lung lavage of IKTA mice and participate in lung injury. In IKTA mice, lung inflammation and injury are progressive. Evidence of inflammation and edema are present by 3 days of dox treatment, followed by impaired gas exchange and death after as little as 7 days of dox treatment. Since the onset of detectable transgene expression occurs by 24-48 hours after adding dox to drinking water (data not shown), induction of lung injury in dox-treated IKTA mice occurs in a time frame similar to that observed in our endotoxemia model. Systemic delivery of LPS via intraperitoneal osmotic pump results in neutrophilic lung inflammation and edema, both of which were markedly reduced in DNTA mice. Together, our studies indicate that prolonged activation of NF-κB in airway epithelium is necessary and sufficient to produce progressive lung injury.

While much attention has been focused on the NF-κB pathway in immune cells, prior investigations have suggested that activity of the NF-κB pathway in epithelial cells can impact organ inflammation and injury. In the lungs, expression of NF-κB activating transgenes delivered by adenoviral vectors to airway epithelial cells results in acute neutrophilic inflammation[14]. Transgenic mice expressing a dominant inhibitor of the NF-κB pathway in CC10 expressing airway epithelial cells or surfactant protein C expressing distal epithelial cells exhibit decreased neutrophilic lung inflammation in response to airway instillation of *E. coli* LPS[16,17]. In the gastrointestinal tract, selective deletion of IKK2 in intestinal epithelial cells impairs NF-κB activation and results in decreased lung and systemic inflammation in a gut ischemia-reperfusion model through reduction of TNFα expression[18]. However, local tissue injury in the intestinal mucosa was exacerbated in this model related to increased apoptosis. In combination with the present study, these findings point to the NF-κB pathway in epithelial cells as an important target for therapies designed to modulate inflammation-induced tissue injury.

In humans with ARDS, evidence supports the role of NF-κB dependent mediators in inducing lung injury, although the cellular source of these mediators is not well defined. A variety of NF-κB linked cytokines and chemokines has been reported to be increased in lung lavage fluid obtained from patients with ARDS, including TNFα, IL-1β, IL-6, and IL-8 [3,19,20]. Increased concentrations of IL-8, the predominant CXC chemokine in humans, are found in lung lavage of at-risk patients who progress to ARDS, and high levels of IL-8 and neutrophils in lung lavage have been correlated with increased mortality in ARDS patients[21-23]. Our mouse model indicates that prolonged activation of NF-κB is sufficient to produce an inflammatory profile similar to human ARDS, as well as the pathophysiological and histological abnormalities. These

findings solidify the NF-κB pathway as an important therapeutic target for interventions targeted to limit lung injury in ARDS.

In summary, our findings implicate the NF-κB pathway in airway epithelial cells in lung injury. Persistent NF-κB activation in epithelium may drive the dysregulated inflammatory response that culminates in ARDS. While interventions that reduce inflammation by blocking NF-κB activation in epithelium must be rigorously examined to define their effects on host defense, the airway epithelium may prove to be an important and feasible target for reducing or preventing lung injury in patients at risk for ARDS.

Methods

Transgenic mouse models.

IKTA transgenic mice: The pBSIIFlag-IKK2 plasmid containing FLAG-cIKK2, a constitutively active form of human IKK2 containing S177E, S181E mutations, was a gift of Dr. Frank Mercurio (Signal Pharmaceutical, San Diego, CA). This plasmid was digested with BssH II to obtain a fragment containing the FLAG-IKK2. The ends of this fragment were filled in prior to ligation into the EcoRV site of a modified pBluescript II SK expression vector (pBSII KS/Asc). This vector contains a $(tet\text{-}O)_7$-CMV promoter that consists of seven copies of the tet operator DNA binding sequence linked to a minimal CMV promoter together with bovine growth hormone polyadenylation sequences to ensure transcript termination. The final plasmid ($(tet\text{-}O)_7$-FLAG-cIKK2-BGH.polyA) was verified by sequencing. To prevent basal leakiness, we used a construct expressing a tetracycline-controlled transcriptional silencer (tTS) under control of the CC10 promoter (CC10-tTS-hGH-polyA)[12]. The $(tet\text{-}O)_7$-FLAG-cIKK2 microinjection fragment was excised from the plasmid as a 3.3kb XmnI-AscI fragment. We purified both CC10-tTS and $(tet\text{-}O)_7$–FLAG-cIKK2 constructs using a GELase™ Agarose Gel-Digesting preparation kit following the manufacturer's instruction (Epicentre, Madison, WI), and these constructs were co-injected at the Vanderbilt transgenic/ES cell shared resource to generate transgenic lines of mice (FVB background) that have co-integrated both the CC10-tTS and $(tet\text{-}O)_7$-FLAG-cIKK2 transgenes. Genotyping of founder animals was performed by Southern Blot and later stages of genotyping were performed by PCR analysis. Primers used for PCR of the $(tet\text{-}O)_7$-FLAG-cIKK2 transgene are as follows: 5'-primer (located in the CMV minimal promoter) 5'-GAC GCC ATC CAC GCT GTT TTG-3'; 3' primer (located in the cIKK2 coding region) 5'-CTT CTC ATG ATC TGG ATC TCC-3'. The product size is 452 bp. Primers used

for identification of cc10-tTS transgene are as follows: upstream 5'- GAG TTG GCA GCA GTT TCT CC-3'; downstream 5'-GAG CAC AGC CAC ATC TTC AA-3'. The product size is 472 bp. PCR protocols for both $(tet\text{-}O)_7$-FLAG-cIKK2 and CC10-tTS were: 1 cycle 94ºC for 2 min; 30 cycles at 94ºC for 1 min, 56ºC for 30 seconds and 72ºC for 1 min; and 1 cycle at 72ºC for 10 min. Mice transgenic for CC10-tTS/$(tet\text{-}O)_7$-FLAG-cIKK2 were mated with cc10-rTTA homozygous mice (gift from Dr. Jeffrey A. Whitsett, University of Cincinnati) to obtain transgenic mice carrying all three transgenes, designated IKTA mice. IKTA mice from 3 separate founder lines were used for these studies.

DNTA transgenic mice: In order to tag the IκB-α dominant inhibitor (IκB-αDN)[8,14,15], a 1.35kb BamHI/DraI fragment was excised from pCMX-pp40 and blunt-end ligated into BamHI/EcoRV digested pEF4/Myc-HisA (Invitrogen Corp, CA). The IκB-αDN-Myc-His tagged fragment was then excised by BamHI digest, fill-in of the overhanging ends and Pme I digestion. The resulting fragment was blunt-end ligated into the pBSII KS/Asc vector described above which had been PstI digested and filled in. Plasmid constructs were verified by sequencing. A 2.1 kb AscI microinjection fragment was prepared and co-injected with the CC10-tTS microinjection fragment as described above at the Vanderbilt transgenic/ES cell shared resource to generate transgenic lines of mice (FVB background) that have co-integrated both the CC10-tTS and $(tet\text{-}O)_7$-IκB-αDN-Myc-His transgenes. Genotyping of founder animals was performed by Southern Blot and later stages of genotyping were performed by PCR analysis. Primers used for PCR of the $(tet\text{-}O)_7$-IκB-αDN-Myc-His transgene are as follows: sense-primer 5'- TGA GGA TGA GGA GAG CAG TGA ATC -3'; antisense primer 5'- CAC CCC CCA GAA TAG AAT GAC AC -3'. The product size is 422 bp. Primers used for identification of CC10-tTS transgene (as above). PCR protocols for $(tet\text{-}O)_7$-IκB-αDN-Myc-His was: 1 cycle 95ºC for 4 min; 30 cycles

at 95ºC for 30 secs, 55ºC for 30 seconds and 72ºC for 1 min; and 1 cycle at 72ºC for 10 min. Mice transgenic for CC10-tTS/(tet-O)$_7$-IκB-αDN-Myc-His were mated with CC10-rTTA homozygous mice to obtain transgenic mice carrying all three transgenes, designated DNTA mice. DNTA mice from two separate founder lines were used for these studies.

Doxycycline (dox) treatment: All IKTA or DNTA mice (or appropriate controls) were maintained on normal water until transgene activation was desired. At that time, 2 g/l of freshly prepared dox (Sigma) was added to the animals' drinking water. 2% sucrose was also added to decrease the bitter taste of dox water. The bottle with dox and 2% sucrose water was wrapped with foil to prevent light-induced dox degradation and dox water was replaced twice per week.

LPS pump model. Male and female mice weighing between 20-25 grams were used for these studies. *Escherichia coli* LPS (serotype 055:B5) was obtained from Sigma-Aldrich (St. Louis, MO). LPS was delivered by an osmotic pump (2001D Alzet pump, Alza Corporation, Palo Alto, CA) filled with LPS solution (1 μg/μl in PBS) and surgically implanted in the peritoneal cavity using sterile technique. The pump delivered 8 μg LPS (8 μl) per hour for 24 hours. In some experiments, osmotic pumps (1003D) were used. These pumps were filled with LPS solution (8 μg/μl in PBS) to deliver 8 μg per hour (1 μl/hour) over 72 hours. A priming dose of 3 μg LPS per gram body weight was injected IP following pump implantation.

Implantation of carotid artery catheter and blood gas analysis. The common carotid artery was separated from the vagus nerve and muscle, and then two 6-0 silk threads were passed under the artery. The cephalic thread was tied to prevent bleeding and then the artery was clamped by

small bulldog clamp. A small incision was made just below the ligature and the catheter was inserted into the lumen. The clamp was taken off and the catheter was pushed in 10 mm. The catheter was fixed with a second thread and the thread previously used to prevent bleeding. A blunt 16 gauge needle was carefully inserted through the incision and pushed subcutaneously until the end protruded through the incision in the neck. The incision in the skin was then sutured and the catheter was connected to a stainless steel tube. The implanted catheter was flushed with saline containing 200 IU heparin/ml and 1 mg ampicillin/ml every day. For blood gas analysis, 100 µl of arterial blood was collected via the catheter and immediately placed in ice. Blood gas analysis was done using an ABL-5 blood gas machine (Radiometer America, Westlake, OH) at 37 °C. Prior to each measurement, the blood gas machine was calibrated with a standard solution.

Lung histology and immunohistochemistry. Lungs were inflated and fixed with 1 ml of 10% formalin and then were removed en bloc after tracheal ligation. For immunohistochemical analysis, 5 um paraffin sections were deparaffinized, dehydrated, washed with PBS, treated with 0.05% trypsin and incubated with 1% bovine serum albumin in PBS for 20 min. prior to incubation with rabbit polyclonal anti-FLAG antibody (Rockland Inc., Gilberstville, PA) or rabbit polyclonal anti-myc antibody (Santa Cruz Biotechnology, Santa Cruz, CA). After incubation with primary antibody, a standard ABC complex protocol (Vectastain ABC kit, Vector Laboratories, Burlingame, CA) using anti-rabbit secondary antibodies was used.

Electrophoretic mobility shift assay (EMSA). Tissue nuclear proteins were extracted from whole lung tissue by the method described previously[24]. After preparation of nuclear protein extract,

EMSA for NF-κB binding activity was performed using oligonucleotides containing a consensus NF-κB binding sequence (5'-AGT TGA GGG GAC TTT CCC AGG C-3').

Western blot analysis. Protein extracts from tissue homogenates (100 μg) were separated on a polyacrylamide gel and transblotted for detection of FLAG-cIKK2 or IκB-αDN-Myc-His. For FLAG-cIKK2, proteins were separated on a 10% acrylamide gel and anti-FLAG antibodies (anti-FLAG conjugated with HRP M_2 monoclonal antibody, Sigma-Aldrich, St. Louis, MO) were used. Horseradish peroxidase was detected by chemoluminescence using Lumi-Light^{PLUS} western blotting substrate (Roche Diagnostics, Indianapolis, IN). For IκB-αDN-Myc-His, proteins were separated on a 12% polyacrylamide gel and monoclonal anti-myc antibodies (Sigma) were used for immunodetection. For detection of RelA in lung tissue nuclear protein fractions, nuclear proteins were prepared as described [24], 20 μg protein was separated on a 10% acrylamide gel, and RelA was immunodetected using rabbit polyclonal anti-RelA antibodies (Santa Cruz Biotechnology). TATA binding protein was detected as a loading control using specific antibodies (Santa Cruz Biotechnology).

RNA isolation and Ribonuclease Protection Assay (RPA). Lung tissue was homogenized in Trizol Reagent (Invitrogen Life Technologies, Inc., Carlsbad, CA) and RNA was isolated following manufacturer's instructions. RPA employing chemokine template mCK-5 was done with the RiboQuant multiprobe RPA system (BD pharMingen, San Diego, CA) according to the manufacturer's direction.

Total and differential cell counts and protein measurement in lung lavage. Lung lavage was performed with 3 aliquots of 800 µl sterile normal saline. Fluid was combined and centrifuged at 400x g for 10 min to separate cells from supernatant. Supernatant was stored at -70 ºC for cytokine and chemokine measurements. The total and differential cell counts were done as previously described[15]. Protein concentration was quantified using the Bradford assay (Bio-Rad, Hercules, CA).

Lung wet/dry ratio measurement. Lungs were removed and the wet weight recorded. Lungs were then placed in an incubator at 65^{o}C for 48 hours and the dry weight was determined.

Cytokine and chemokine measurements. Measurement of cytokines and chemokines in lung lavage fluid and cell culture supernatant was done using the Bio-plex^{TM} mouse cytokine 23-plex kit (Bio-Rad, Hercules, CA) following manufacturer's direction and using Luminex technology. MIP-2 and KC levels were measured using a specific ELISA according to manufacturer's instructions (R&D System, Minneapolis, MN)

Tracheal epithelial cell culture. Mouse tracheal epithelial cell (MTEC) culture was done by following the previously published protocol with minor modification[13]. After removing muscle and vessels, tracheas were incubated in Ham's F-12 pen-strep containing 1.5 mg/ml pronase (Roche Molecular Biochemicals, Indianapolis, IN) for 18 h at 4 °C to dislodge the epithelial cells. Cells were treated with 0.5 mg/ml crude pancreatic DNase I (Sigma-Aldrich) on ice for 5 min. After incubation in tissue culture plates (Becton-Dickinson Labware, Franklin Lakes, NJ) for 3-4 h in 5% CO_2 at 37 °C to adhere fibroblasts, nonadherent cells were collected by centrifugation.

Supported polycarbonate and polyester porous (0.4 µM pores) membranes (Transwell; Corning-Costar, Corning, NY) were coated with type I rat tail collagen (Becton-Dickinson) in 0.02 N acetic acid for 18 h at 25 °C. Membranes were seeded with cells and incubated with DMEM-Ham's F-12 media containing 15 mM HEPES, 3.6 mM sodium bicarbonate, 4 mM L-glutamine, 100 U/ml penicillin, 100 µg/ml streptomycin, and 0.25 µg/ml fungizone, 10 µg/ml insulin, 5 µg/ml transferrin, 0.1 µg/ml cholera toxin, 25 ng/ml epidermal growth factor (Becton-Dickinson, Bedford, MA), 30 µg/ml bovine pituitary extract, 5% FBS, and freshly added 0.01 µM retinoic acid, filling upper and lower chambers in 5% CO_2 at 37 °C. Media were changed every 2 days until the transmembrane resistance (R_t) was >1,000 $\Omega \cdot cm^2$, as measured by an epithelial Ohm-voltmeter (World Precision Instruments, Sarasota, FL). Media were then removed from the upper chamber to establish an air-liquid interface, and lower chambers only were provided fresh DMEM-Ham's F-12 media supplemented with 2% NuSerum (Becton-Dickinson) and 0.01 µM retinoic acid.

Membrane cultures were prepared for scanning electron microscopy, as previously described[25]. Briefly, samples were fixed with 2.5% glutaraldehyde, stained with 1.25% osmium tetroxide, critical point dried under liquid carbon dioxide, gold sputter coated, and visualized on a Hitachi S-3000N microscope (Tokyo, Japan).

For immunofluorescent detection of FLAG-cIKK2 expression, membranes were fixed with 4% paraformaldehyde, pH 7.4, for 10 min at 25 °C, washed in PBS. A piece of membrane was cut and used for staining. Nonspecific antibody binding was blocked using 5% nonspecific serum and 3% BSA in PBS for 30 min at 25°C. Samples were incubated for 18 h at 4 °C with anti-FLAG M2-FITC conjugate antibody (Sigma- Aldrich) in blocking solution. Membranes were mounted on slides with Vecta Shield (Vector, Burlingame, CA) containing 4',6 diamidino-

2-phenylindole to stain intracellular DNA. The microscopic images were obtained by using a Zeiss LSM 510 confocal microscope (Carl Zeiss).

Statistical analysis. To assess differences among groups, analyses were performed with GraphPad Instat (GraphPad Software, San Diego, CA) using an unpaired *t* test or one-way analysis of variance (ANOVA). Mortality differences were evaluated using a Fisher's exact test. Results are presented as mean +/- standard error of the mean (SEM). Two-tailed p values < 0.05 were considered significant.

Acknowledgements

The authors wish to thank Dr. Jeffrey A. Whitsett of the University of Cincinnati College of Medicine for the generous donation of CC-10 rtTA expressing transgenic mice used in these studies. We also wish to thank the Vanderbilt University Mouse Metabolic Phenotyping Core, the Vanderbilt Transgenic/ES Shared Resource, and the Mouse Pathology Core for their valuable assistance.

Table 1

Lung lavage cytokine levels (pg/ml)

	WT + dox	IKTA no dox	IKTA + dox
TNFα	5.6 ± 3.4	4.6 ± 4.6	32.9 ± 11.0
IL-1α	1.3 ± 0.8	0	11.0 ± 2.3*
IL-1β	0	0	40.0 ± 1.6*
IL-2	12.6 ± 5.8	8.7 ± 1.6	25.8 ± 0.5
IL-5	1.0 ± 0.4	0.6 ± 0.6	12.8 ± 5.7*
IL-6	1.4 ± 0.9	1.2 ± 0.1	197.0 ± 54.0*
IL-9	17.9 ± 0	11.3 ± 10.2	31.6 ± 2.5
IL-10	1.5 ± 0.8	0	7.4 ± 2.6
IL-12p40	80.4 ± 9.5	28.2 ± 5.9	258.9 ± 83.3*
IL-17	1.1 ± 0.6	1.1 ± 0.6	13.7 ± 3.0*
Eotaxin	32.1 ± 26.3	44.8 ± 22.9	130.5 ± 18.6
RANTES	0	0	530.8 ± 106.0*
MIP-2	2.0 ± 0.6	0	35.4 ± 10.7*
MIP-1β	10.4 ± 0.8	11.1 ± 2.4	31.8 ± 9.2
KC	42.9 ± 3.7	65.3 ± 11.0	447.5 ± 125.4*
MCP-1	22.3 ± 10.1	12.1 ± 10.1	567.7 ± 144.2*
G-CSF	2.8 ± 0.4	9.6 ± 7.1	94.5 ± 9.1*
GM-CSF	6.8 ± 3.2	11.4 ± 2.9	37.9 ± 16.6

Values measured by luminex or ELISA are presented as mean (± SEM). N=3-5 per group.

*=$p<0.05$ compared with all other groups by ANOVA. Levels of IL-3, IL-4, IL-12p70, IL-13, MIP-1α, and IFNγ were below the limits of detection.

References

1. Ware,L.B. & Matthay,M.A. The acute respiratory distress syndrome. *N. Engl. J. Med* **342**, 1334-1349 (2000).

2. Kollef,M.H. & Schuster,D.P. The acute respiratory distress syndrome. *N. Engl. J. Med* **332**, 27-37 (1995).

3. Bhatia,M. & Moochhala,S. Role of inflammatory mediators in the pathophysiology of acute respiratory distress syndrome. *J. Pathol.* **202**, 145-156 (2004).

4. Blackwell,T.S. & Christman,J.W. The role of nuclear factor-kappa B in cytokine gene regulation. *Am. J. Respir. Cell Mol Biol.* **17**, 3-9 (1997).

5. Ghosh,S., May,M.J. & Kopp,E.B. NF-kappa B and Rel proteins: evolutionarily conserved mediators of immune responses. *Annu. Rev. Immunol.* **16**, 225-260 (1998).

6. Mercurio,F. *et al.* IKK-1 and IKK-2: cytokine-activated IkappaB kinases essential for NF-kappaB activation. *Science* **278**, 860-866 (1997).

7. Muir,A. *et al.* Toll-like receptors in normal and cystic fibrosis airway epithelial cells. *Am. J. Respir. Cell Mol Biol.* **30**, 777-783 (2004).

8. Sadikot,R.T. *et al.* Targeted Immunomodulation of the NF-{kappa}B Pathway in Airway Epithelium Impacts Host Defense against Pseudomonas aeruginosa. *J. Immunol.* **176**, 4923-4930 (2006).

9. Everhart,M.B. *et al.* Duration and Intensity of NF-{kappa}B Activity Determine the Severity of Endotoxin-Induced Acute Lung Injury. *J. Immunol.* **176**, 4995-5005 (2006).

10. Deuschle,U., Meyer,W.K. & Thiesen,H.J. Tetracycline-reversible silencing of eukaryotic promoters. *Mol Cell Biol.* **15**, 1907-1914 (1995).

11. Forster,K. *et al.* Tetracycline-inducible expression systems with reduced basal activity in mammalian cells. *Nucleic Acids Res.* **27**, 708-710 (1999).

12. Zhu,Z., Ma,B., Homer,R.J., Zheng,T. & Elias,J.A. Use of the tetracycline-controlled transcriptional silencer (tTS) to eliminate transgene leak in inducible overexpression transgenic mice. *J. Biol. Chem.* **276**, 25222-25229 (2001).

13. You,Y., Richer,E.J., Huang,T. & Brody,S.L. Growth and differentiation of mouse tracheal epithelial cells: selection of a proliferative population. *Am. J. Physiol Lung Cell Mol Physiol* **283**, L1315-L1321 (2002).

14. Sadikot,R.T. *et al.* Selective I kappa B kinase expression in airway epithelium generates neutrophilic lung inflammation. *J. Immunol.* **170**, 1091-1098 (2003).

15. Blackwell,T.S. *et al.* Multiorgan nuclear factor kappa B activation in a transgenic mouse model of systemic inflammation. *Am. J. Respir. Crit Care Med* **162**, 1095-1101 (2000).

16. Poynter,M.E., Irvin,C.G. & Janssen-Heininger,Y.M. A prominent role for airway epithelial NF-kappa B activation in lipopolysaccharide-induced airway inflammation. *J. Immunol.* **170**, 6257-6265 (2003).

17. Skerrett,S.J. *et al.* Respiratory epithelial cells regulate lung inflammation in response to inhaled endotoxin. *Am. J. Physiol Lung Cell Mol Physiol* **287**, L143-L152 (2004).

18. Chen,L.W. *et al.* The two faces of IKK and NF-kappaB inhibition: prevention of systemic inflammation but increased local injury following intestinal ischemia-reperfusion. *Nat. Med* **9**, 575-581 (2003).

19. Goodman,R.B. *et al.* Inflammatory cytokines in patients with persistence of the acute respiratory distress syndrome. *Am. J. Respir. Crit Care Med* **154**, 602-611 (1996).

20. Schutte,H. *et al.* Bronchoalveolar and systemic cytokine profiles in patients with ARDS, severe pneumonia and cardiogenic pulmonary oedema. *Eur. Respir. J.* **9**, 1858-1867 (1996).

21. Miller,E.J. *et al.* Elevated levels of NAP-1/interleukin-8 are present in the airspaces of patients with the adult respiratory distress syndrome and are associated with increased mortality. *Am. Rev. Respir. Dis.* **146**, 427-432 (1992).

22. Donnelly,S.C. *et al.* Interleukin-8 and development of adult respiratory distress syndrome in at-risk patient groups. *Lancet* **341**, 643-647 (1993).

23. Baughman,R.P., Gunther,K.L., Rashkin,M.C., Keeton,D.A. & Pattishall,E.N. Changes in the inflammatory response of the lung during acute respiratory distress syndrome: prognostic indicators. *Am. J. Respir. Crit Care Med* **154**, 76-81 (1996).

24. Blackwell,T.S., Blackwell,T.R. & Christman,J.W. Impaired activation of nuclear factor-kappaB in endotoxin-tolerant rats is associated with down-regulation of chemokine gene expression and inhibition of neutrophilic lung inflammation. *J. Immunol.* **158**, 5934-5940 (1997).

25. Look,D.C. *et al.* Effects of paramyxoviral infection on airway epithelial cell Foxj1 expression, ciliogenesis, and mucociliary function. *Am. J. Pathol.* **159**, 2055-2069 (2001).

Figure Legends

Figure 1. Doxycycline-induced expression of FLAG-cIKK2 is localized to lung epithelial cells and sufficient to activate NF-κB. a) Schematic for construction of IKTA transgenic mice. b) Western blot for FLAG expression in tissue homogenates obtained from untreated IKTA mice, triple transgenic IKTA mice treated with dox for 3 days, or double transgenic $(tet\text{-}O)_7$-FLAG-cIKK2/CC10-tTS mice treated with dox. Transgene expression is detected only in the lungs of IKTA mice following dox treatment. c) Immunohistochemistry for FLAG in lung tissue from an untreated IKTA mouse (left panel) or an IKTA mouse treated with dox for 3 days (right panel). FLAG-cIKK2 staining (brown stain) is localized in airway epithelial cells in dox-treated IKTA mice. d) Electrophoretic mobility shift assay for NF-κB binding using lung nuclear protein extracts from WT control mice treated with dox (WT+Dox), untreated IKTA mice (IKTA-Dox), and IKTA mice treated with dox for 3 days (IKTA+Dox). Increased intensity of both NF-κB bands (RelA/p50 and p50/p50) is present in the IKTA+Dox group.

Figure 2. NF-κB activation in airway epithelium results in progressive lung inflammation and injury. a) H&E stained lung sections from untreated IKTA mice and IKTA mice (line 3) treated with dox for 3 or 7 days. While untreated IKTA mice have normal lung histology, a progressive inflammatory cell infiltrate is observed at 3 and 7 days after dox treatment, along with hemorrhage and edema at 7 days. b) Total neutrophils, macrophages and lymphocytes in lung lavage from IKTA mice treated with dox for 3 or 7 days compared with WT mice treated with dox for 7 days. (n=3-4 per group, *=$p<0.05$ compared with WT, **=$p<0.05$ compared with WT and IKTA mice treated with dox for 3 days). c) Lung lavage protein concentration in untreated WT and IKTA mice (Day 0) and in both groups after 3 or 7 days of dox treatment. (n=4 per

group, *=p<0.01 compared with WT). d) Lung wet/dry ratios for WT and IKTA mice treated with dox for 3 days. (n=3-6 per group, *=p<0.01 compared with WT).

Figure 3. Treatment of IKTA mice with dox results in hypoxemia and increased mortality. a) Serial arterial blood gas measurements were obtained from indwelling carotid artery catheters. PO_2 and PCO_2 were assessed in IKTA mice at baseline and up to 7 days of dox treatment. (n=3-4 per time point, *=p<0.01 compared with baseline). b) Mortality rates in mice from IKTA lines 3 and 31 compared to WT controls through 14 days of dox treatment. While all WT mice survived, 60% of mice in IKTA line 31 and 70% of mice in IKTA line 3 died between day 7 and 14. (n=10 mice per group).

Figure 4. DNTA transgenic mice express a dominant inhibitor of the NF-κB pathway in airway epithelium. a) Schematic for construction of DNTA transgenic mice. b) Western blot for Myc-His tagged IκB-αDN expression in tissue homogenates obtained from WT and DNTA mice, and DNTA mice treated with dox for 7 days. Transgene expression is detected only in the lungs of DNTA mice following dox treatment. c) DNTA mice were crossed with IKTA mice (line 26) to create IKDNTA mice that express both transgenes. Total cell counts in lung lavage are shown for IKTA mice (line 26), DNTA mice, and IKDNTA mice following 7 days of dox treatment, and IKDNTA mice without dox treatment. The inflammatory cell influx was inhibited in dox-treated IKDNTA mice, indicating that expression of IκB-αDN blocks cIKK2-induced inflammation. (n=3-8 per group, *=p<0.05 compared to other groups)

Figure 5. DNTA mice are protected from *E. coli* LPS-induced lung inflammation and injury. WT or DNTA mice were treated with dox (2 g/l) in drinking water for 1 week followed by intraperitoneal implantation of osmotic pumps delivering LPS. a) Western blot from lung nuclear protein extracts showing impaired nuclear translocation of RelA in DNTA mice at 4 hours after LPS pump implantation (DNTA+LPS) compared to WT mice (WT+LPS). Samples from DNTA mice and WT mice without LPS pumps are shown as controls. TATA binding protein (TBP) was identified as a loading control. b) H&E stained lung sections from WT and DNTA mice harvested 48 hours after intraperitoneal placement of pumps that deliver LPS continuously for 24 hours. Lung inflammation and edema were markedly reduced in dox-treated DNTA mice. c) Lung lavage neutrophils obtained at 48 hours after LPS pump placement. (n=10 per group, *=$p<0.05$). d) Lung wet/dry ratios for WT and DNTA mice treated with LPS pumps, presented as increase above untreated controls. (n=10 per group, *=$p<0.01$). e) Lung lavage protein concentration in untreated WT mice and WT and DNTA mice at 48 hours after treatment with LPS pump (n=6 per group, *=$p<0.05$ compared with untreated mice and LPS pump-treated DNTA mice). f) Mortality rates in dox-treated WT and DNTA mice following intraperitoneal implantation of osmotic pumps that deliver LPS at 8 μg/hour over 72 hours. (n=10 per group, *=$p<0.05$).

Fig. 1a

Construction of cIKK2 TransActivated (IKTA) transgenic mice

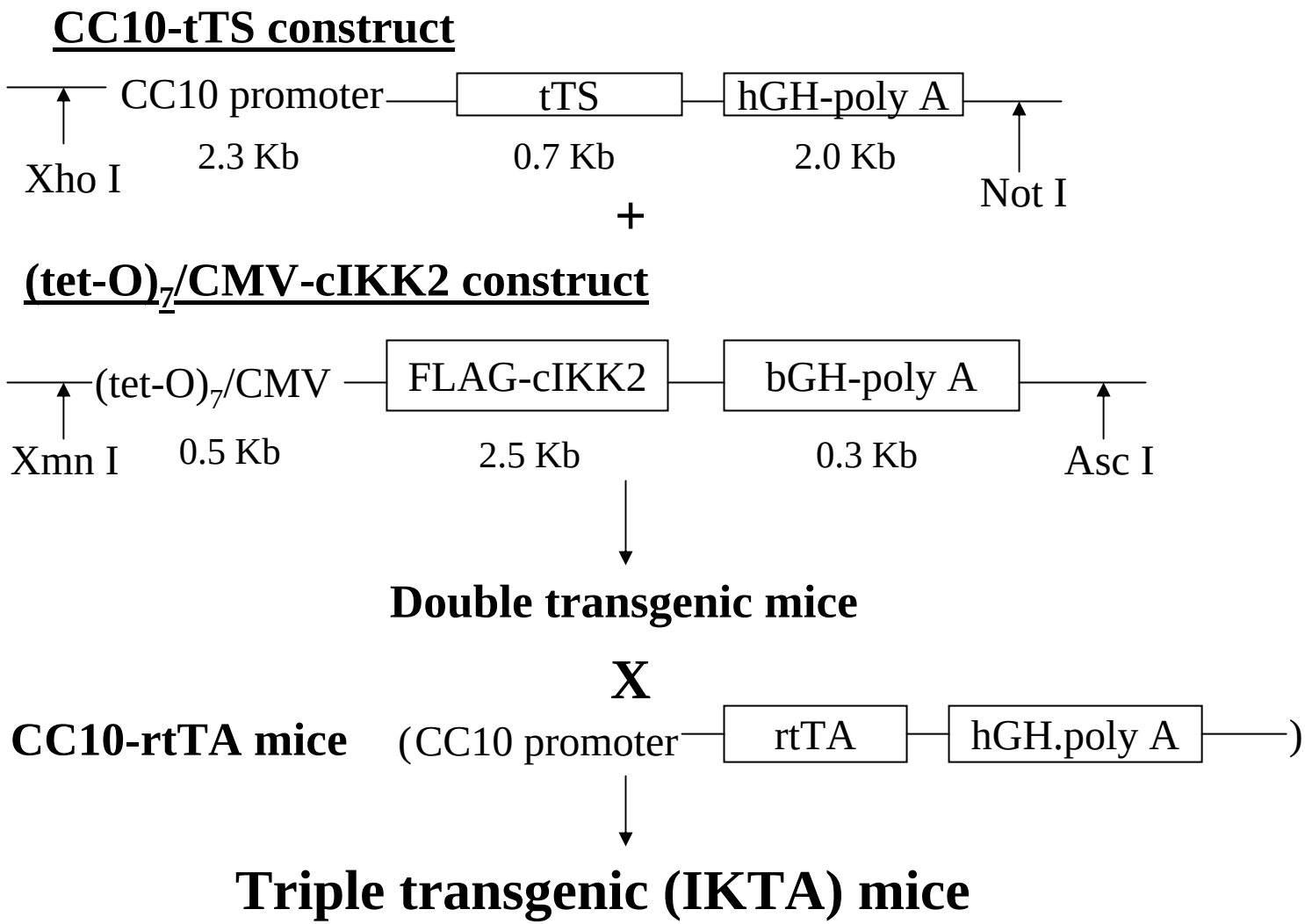

Fig. 1b

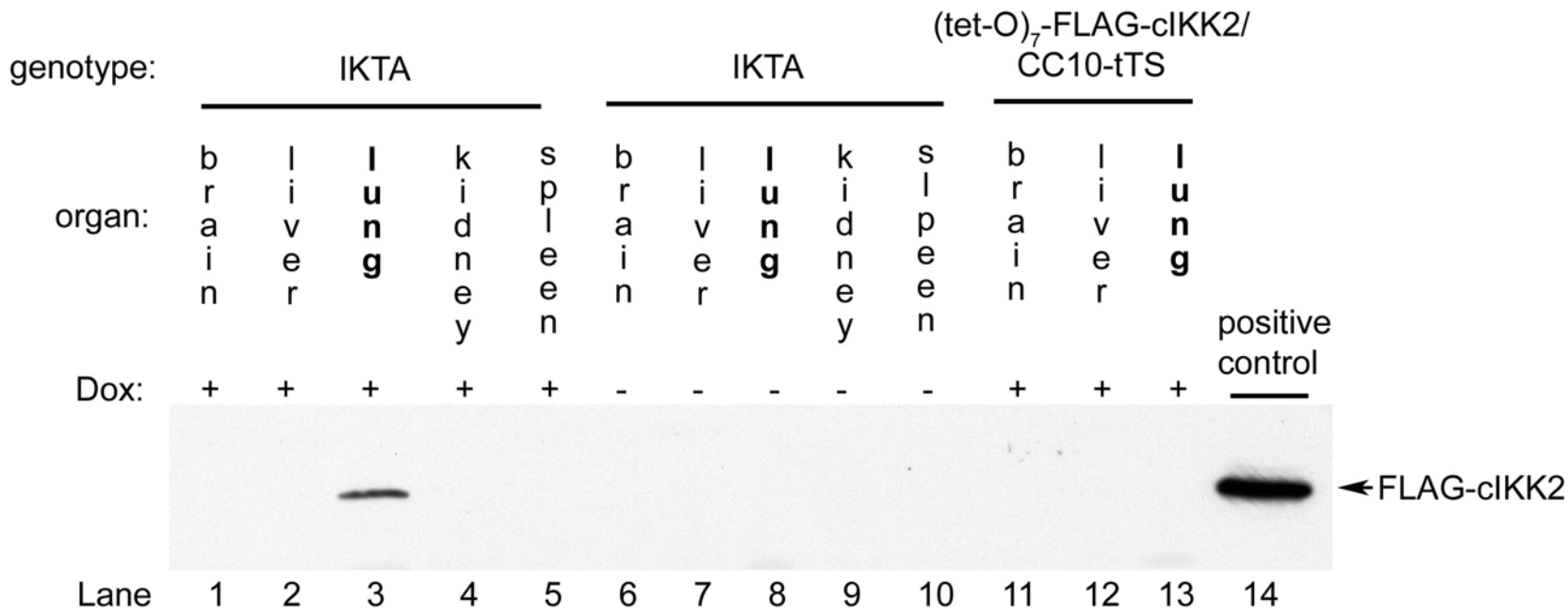
genotype:
IKTA
IKTA
(tet-O)7-FLAG-cIKK2/
CC10-tTS
organ:
brain
liver
lung
kidney
spleen
brain
liver
lung
kidney
spleen
brain
liver
lung
positive
control
Dox:
+ + + + + - - - - - + + + +
FLAG-cIKK2
Lane
1 2 3 4 5 6 7 8 9 10 11 12 13 14

Fig. 1c

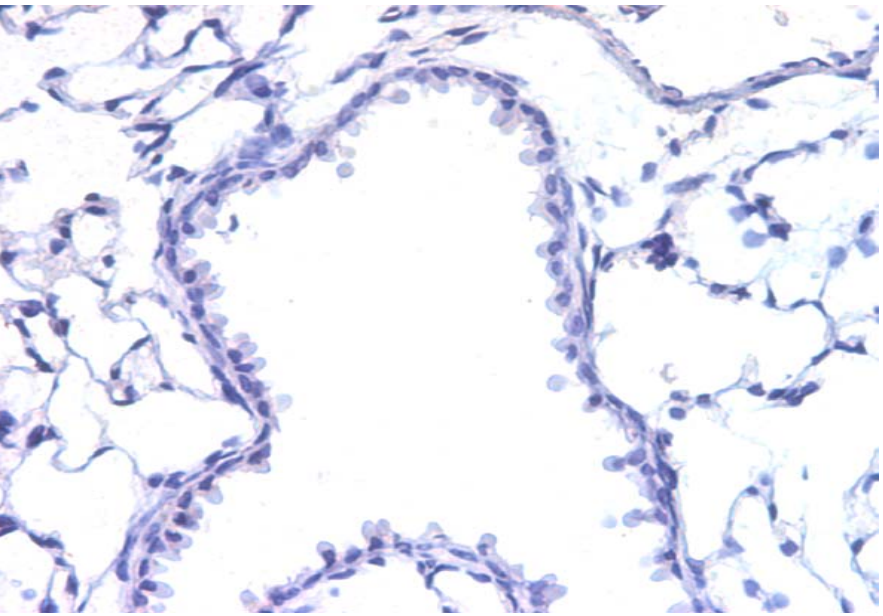

IKTA – no dox

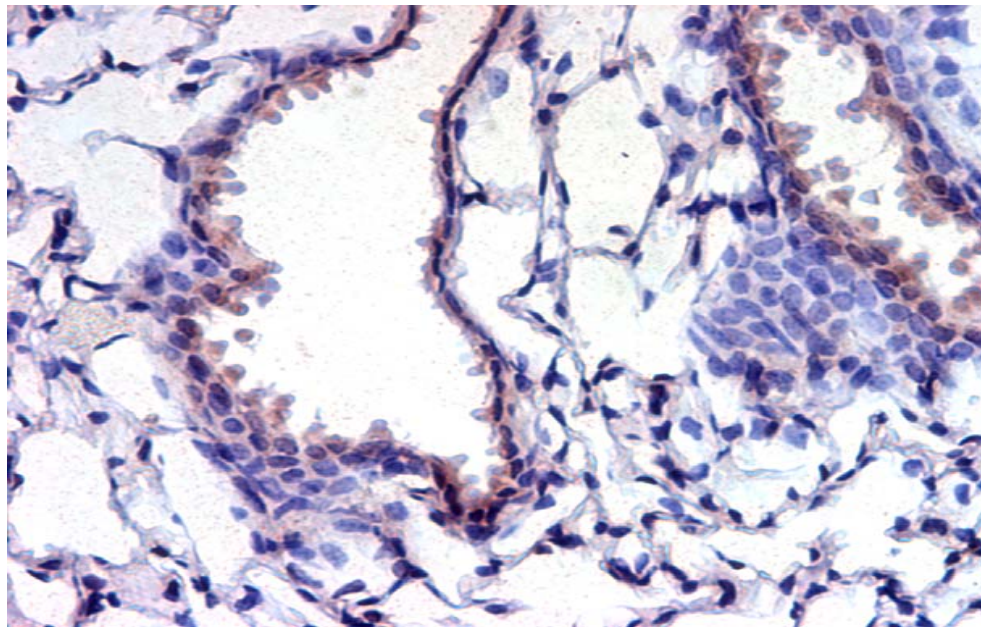

IKTA + dox

Fig. 1d

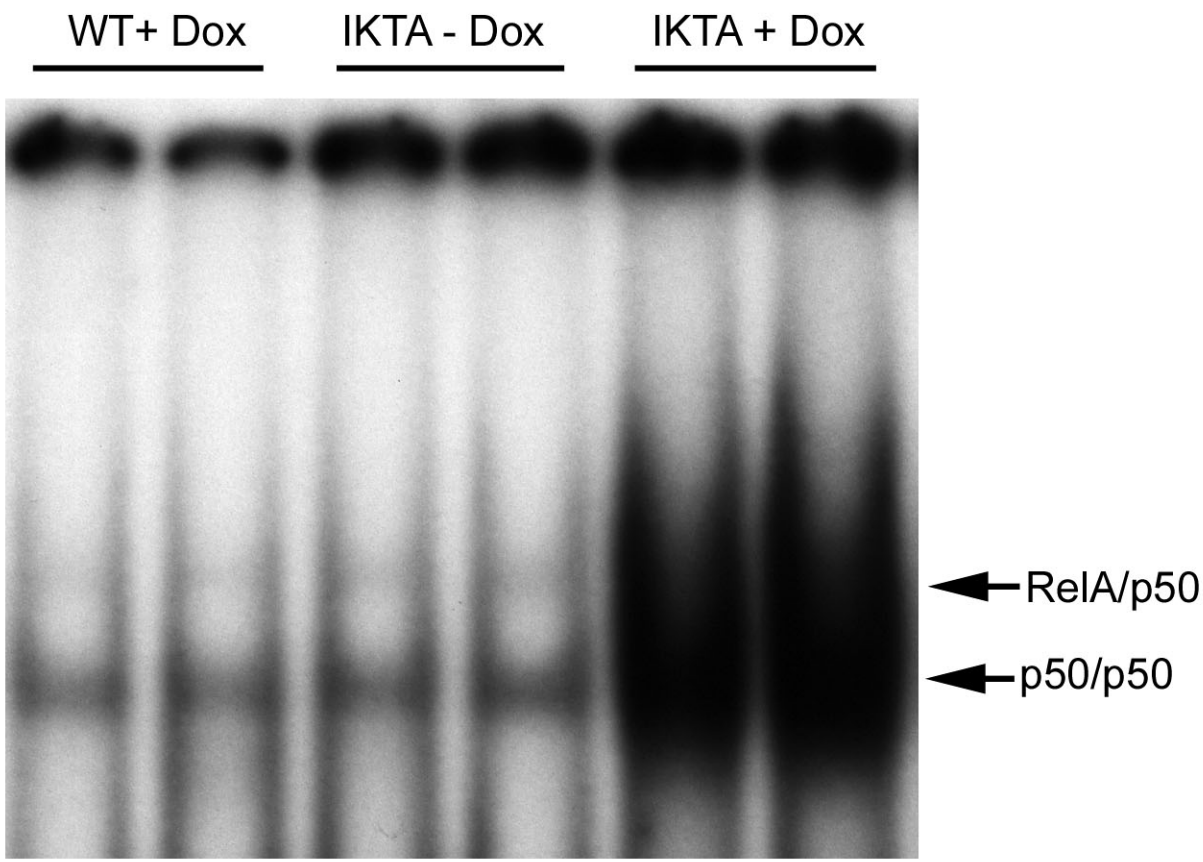

Fig. 2a

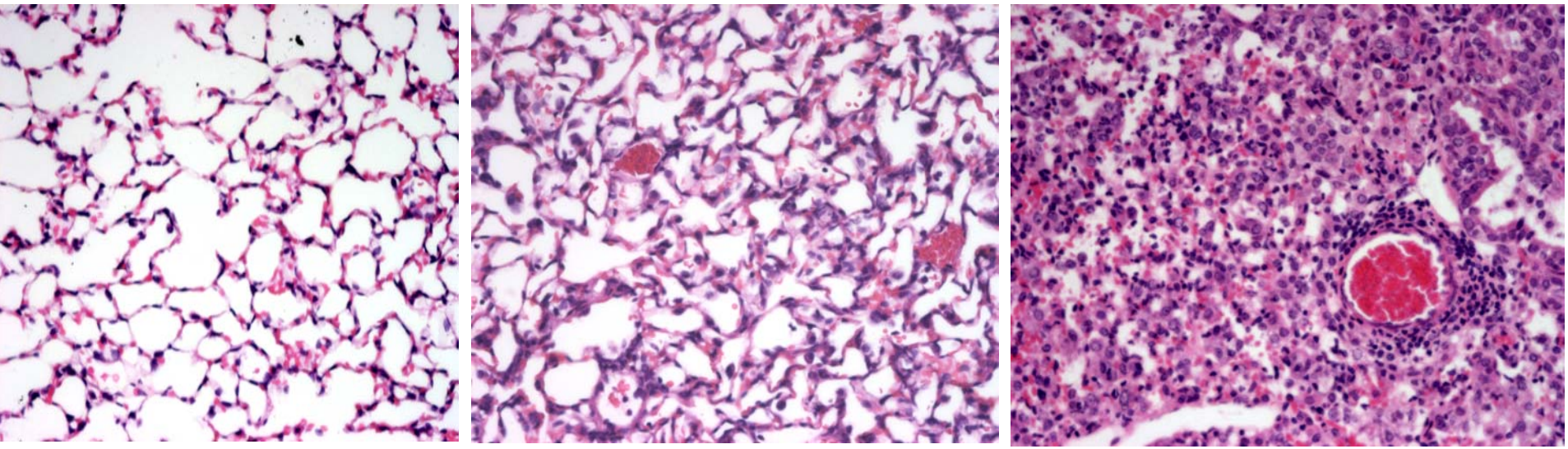

no dox

3 days

7 days

Fig. 2b

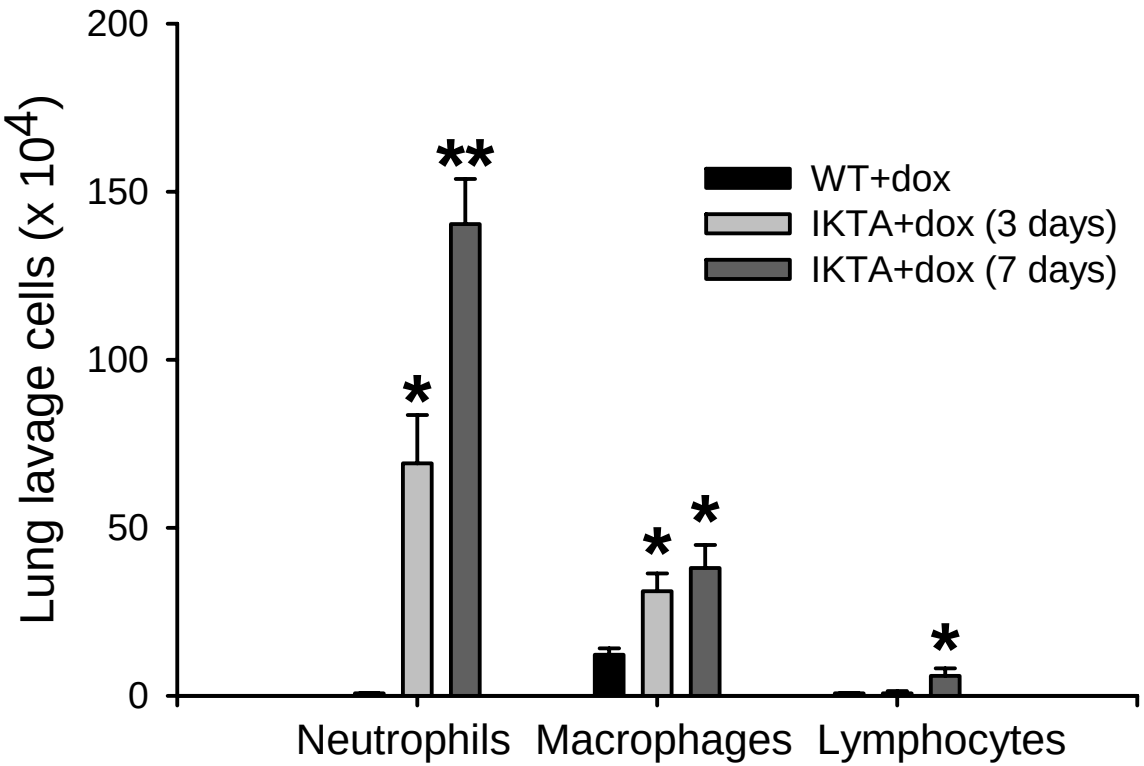
200
150
100
50
0
Lung lavage cells (x 10^4)
WT+dox
IKTA+dox (3 days)
IKTA+dox (7 days)
*
**
*
*
*
Neutrophils
Macrophages
Lymphocytes

Fig. 2c

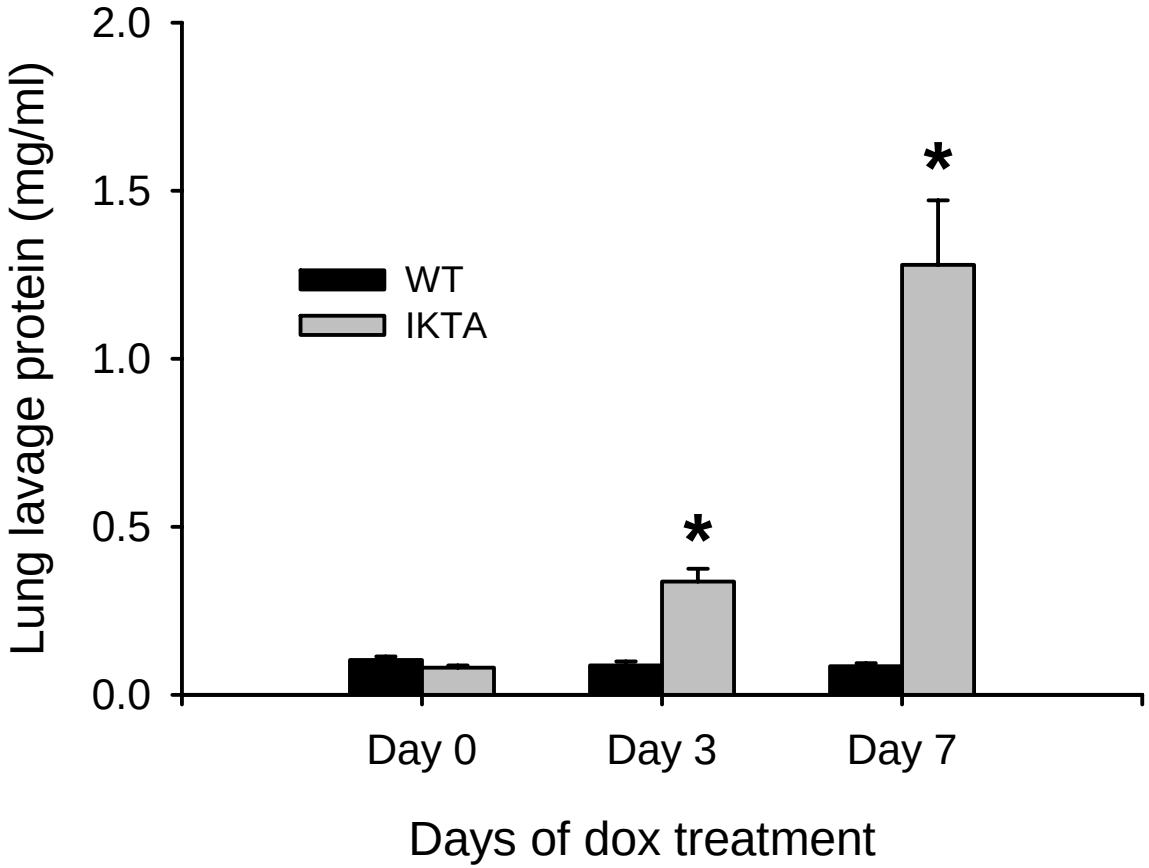
2.0
1.5
1.0
0.5
0.0
Lung lavage protein (mg/ml)
WT
IKTA
*
*
Day 0
Day 3
Day 7
Days of dox treatment

Fig. 2d

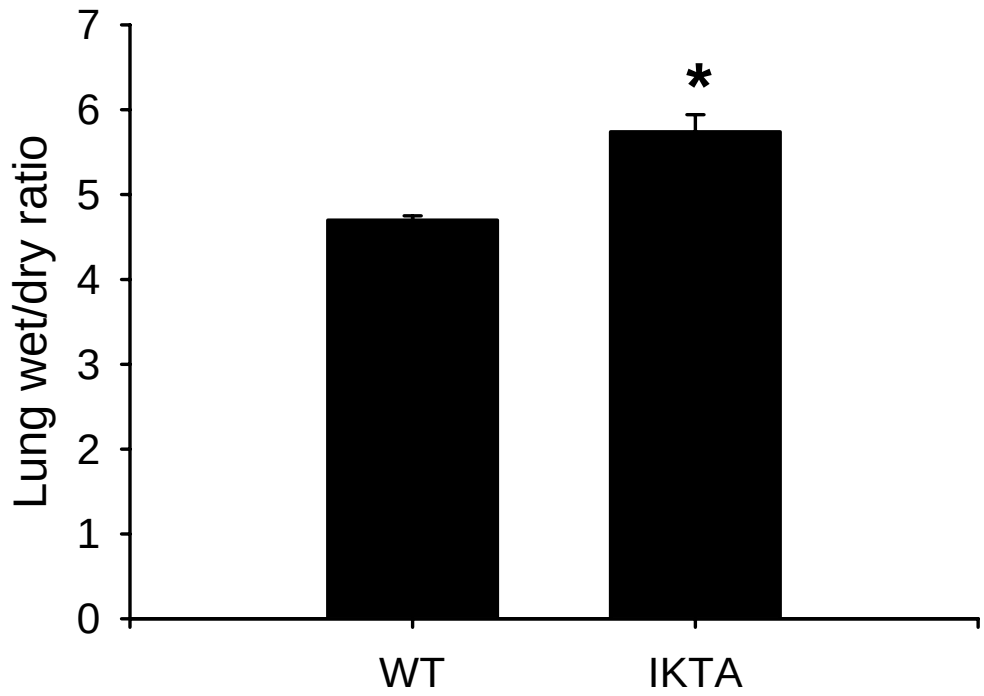

Fig. 3a

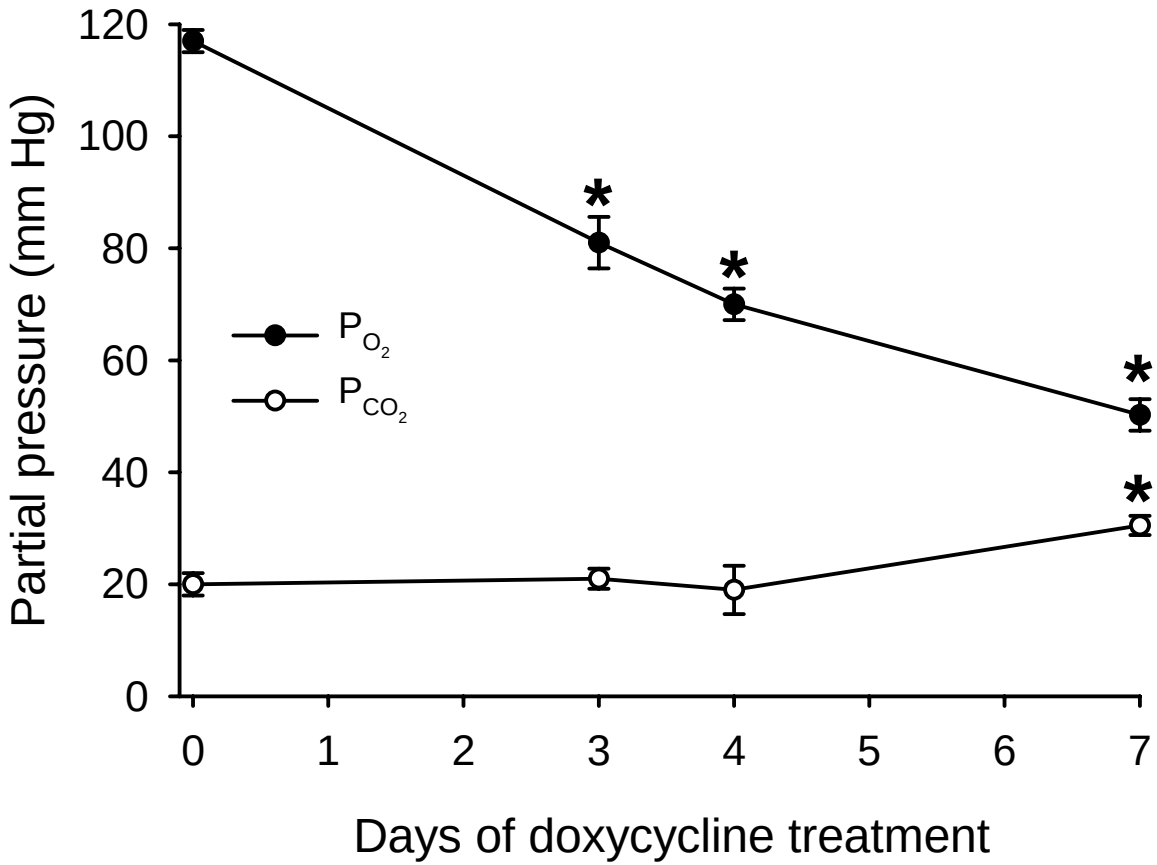
120
100
80
60
40
20
0
Partial pressure (mm Hg)
P_{O_2}
P_{CO_2}
*
*
*
*
0
1
2
3
4
5
6
7
Days of doxycycline treatment

Fig. 3b

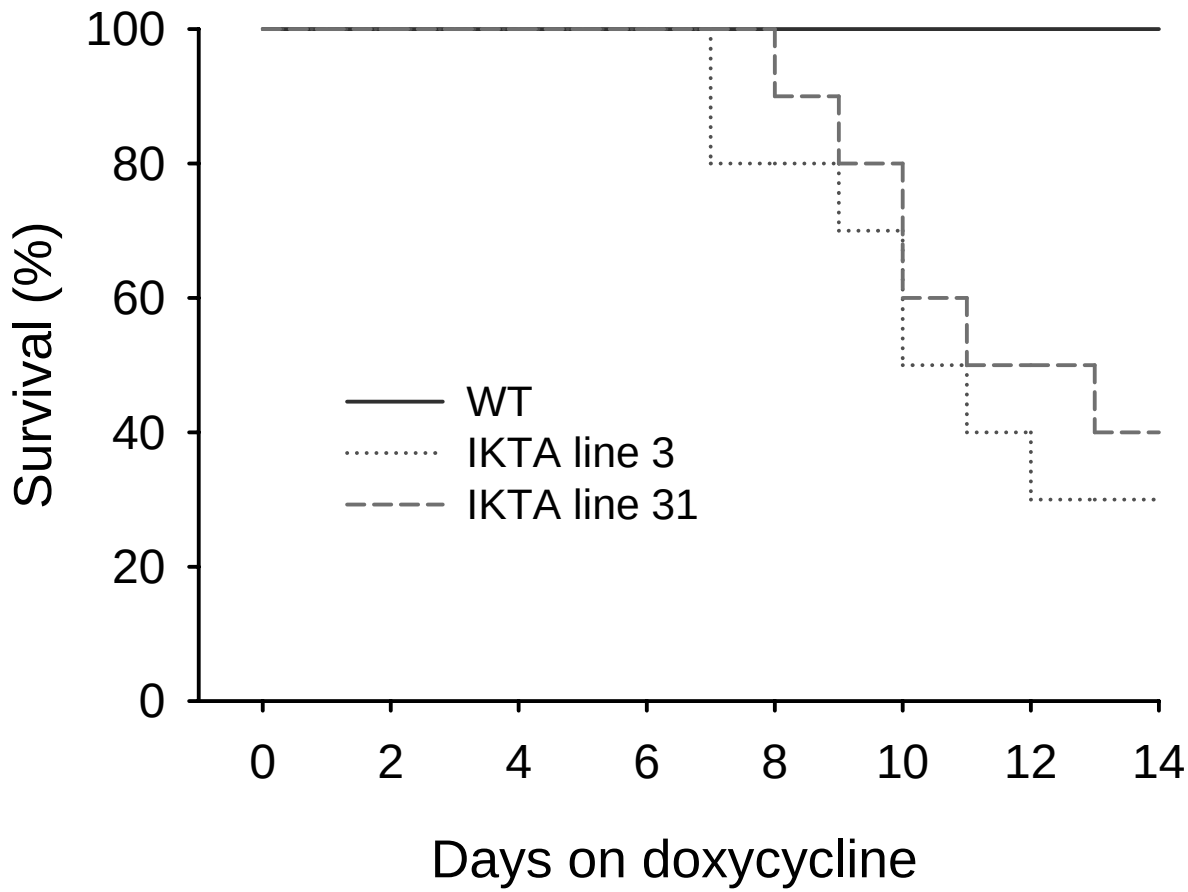
100
80
60
40
20
0
Survival (%)
WT
IKTA line 3
IKTA line 31
0
2
4
6
8
10
12
14
Days on doxycycline

Fig. 4a

Construction of IκB-αDominant Negative TransActivated (DNTA) transgenic mice

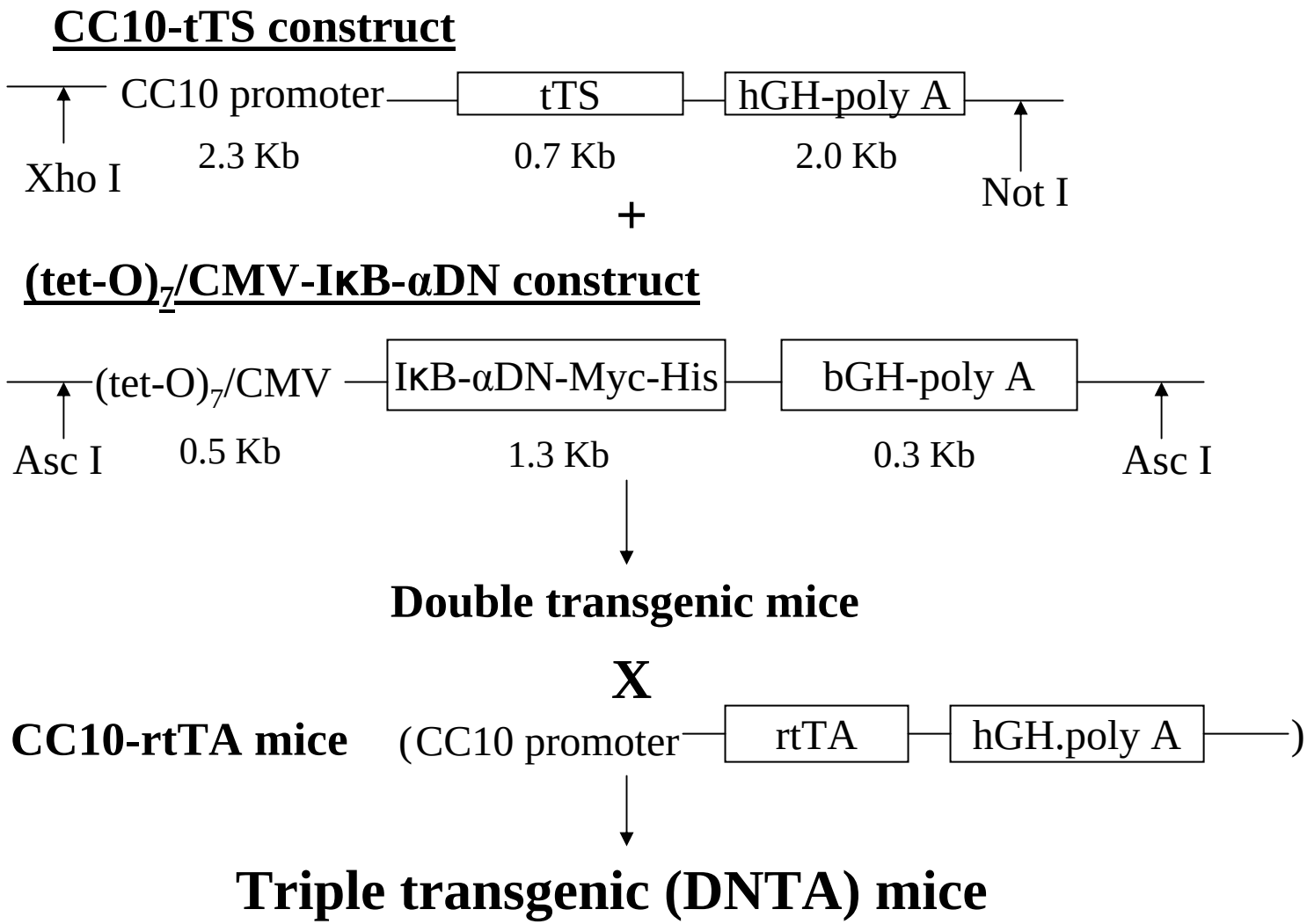

Fig. 4b

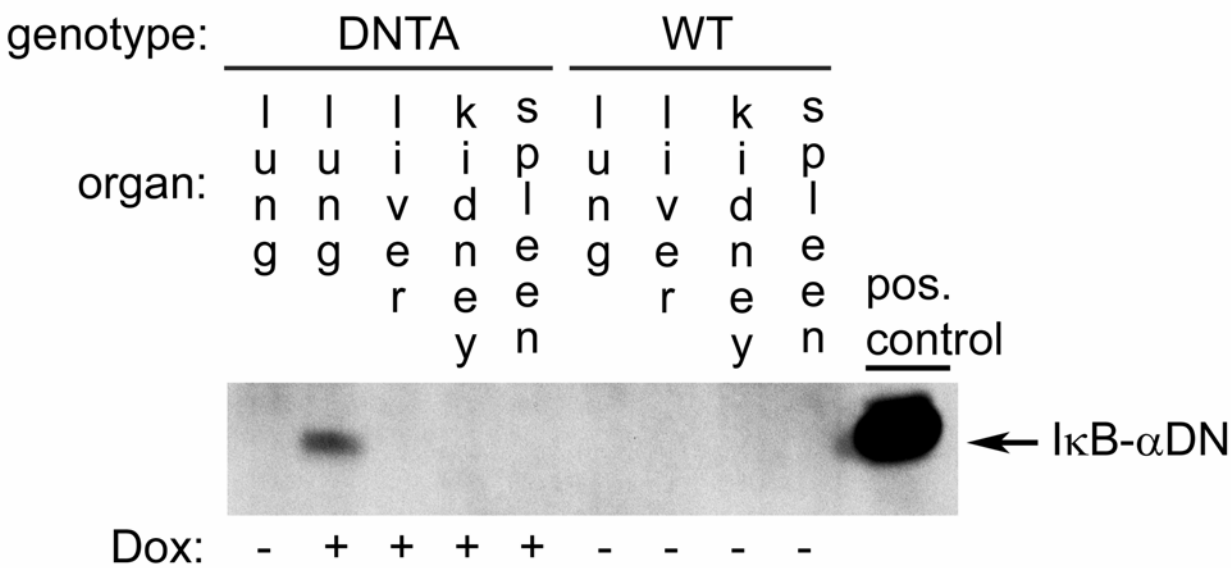
genotype:
DNTA
WT
organ:
lung
lung
liver
kidney
spleen
lung
liver
kidney
spleen
pos. control
IκB-αDN
Dox:
- + + + + - - - -

Fig. 4c

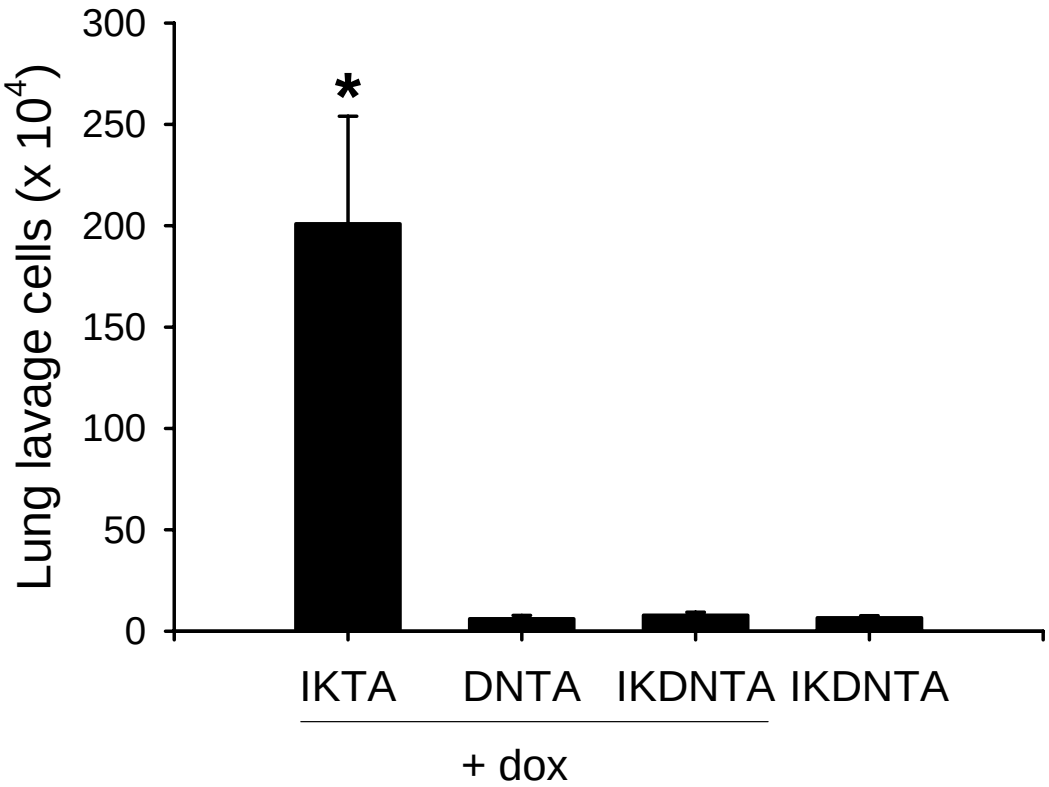
300
250
200
150
100
50
0
Lung lavage cells (x 10^4)
*
IKTA
DNTA
IKDNTA
IKDNTA
+ dox

Fig. 5a

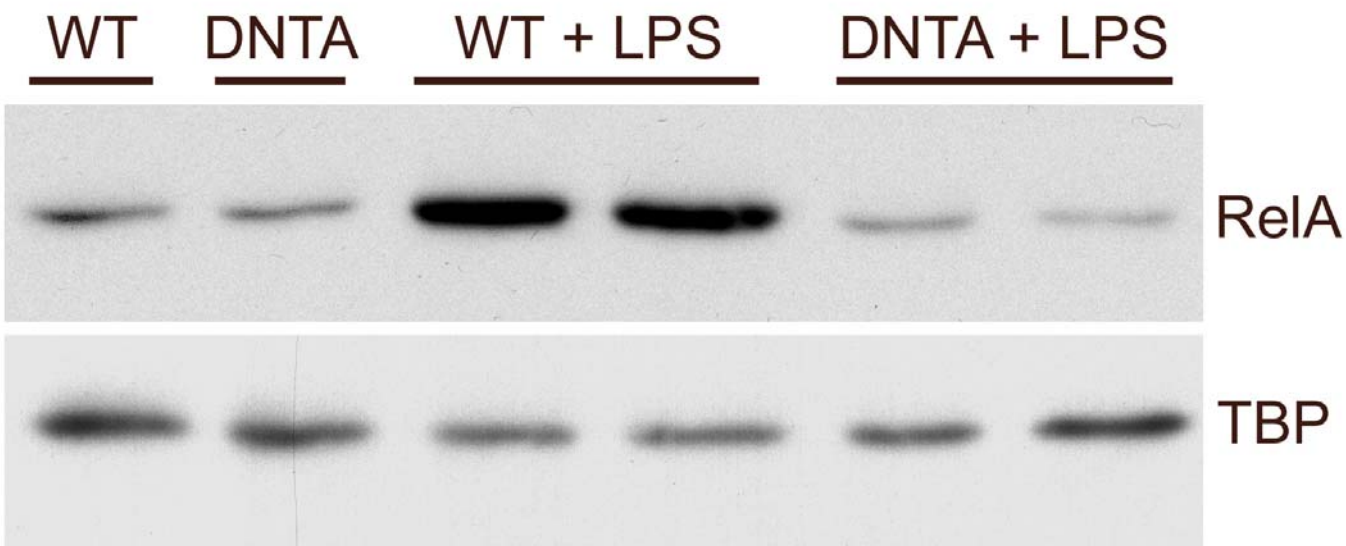

Fig. 5b

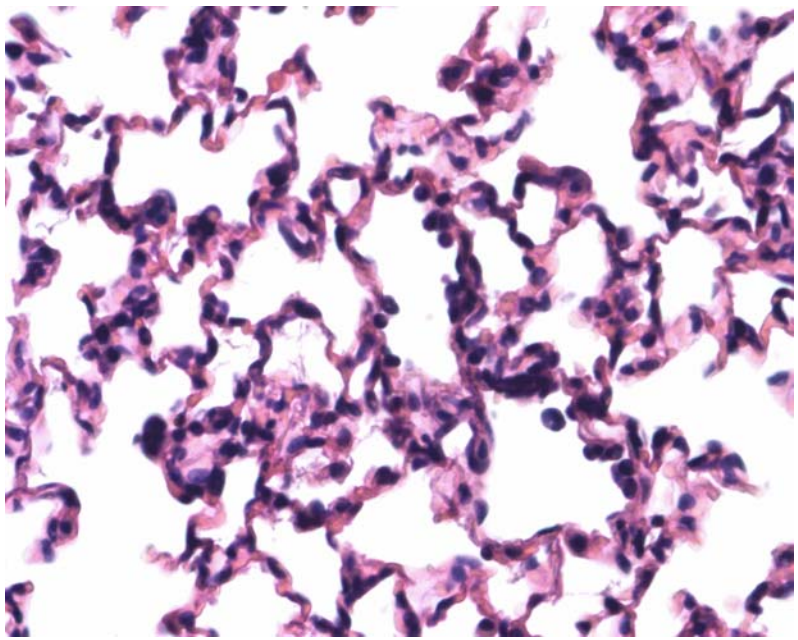

WT

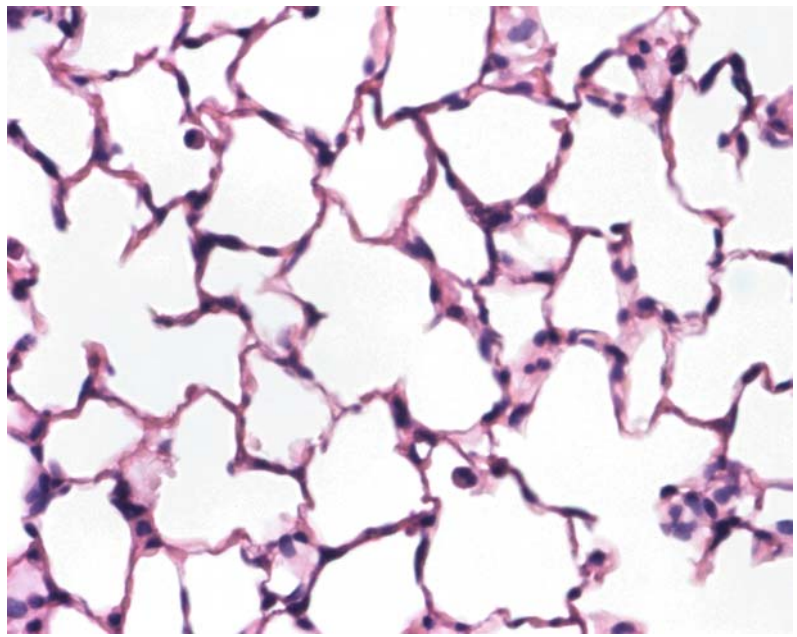

DNTA

Fig. 5c

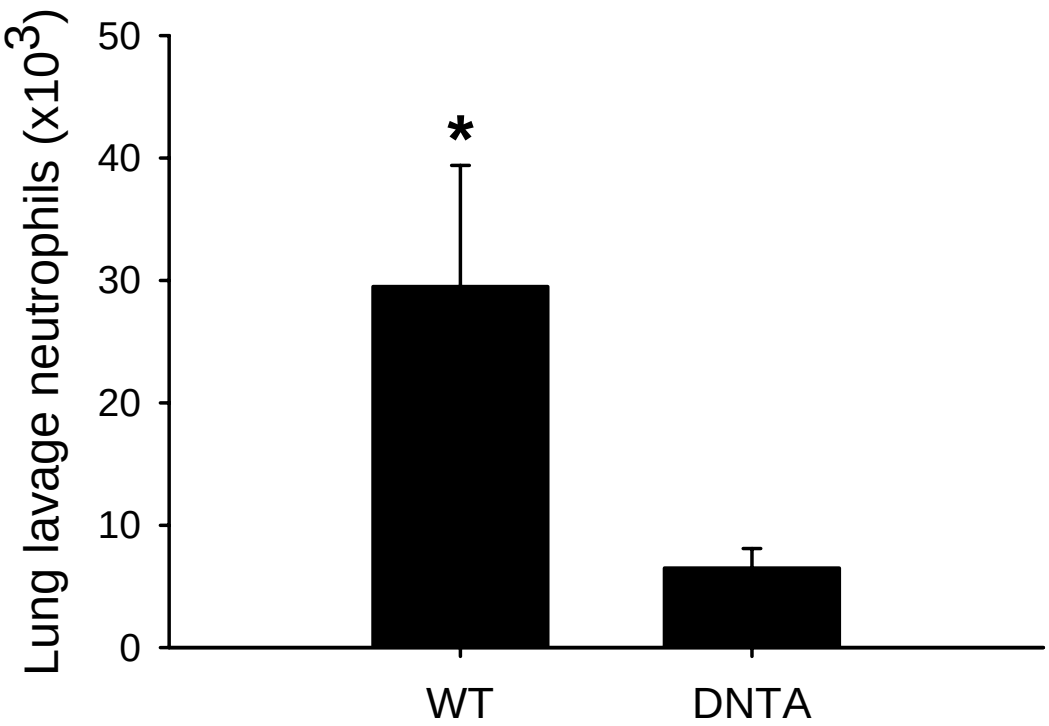

Fig. 5d

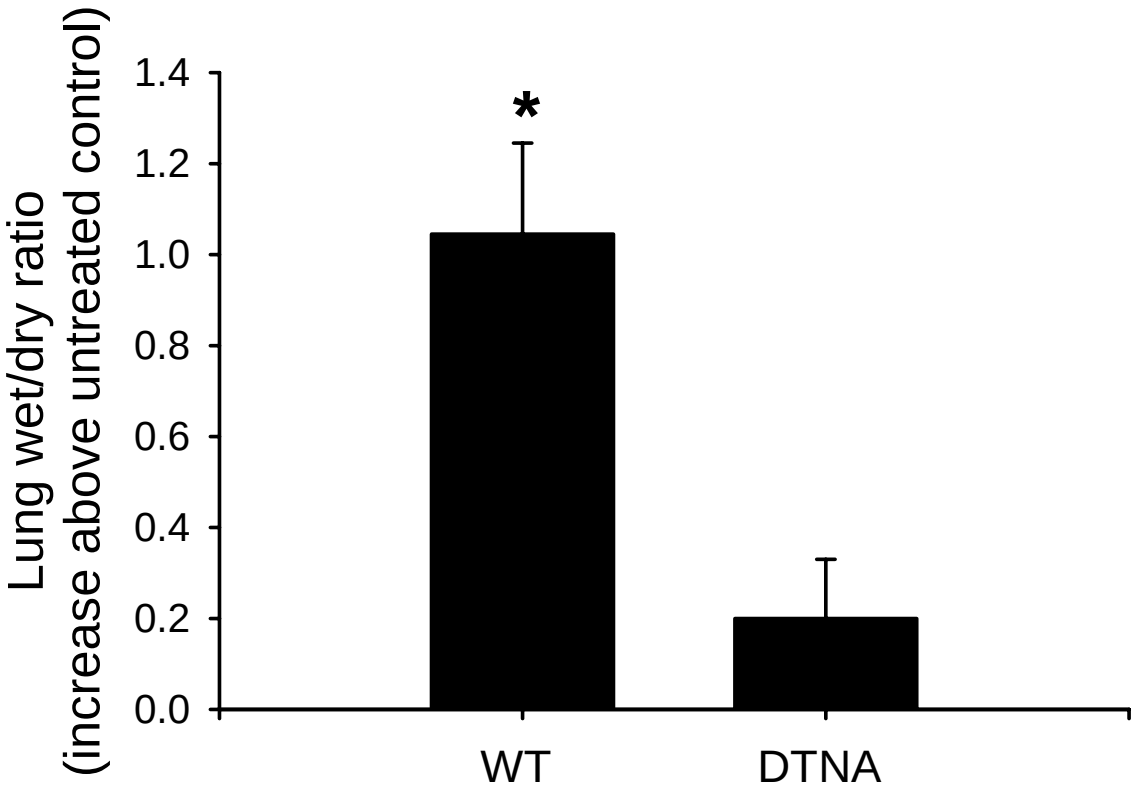
Lung wet/dry ratio
(increase above untreated control)
1.4
1.2
1.0
0.8
0.6
0.4
0.2
0.0
*
WT
DTNA

Fig. 5e

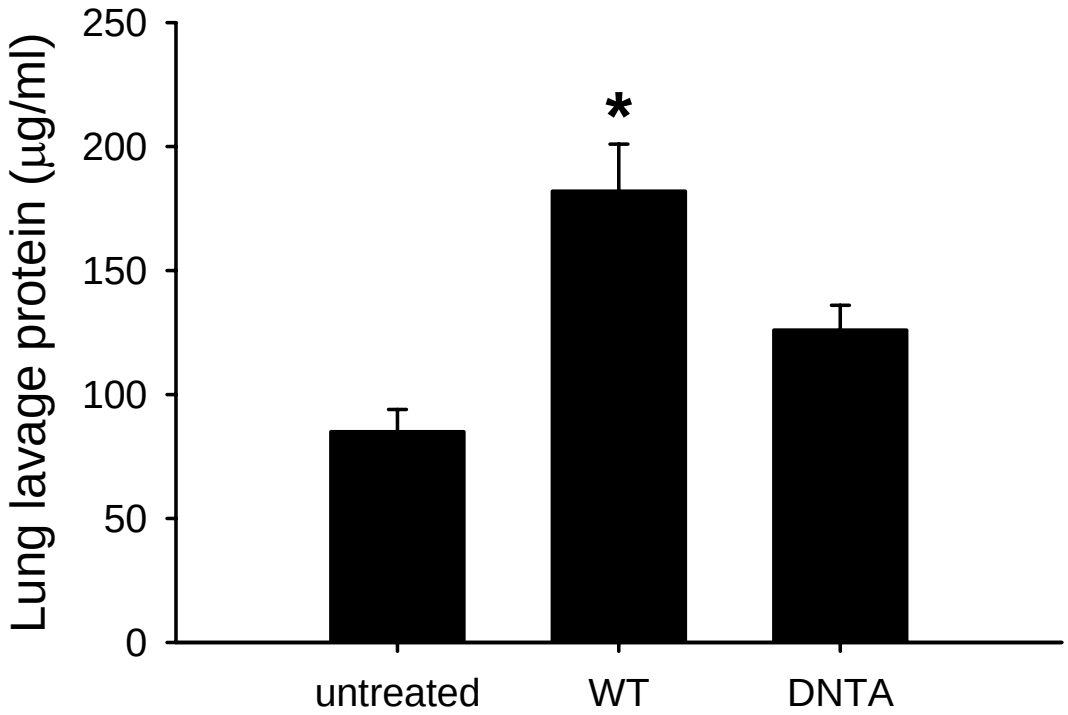
Lung lavage protein (μg/ml)
250
200
150
100
50
0
*
untreated
WT
DNTA

Fig. 5f

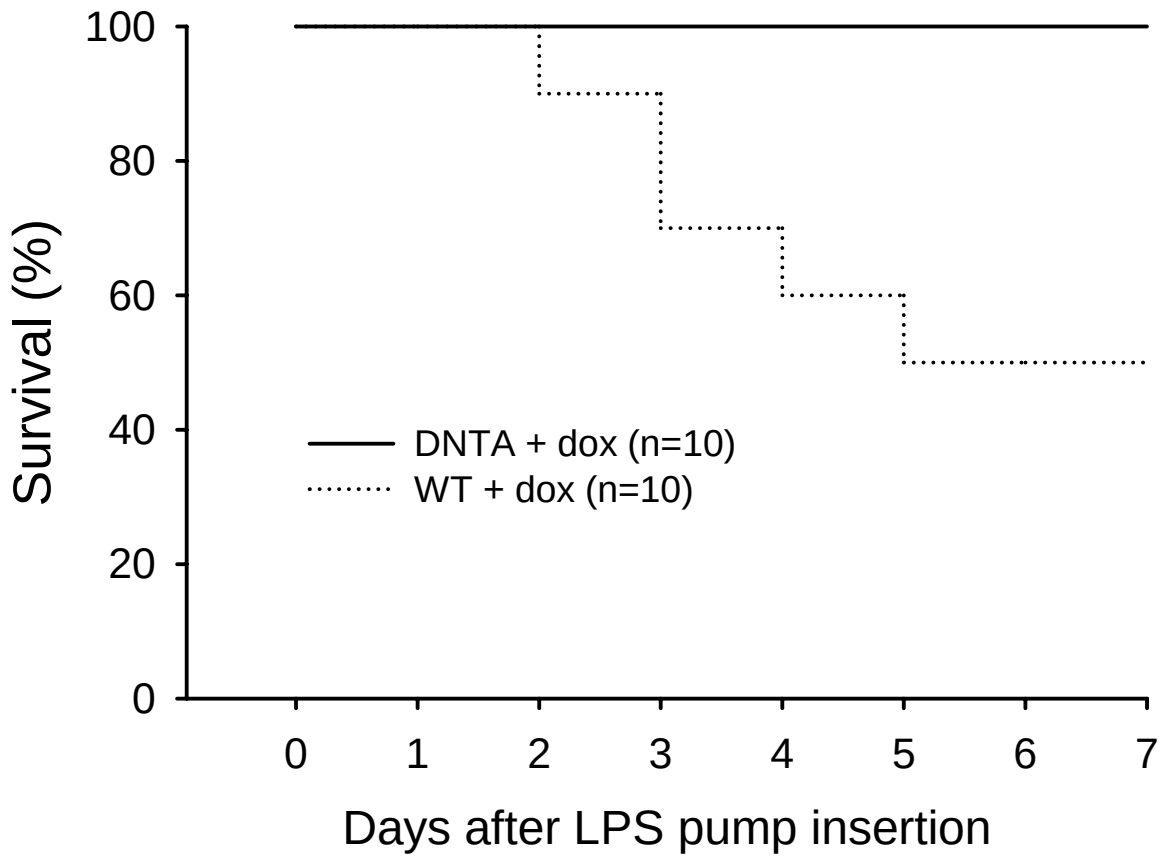
100
80
60
40
20
0
Survival (%)
DNTA + dox (n=10)
WT + dox (n=10)
0
1
2
3
4
5
6
7
Days after LPS pump insertion

Supplemental fig. 1

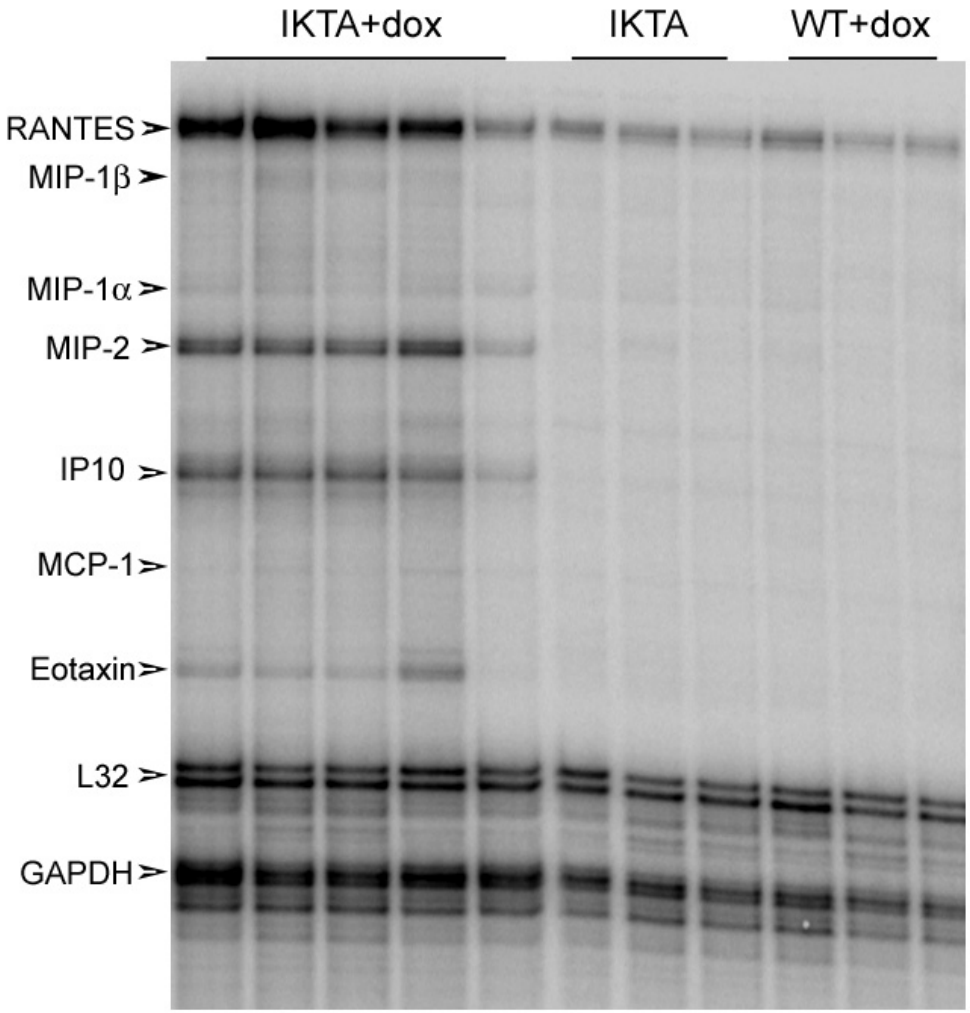

Supplemental fig. 2a

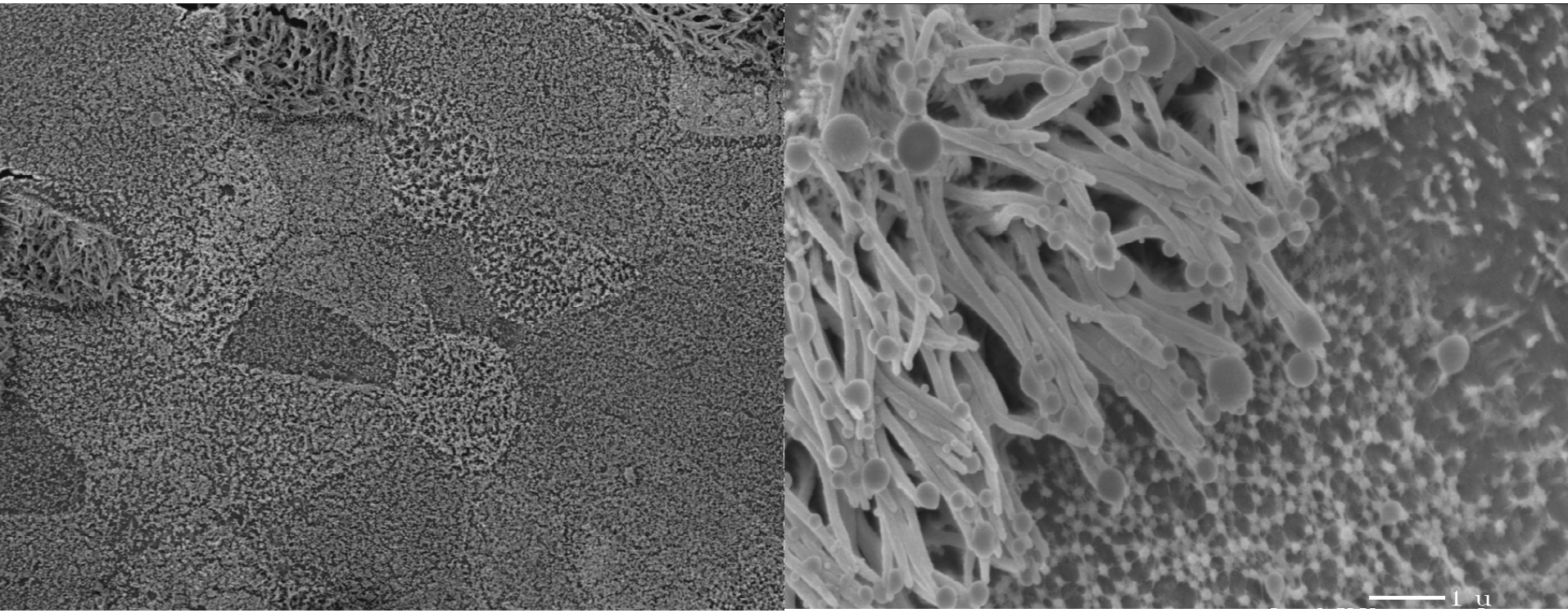

Supplemental fig. 2b

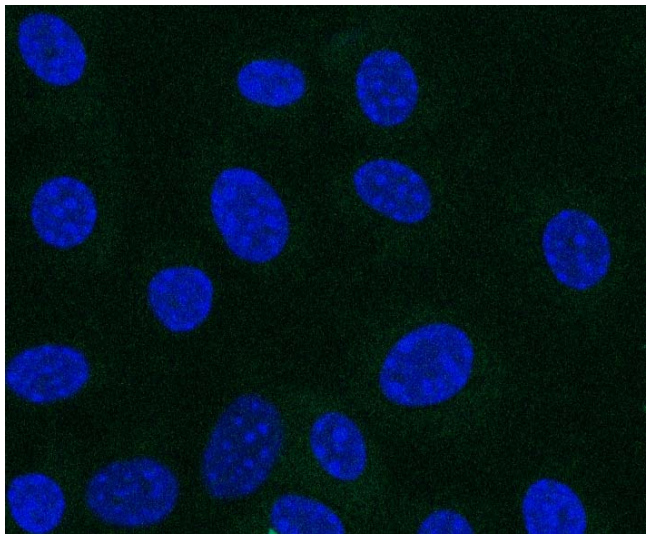

IKTA

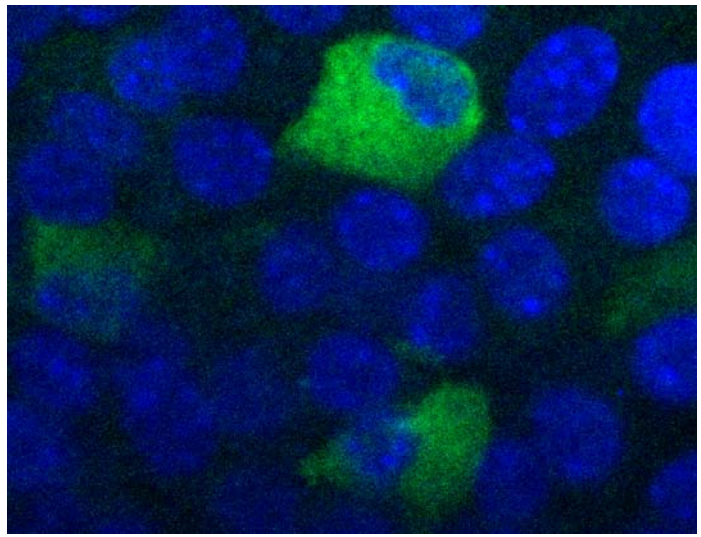

IKTA+dox

Supplemental Table 1

Mediator Concentration in mouse tracheal epithelial cell (MTEC) supernatant (pg/ml)

	IKTA	**IKTA+dox**
IL-1α	0	6 (4)
IL-1β	0	6 (1)
IL-6	11 (3)	554 (102)*
IL-12 (p70)	0	0
G-CSF	3247 (199)	9366 (460)*
GM-CSF	236 (61)	3816 (280)*
MIP-1α	0	0
MIP-2	121 (8)	833 (5)*
KC	9859 (507)	15908 (434)*
RANTES	242 (78)	14267 (632)*
TNFα	0	0
IFN-γ	0	0

Values measured by luminex or ELISA are presented as mean (± SEM). N=3 per group.

*=$p<0.05$ compared with IKTA cells (without dox treatment).

Supplemental Table 2

Mediators in lung lavage at 48 hours after implantation of LPS pump (pg/ml)

	WT mice	**DNTA mice**
TNFα	22.7 ± 17.7	1.2 ± 0.5
IL-1α	81.1 ± 9.3	61.1 ± 6.2
IL-1β	10.2 ± 6.1	3.7 ± 1.6
IL-2	24.2 ± 2.4	12.4 ± 4.1*
IL-3	2.7 ± 0.6	1.0 ± 0.5
IL-5	3.6 ± 1.1	1.6 ± 0.3
IL-6	16.2 ± 2.2	9.3 ± 2.2
IL-9	170.0 ± 31.0	93.0 ± 20.0
IL-10	7.7 ± 2.8	0
IL-12p40	65.2 ± 19.1	49.0 ± 10.4
IL-12p70	8.6 ± 3.8	4.1 ± 2.0
Eotaxin	76.0 ± 39.3	10.7 ± 10.4
RANTES	31.8 ± 2.8	19.1 ± 3.0*
MIP-2	21.9 ± 3.2	4.1 ± 1.5*
MIP-1β	33.8 ± 8.9	8.9 ± 2.6*
KC	696 ± 77	290 ± 36*
MCP-1	668 ± 134	288 ± 59*
G-CSF	16,597 ± 5,651	2,729 ± 509*
GM-CSF	23.3 ± 5.3	9.7 ± 2.5*
IFNγ	8.7 ± 5.4	6.0 ± 3.0

Values measured by luminex or ELISA are presented as mean (± SEM). N=6 mice per group. *=$p<0.05$ compared with WT+ dox group treated with LPS pump. Levels of IL-4, IL-13, IL-17, and MIP-1α were below the limits of detection.